

See discussions, stats, and author profiles for this publication at: <https://www.researchgate.net/publication/44681847>

# Electrochemistry of Conducting Polymers— Persistent Models and New Concepts

ARTICLE *in* CHEMICAL REVIEWS · AUGUST 2010

Impact Factor: 46.57 · DOI: 10.1021/cr900226k · Source: PubMed

---

CITATIONS

293

READS

336

3 AUTHORS, INCLUDING:



Bernardo A. Frontana-Uribe

Universidad Nacional Autónoma de México

64 PUBLICATIONS 818 CITATIONS

[SEE PROFILE](#)



Sabine Ludwigs

Universität Stuttgart

75 PUBLICATIONS 1,942 CITATIONS

[SEE PROFILE](#)

# Electrochemistry of Conducting Polymers—Persistent Models and New Concepts<sup>†</sup>

Jürgen Heinze,<sup>\*,‡,§</sup> Bernardo A. Frontana-Uribe,<sup>||,#</sup> and Sabine Ludwigs<sup>§,⊥</sup>

Institute for Physical Chemistry, University of Freiburg,  
79104 Freiburg, Germany, Freiburg Materials Research Center, University of Freiburg, 79104 Freiburg, Germany, Centro Conjunto de Investigación en Química Sustentable, UAEM-UNAM, 50200 Toluca, Edo. Mex., México, and Freiburg Institute for Advanced Studies (FRIAS), University of Freiburg, 79104 Freiburg, Germany

Received June 23, 2009

## Contents

1. Introduction	4724
2. Electropolymerization Mechanism of Conducting Polymers (CPs)	4726
2.1. Anodic Electropolymerization	4726
2.1.1. General Principles	4726
2.1.2. First Steps of Electropolymerization: Oligomerization and Nucleation	4726
2.1.3. Deposition, Growth, and Solid-State Processes	4730
2.2. Cathodic Electropolymerization	4732
2.2.1. Electropolymerization of PPXs and PPVs	4732
3. Charging—Discharging of Conducting Polymers	4733
3.1. Redox Properties of Oligomers and Polymers	4733
3.2. Specific Phenomena of n-Doping	4739
3.3. Conductivity in Charged Systems	4740
4. Controlling the Electropolymerization Process	4742
4.1. Influence of the Polymerization Technique	4742
4.2. Influence of Experimental Conditions	4743
4.3. Electropolymerization in Novel Electrolytic Media	4745
4.3.1. Electropolymerization in Microemulsion Media	4745
4.3.2. Boron Trifluoride Etherate Catalyzed Electropolymerizations	4745
4.3.3. Electropolymerization in Ionic Liquids	4746
5. Electrosynthesis of Functionalized Conducting Polymers	4747
5.1. Redox-Active Substituents	4748
5.1.1. Organic Redox-Active Substituents	4748
5.1.2. Conjugated Metallopolymers	4751
5.2. Self-doped Conducting Polymers	4753
6. Controlling the Size and Form of Conducting Polymers	4754
6.1. Novel Architectures on the Molecular Scale	4754
6.2. Organic Structure-Directing Agents	4756
6.2.1. Self-assembled Monolayers	4756
6.2.2. Organic Supramolecular Arrays as Organic Templates	4758
6.3. Tuning of Morphologies Using Templates and Patterning Techniques	4760
6.3.1. Soft Templates—The Gas Bubble Technique	4760
6.3.2. Sacrificial Hard Template Methods	4761
6.3.3. Patterning with Scanning Probe Techniques (Direct Writing)	4764
7. Concluding Remarks	4765
8. Acknowledgments	4765
9. References	4766

## 1. Introduction

The existence of materials now included among the class of conducting polymers (CP) has long been known. The first electrochemical synthesis and their characterization as insoluble material took place almost 150 years ago. In 1862, Letheby reported the anodic oxidation of aniline in a solution of diluted sulphuric acid and that the blue–black shiny powder was insoluble in water.<sup>1</sup>

The modern development of conducting polymers began in 1977 as the American scientists Heeger and MacDiarmid and their Japanese colleague Shirakawa discovered that doping chainlike polyacetylene (PA) with iodine endowed the polymer with metal-like properties, producing copper-colored films with an increase of conductivity of 10 orders of magnitude.<sup>2,3</sup> These unconventional properties of an organic material stimulated worldwide efforts to find applications such as batteries or electronic devices. However, PA was not stable and was easily destroyed by oxidative degradation. Therefore, numerous other conducting polymers with properties similar to those of PA were synthesized, such as polyphenylene (PP), polyphenylenevinylene, polypyrrole (PPy), polythiophene (PTh), and, last but not least, polyaniline (PANI).<sup>4–10</sup>

Nowadays, a great number of different monomers are known that form conducting polymers. Such starting systems include substituted derivatives of the already mentioned hydrocarbons and heterocycles but also novel compounds, e.g. 3,4-ethylenedioxythiophene (10),<sup>11,12</sup> which has considerably improved the properties of conducting materials (Figure 1).

The interest of electrochemists in conducting polymers is based on several topics. The method of choice for preparing conducting polymers, with the exception of PA, is the anodic oxidation of suitable monomeric species, such as pyrrole,<sup>6</sup>

\* Corresponding author: Telephone: +49-761-2036202. Fax: +49-761-2036237. E-mail: juergen.heinze@physchem.uni-freiburg.de.

<sup>†</sup> This paper was part of the Molecular and Biomolecular Electrochemistry thematic issue (<http://pubs.acs.org/toc/chreay/108/7>).

<sup>‡</sup> Institute for Physical Chemistry, University of Freiburg.

<sup>§</sup> Freiburg Materials Research Center, University of Freiburg.

<sup>||</sup> Centro de Investigación en Química Sustentable, UAEM-UNAM.

<sup>#</sup> Researcher of the Instituto de Química, UNAM.

<sup>⊥</sup> Freiburg Institute for Advanced Studies (FRIAS), University of Freiburg.



Jürgen Heinze is working at the University of Freiburg at the Materials Research Center (FMF) and the Institute for Physical Chemistry. He habilitated in Physical Chemistry in 1980 and was appointed professor in 1987. He was chairman and head of numerous national and international priority research programs. In 2004 he was honored with the Fellowship of the International Society of Electrochemistry. His main research interests are molecular electrochemistry, electroactive materials, and the further development of electrochemical methods, in particular, those involving microelectrodes, nanodes, and scanning electrochemical microscopy (SECM). Further interests include ionic liquids, diamond electrodes, and sensors. Results have been published in about 280 scientific papers involving original contributions, book chapters, and reviews.



Bernardo Antonio Frontana-Uribe obtained his B.Sc. in Chemistry (1993) and received his M.Sc. degree in Organic Chemistry (1995) at the National Autonomous University of Mexico (UNAM), working on the electrochemical transformation of natural products. He received his Ph.D. degree in 1999 at the University of Rennes I in France, under the supervision of Prof. C. Moinet and A. Tallec, working on the electrosynthesis of nitrogenated heterocycles. He carried out research investigations at the University of California—Santa Barbara in the U.S.A. and the University of Freiburg in Germany. He is currently the head of the “Electrochemistry and Electrosynthesis Laboratory” at the Center of Sustainable Chemistry UAEM-UNAM in Mexico. During these years his research interests have been in the electrotransformations of natural products, electrocatalytic properties of conducting polymer electrodes, and electroassisted crystallization of proteins.

thiophene,<sup>8</sup> or aniline.<sup>9,10</sup> From the viewpoint of molecular electrochemistry, the most relevant aspect concerns the mechanism of electropolymerization involving initially the formation of oligomers followed by nucleation and growth steps, leading to polymeric materials. Mechanistic details are important for optimizing the conditions of electropolymerization. They play a decisive role in determining the quality of the fabricated materials.

A central point of electrochemical research is the analysis of the “doping” process. Even in the earliest stage of research on CPs, there was no doubt that these processes were not



Sabine Ludwigs studied chemistry at the University of Bayreuth, Germany (1997–2002) and completed her Ph.D. in 2004 in the field of “Physical chemistry of polymers” at Bayreuth University in the group of Prof. G. Krausch. Following her Ph.D. studies, she carried out a postdoc with Ullrich Steiner at the Cavendish Laboratory in Cambridge, U.K., from 2004 to 2006. She then returned to Germany, where she joined the Institute for Macromolecular Chemistry and the Freiburg Materials Research Center at the University of Freiburg, Germany, and started to establish her own research team. Sabine was recently awarded with an Emmy Noether grant from the German Science Foundation (DFG). In November 2008 she was appointed as a Junior Fellow at the Freiburg Institute for Advanced Studies (FRIAS) in the School of Soft Matter Research. Her interdisciplinary research team of physical and macromolecular chemists is working on the synthesis and the morphological and electrochemical characterization of tailor-made optoelectronic polymers and inorganic nanoparticles.

comparable with the classic doping of inorganic semiconductors. Rather, they correspond to oxidation in the case of p-doping or reduction in the case of n-doping. That means, using the electrochemical terminology, the doping process corresponds to redox reactions in the polymer matrix. Especially for applications, it is important to know the phenomenological details of such redox reactions, e.g. in

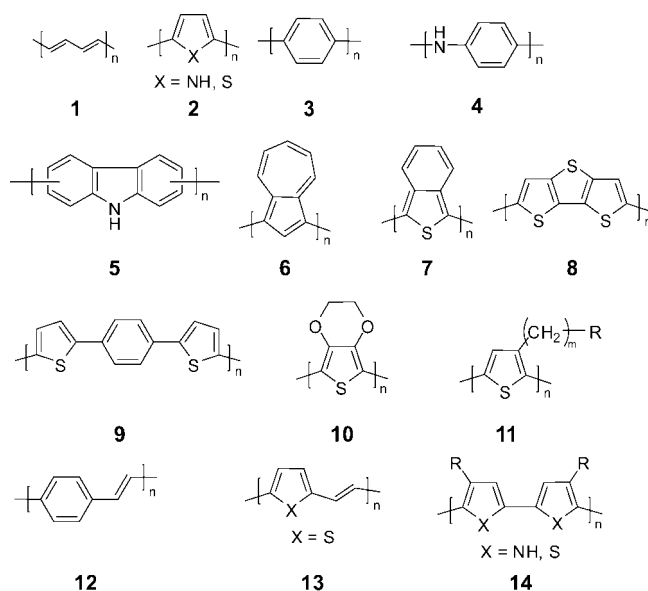


**Figure 1.** Selected building units of conducting polymers: **1**, polyacetylene (PA); **2**, polypyrrole (PPy), polythiophene (PTh); **3**, poly-p-phenylene (PPP); **4**, polyaniline (PANI); **5**, polycarbazole; **6**, polyazulene; **7**, poly(isothionaphthalene); **8**, poly(dithieno-thiophene); **9**, poly(dithienylbenzene); **10**, poly(ethylenedioxy-thiophene) (PEDOT); **11**, poly(3-alkylthiophene); **12**, poly(phe-nylenevinylene) (PPV); **13**, poly(thienylenevinylene); **14**, poly(bipyrrole), poly(bithiophene).

which potential range the charging occurs and what is the maximum level of oxidation before the material starts to degrade.

At the end of the 20th century, the interest in CPs had significantly settled down. However, in 2000, Heeger, MacDiarmid, and Shirakawa were awarded the Nobel Prize for their pioneering work in the field of CPs.<sup>13–15</sup> This distinction excited a new impetus, and a main focus on applications developed in connection with materials research. Between 2000 and 2009, the number of publications doubled from 18 000 to more than 42 000.<sup>16</sup> Therefore, it is surprising that, despite substantial progress in applications, some crucial phenomena of CPs are still under debate. This concerns *inter alia* the mechanism of electropolymerization, the charging/discharging behavior, and even spectroscopic and electrical properties. A reason for this situation may be that, at an early stage in experimental work on these systems, models were introduced using *deduction* to describe basic processes and properties of conducting polymers. For instance, it was postulated that electropolymerization proceeded as a chain propagation reaction<sup>17,18</sup> similar to that known from chemical radical and ionic polymerization of ethylene. Nowadays, it is clear that this mechanism cannot be correct because the reactivity of the charged chain decreases considerably as a function of chain length (see below).<sup>19–21</sup> Other discrepancies concern the interpretation of conductivity after doping<sup>22</sup> or the well-known memory effect.<sup>23</sup>

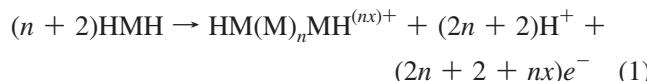
Against this background of accelerated progress between 2000 and 2009,<sup>16</sup> the scope of this review will be mainly limited to novel electrochemical findings in the field of CPs, involving the formation with mechanistic and electrosynthetic aspects, the charge storage mechanism, and related details. On the one hand, basic properties and processes of CPs will be discussed in light of recent results. On the other hand, an overview of recent electropolymerization methods, including the preparation of nanostructures and new architectures as well as new strategies for tuning their properties, will be given. For those readers who are interested in detailed descriptions of properties and applications of CPs, several just published textbooks are available.<sup>24–26</sup>

## 2. Electropolymerization Mechanism of Conducting Polymers (CPs)

### 2.1. Anodic Electropolymerization

#### 2.1.1. General Principles

The most important electrochemical method of preparing conducting polymers is the anodic oxidation of suitable monomer species. This process involves a reaction sequence in which each coupling step has to be activated by two species. It has an electrochemical stoichiometry of 2.07–2.6 F·mol<sup>-1</sup> of reacting monomer.<sup>17,18</sup> The film-forming process needs two electrons per molecule, that is 2 F·mol<sup>-1</sup>, and the additional charge normally serves the partial reversible oxidation of the conjugated polymer. As the potential needed for the oxidation of the monomer is always higher than the charging of oligomeric intermediates or the resulting polymer, the two processes—polymer formation and its oxidation (doping)—occur simultaneously. On the basis of this stoichiometry, the complete reaction equation for the polymerization of a suitable starting species HMH is (eq 1):

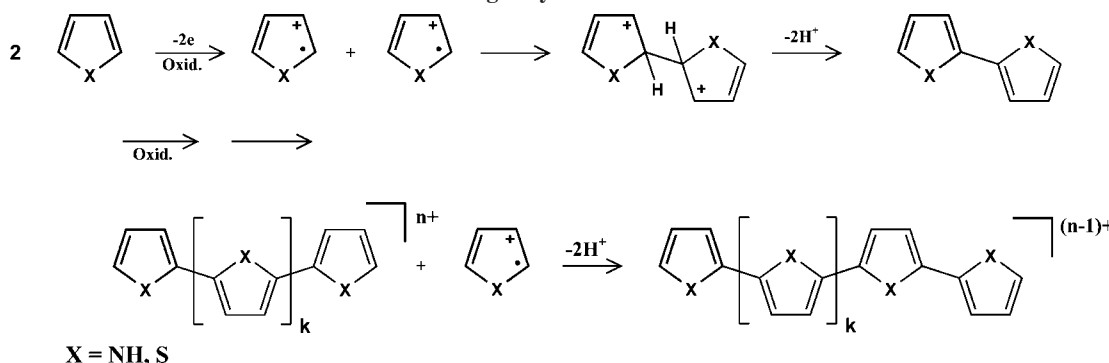


(2n + 2) electrons are used for the polymerization process itself, while the additional charging of the polymer film requires nx electrons. In general, x lies between 0.25 and 0.4 and represents the doping level of the polymer. This means that every third to fourth monomeric subunit has been charged at the end of the electropolymerization.

#### 2.1.2. First Steps of Electropolymerization: Oligomerization and Nucleation

The mechanism of electropolymerization of conducting polymers is still not fully understood and remains subject to controversial discussion. Diaz presented the very first mechanistic concept for the formation of CPs.<sup>17,18</sup> He suggested, in analogy with radicalic or ionic polymerization processes, that in the polymerization of pyrrole the monomers dimerize at the α-position after oxidation at the electrode and that proton elimination occurs from the doubly charged σ-dimer, forming an aromatic neutral dimer. As this dimer, on account of its greater conjugation, is more easily oxidized than the monomer, it is immediately oxidized to its cation, undergoing a next coupling step with a monomeric radical cation, and then from the resulting charged trimer again protons are eliminated. A sort of chain propagation reaction is running, involving a cascade of E(CCE)<sub>n</sub> steps (Scheme 1).

This mechanism, with some marginal modifications,<sup>27,28</sup> is still widely accepted in the literature.<sup>25,26,29,30</sup> However, different experimental findings give evidence that the chain propagation model is far too simple. For example, despite a very high reactivity of 3-methoxythiophene, its electropolymerization in dry acetonitrile stops at the level of its soluble tetramer.<sup>31</sup> Similarly, pyrrole preferably forms oligomeric species during anodic oxidation in acetonitrile but yields a high quality polymer only after addition of 1% of water.<sup>32,33</sup> In this context, the so-called *oligomer approach* has been a very helpful instrument, which as a bottom-up strategy has opened the way to characterize the properties and processes of conjugated oligomers as a function of chain length.<sup>21</sup> Measurements of oligomeric pyrroles<sup>34,35,20</sup> and thiophenes<sup>36</sup> showed that the reactivities of the monomeric starting species were always high but decreased drastically for oligomers.<sup>37,38</sup> Consequently, it was concluded that in the very first step a radical ion dimerization of the monomeric starting molecules took place but the coupling tendency between charged oligomers and a monomer radical cation decreased as a function of the oligomeric chain length. There are two reasons why the chain propagation between an oligomer and a monomer is rather improbable. First, because the rate constants of dimerization of radical cations such as Py<sup>+</sup> or Th<sup>+</sup> with values about 10<sup>9</sup> M<sup>-1</sup>·s<sup>-1</sup> are extremely high;<sup>34</sup> even at low concentrations dimerization of these monomeric cations dominates. Second, recent studies have shown it is not the rate of coupling but rather the elimination of protons from the intermediate σ-dimers that may be rate determining.<sup>31</sup> Thus, the acidity of intermediate σ-dimers diminishes in a growing chain as a function of their lengths due to the resonant stabilizing effect of a large conjugated oligomer.<sup>39–41</sup> Therefore, a permanent elongation of the chain based on the successive coupling of monomeric cations with the chain is

**Scheme 1.** Classical Formation Mechanism of Conducting Polymers

extremely unlikely. Experimental studies using fast double potential step chronoamperometry have confirmed this conclusion.<sup>35</sup>

The importance of proton elimination has been overlooked for a long time. Originally, it was assumed that proton elimination is always a fast reaction, the driving force of which is the rearomatization of the system. Experiments conducted by different groups showed that rates of proton elimination from “dimeric” coupling intermediates may diminish so drastically that charged  $\sigma$ -dimers with more than four units in a conjugated chain segment are fairly stable.<sup>20,31</sup> Proton elimination from such species takes place only when  $\sigma$ -intermediates are oxidized to a higher charging level, which increases the reactivity of the system. Thus, the charged  $\sigma$ -dimer of the thiophene octamer does not undergo a deprotonation step as long as the electrode potential does not exceed the oxidation potential of the octathienophene trication.<sup>42</sup> In general, it can be stated that the stability of the positive charges in a  $\sigma$ -dimer is dependent on electronic factors and the extent of the conjugated system. The chain length criterion proves greater stability—meaning a lower tendency for proton release—of such intermediates for an increasing chain length. As already mentioned, an important consequence of this behavior is that medium-sized oligomeric chains cannot grow via a coupling of a monomeric or dimeric species with an oligomeric chain because the resulting intermediates do not eliminate protons.

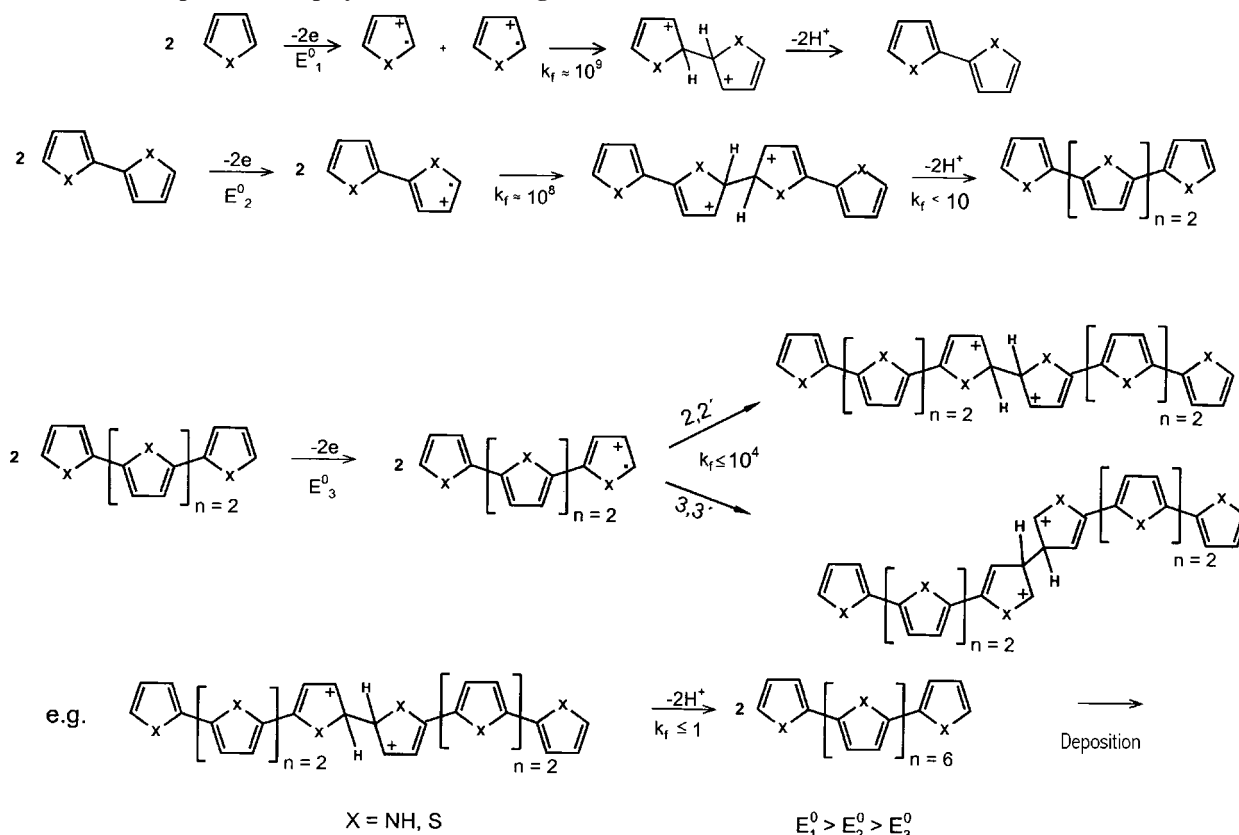
In the literature, several phenomena have been described which, as can be deduced now, are connected with the reactivity of “ $\sigma$ ”-dimers. The most important finding is the “water effect”. As has been shown in numerous publications,<sup>32,43,44</sup> the addition of 1 wt % H<sub>2</sub>O to a solution of pyrrole in acetonitrile increases the rate of electropolymerization and improves the film adherence and morphology. The  $\sigma$ -intermediates of pyrrole oligomers are weak acids. Therefore, sufficiently strong bases are necessary to initiate proton elimination. Water fulfills this condition, but not acetonitrile.<sup>33,45</sup> A similar effect results from the application of a sterically hindered base such as 2,6-di-*tert*-butylpyridine.<sup>46</sup> In addition to the basicity effect, Zotti et al. observed anion effects on the polymerization rate of 2,2'-bipyrrole<sup>47</sup> in the presence of tosylate. They suggested that 2,2'-bipyrrole forms an ion pair with the tosylate anion which may then dimerize at a faster rate than the free radical cation due to the shielding of the positive charge.

Despite the fact that  $\sigma$ -dimers are intermediates during the oxidative formation of conducting polymers, their existence has been questioned for all those cases where substituents at the reactive site of a compound may impede a direct coupling reaction. Thus, on the basis of concentration and

temperature-dependent UV-vis and ESR data, several authors have suggested that the radical cations of substituted oligothiophenes form  $\pi$ -mers.<sup>48–52</sup> In all cases, voltammetric data apparently indicate the reversible formation of radical cations without chemical follow-up steps. Accordingly, based on experimental data, it has been concluded that weakly interacting  $\pi$ -mers form rapidly and also decay relatively quickly on the experimental time scale. However, recent cyclic voltammetric studies of the oxidation of diphenylpolyenes, substituted oligothiophenes, and other systems have indicated strong changes of the voltammetric response as a function of temperature, concentration, and scan rate. A detailed evaluation of these data gave clear evidence that the formation of all these radical ions is followed by a rapid reversible dimerization between the oligomers, accompanied by the formation of a  $\sigma$ -bond.<sup>53–55</sup> Moreover, applying NMR measurements, Merz et al. could show that the radical cations of 5,5'-diphenyl-3,3',4,4'-tetramethoxy-2,2'-bipyrrole reversibly dimerize and form an  $\sigma$ -dimer in solution, the equilibrium constant of which is temperature-dependent.<sup>56</sup> The fact that the reaction enthalpies of the formation of all these  $\sigma$ -dimers normally lie between –60 and –90 kJ mol<sup>–1</sup> (ref 53) is a further strong argument against the  $\pi$ -mer hypothesis. These reaction enthalpies of equally charged species still contain essential repulsive interactions. That means that the true bonding interaction is significantly higher than –60 kJ mol<sup>–1</sup>, which clearly exceeds values of weak  $\pi$ -interactions.

In the early period of research on CPs, the radical cation–radical cation coupling (RR) mechanism has been criticized by the argument that the strong Coulombic repulsion between small cation radicals renders a direct dimerization of such particles improbable. Instead, a radical cation–substrate coupling (RS) was postulated.<sup>57–60</sup> An electrophilic attack by the radical cation on the neutral monomer or oligomer generates a single-charged coupling product, which eliminates its protons only after an additional charge transfer, becoming a rearomatized neutral oligomer. However, the principal objection to the RR path—the strong Coulombic repulsion between charged particles—is not convincing for reactions in the condensed phase. Using the Debye–Smoluchowski theory,<sup>61</sup> it has been shown that even small molecules that are equally charged are able to dimerize at a diffusion-controlled rate.<sup>62,63</sup> In the meantime, a theoretical analysis<sup>64</sup> and careful quantitative kinetic studies of the coupling steps of oligomeric pyrroles and thiophenes have confirmed the R<sup>+</sup>R<sup>+</sup> reaction path.<sup>35,65,66</sup>

But which intermediates are formed during electropolymerization of suitable starting species? The early experimental results of Savéant<sup>35</sup> et al. gave evidence that radical cations of the starting compound and their oligomeric

**Scheme 2. Initial Steps of Electropolymerization Taking Place via  $\sigma$ -Bonded Intermediates**

intermediates are involved in the oligomerization reaction and that they preferably couple between themselves. Studies by Heinze et al. on donor-substituted thiophenes such as methylsulfanyl- or methoxy-substituted derivatives<sup>31,33,67</sup> confirm these findings and unambiguously show that the consecutive oligomerization of conducting polymers starts in solution and preferably takes place via successive “dimerization” steps leading from a dimer to a tetramer and then to an octameric coupling product (Scheme 2). At higher concentrations of the starting species, additional coupling reactions may occur, which produce intermediates such as trimers, hexamers, and so on. Similarly, already in the late 1980s, Costa and Garnier<sup>68</sup> concluded from spectroscopic measurements based on ellipsometry of methylthiophene that the intermediate cations generated at the electrode form oligomers by coupling cations in the solution with a degree of polymerization of 3–4. Lukkari<sup>69</sup> et al. also showed that, during the initial phase of electropolymerization, oligomers are formed in solution and that the beginning of the deposition process involving short or longer oligomers depends on the chemical nature and reactivity of the electrode, e.g. ITO or Pt. Using the technique of bidimensional spectroelectrochemistry, that allows simultaneous acquisition of spectra in both normal and parallel directions to the surface of a plane electrode, Lopez-Palacios et al.<sup>70</sup> gave very clear experimental evidence that during the electropolymerization of bithiophene derivatives always soluble oligomers are formed in front of the electrode. It should be noted that the efficiency of electropolymerization and the amount of soluble oligomers formed during anodic oxidation strongly depend on different experimental parameters such as the formation potential, the concentration of the monomer, and the experimental time scale. High potentials and concentrations, as well as long electrolysis

**Table 1. Peak and Redox Potentials of Oligopyrroles (nPy),<sup>34,72</sup> Oligothiophenes (nTh),<sup>42,73,74</sup> and Mixed Oligomers<sup>73</sup>**

compound	$E_{1,\text{ox}}^0$ (V)	$E_{2,\text{ox}}^0$ (V)	$k_{\text{dim}} (\text{M}^{-1} \cdot \text{s}^{-1})^a$
Py	1.35		$4 \times 10^9$
$\alpha$ 2Py	0.64		$1.2 \times 10^9$
$\alpha$ 3Py	0.32		$5 \times 10^8$
$\alpha$ 4Py	0.20	0.47	$<10^4$
$\alpha$ 5Py	0.16	0.36	$<10^2$
Th	1.7 <sup>b</sup>		$<10^9$
$\alpha$ 2Th	1.29 <sup>b</sup>		$6 \times 10^8$
$\alpha$ 3Th	0.95	1.9 <sup>b</sup>	$(2-3) \times 10^8$
$\alpha$ 4Th	0.80	1.24	
$\alpha$ 6Th	0.60	0.87	
$\alpha$ 3(MeTh)	1.06		$3.5 \times 10^7$
$\alpha$ ThPyTh	0.80		$10^6$

<sup>a</sup> Kinetic data for dimerization of the corresponding radical cations after anodic oxidation. All potentials are related to the Ag/AgCl electrode. <sup>b</sup> Irreversible peak potential.

times, favor an efficient polymerization. Hence, it is not surprising that some authors observed high deposition efficiencies during electropolymerization experiments<sup>71</sup> (see section 2.1.3).

An important factor that significantly influences the results of electropolymerization reactions concerns the selection of the starting compound. This is typically a monomer but may be also a short oligomer ( $n = 2-6$ ) with identical or different hetero- or isocyclic rings. Furthermore, the substitution pattern as a function of its nature or its position is an additional parameter that controls the kinetics of electropolymerization.

The simplest modification involves the elongation of the starting monomer to a dimer or longer oligomers. Under these conditions, two essential parameters change. First, the oxidation potentials get lower for increasing chain length. Second, the kinetics slows down in the same manner (Table 1). The

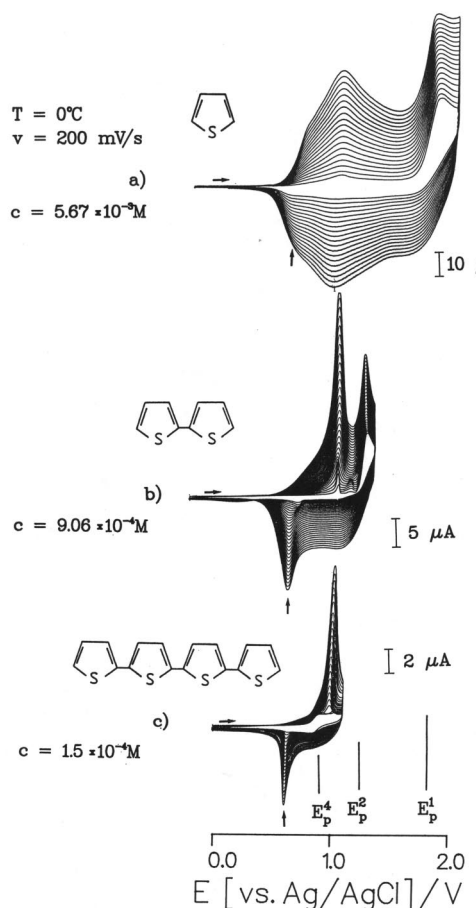
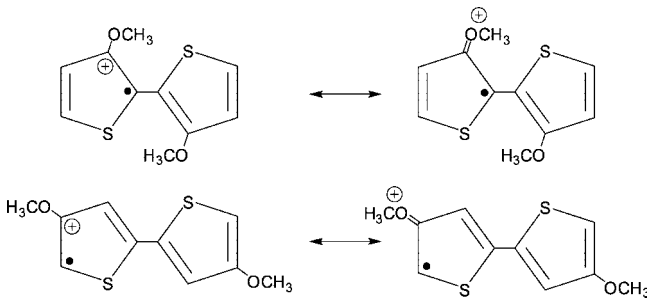


**Figure 2.** Potentiodynamic electropolymerization of thiophene, bithiophene, and quaterthiophene in  $\text{CH}_3\text{NO}_2/0.1 \text{ M TBAPF}_6$ ;  $v = 100 \text{ mV} \cdot \text{s}^{-1}$ ;  $T = 298 \text{ K}$ . The arrow indicates the discharging of octathiophene.

lowering of the oxidation potentials of oligomers facilitates defect-free electropolymerizations because nucleophilic reactions of solvents with growing oligomers do not take place and “polymerizations” even in water become possible. However, with respect to the starting compounds, the most drastic changes concern the kinetics.

As can be seen in Figure 2, the oxidation of thiophene leads to a product with a chain length significantly higher than 8, while the bithiophene oxidation preferably generates octathiophene and the tetrathiophene oxidation exclusively ends at the level of octathiophene. The decreasing coupling rates of the radical cations of the repetitive oligomers and the simultaneous increase of the kinetic stability of the coupling products explain these findings. Similarly, studies of Hapiot et al. have shown that the combination of thiophene and pyrrole<sup>73</sup> units in a trimeric oligomer also lowers oxidation potentials and reaction rates in comparison to the case of the pure terthiophene oligomer. As expected, the introduction of withdrawing substituents increases the oxidation potential and the reactivity of the system, whereas donor groups decrease the oxidation potentials.<sup>36,74</sup> Interestingly, even the position of a substituent may influence the reactivity of the compound. Thus, the rates of electropolymerization of the donor-substituted 3,3'-dimethoxybithiophene and 4,4'-dimethoxybithiophene differ extremely. The initializing dimerization step of the 3,3'-isomer is low, resulting in a dimerization constant of  $<10^5 \text{ [M}^{-1} \cdot \text{s}^{-1}]$ . By contrast, the coupling reaction of the 4,4'-isomer is very fast with a rate constant higher than  $5 \times 10^8 \text{ [M}^{-1} \cdot \text{s}^{-1}]$ . The reason for this

**Scheme 3. Mesomeric Resonance Structures of 3,3'-Dimethoxy- and 4,4'-Dimethoxybithiophene**



behavior rests on electronic effects. The mesomeric resonance structures of the corresponding radical cations reveal that the highest spin density is located at the blocked inner  $\alpha$ -position in the case of the 3,3'-isomer and at the non-blocked outer  $\alpha$ -site in the case of the 4,4'-isomer (Scheme 3).<sup>75,67</sup> As a consequence, the electropolymerization of the 3,3'-isomer stops at the level of the octamer, whereas the 4,4'-isomer yields a typical conducting polymer with excellent properties.

A difficulty of the interpretation of electrochemical measurements in the field of CPs is that the electropolymerization process has been compared with the electrodeposition of metals. However, there are many differences. The most important is that every bond-forming step during electropolymerization has its own electrochemical activation barrier, whereas the deposition of metals is based on one redox step. A typical example of this comparison is the so-called *nucleation loop*, which was first described by Pletcher.<sup>57</sup> This phenomenon is normally observed during the very first voltammetric cycle of an electropolymerization experiment. It involves a crossing effect that appears in all voltammograms on the reverse sweep of the first cycle (Figure 3).<sup>76</sup> As this effect always appears in experiments with freshly polished electrodes, it has been interpreted as the start of the nucleation process of the corresponding polymer. Such behavior is similar in this respect to the electrochemical deposition of a metal on a foreign substrate, in which overpotential is required for nucleation, after which growth of the metallic layer occurs at the characteristic redox potential of the reverse sweep.

Cyclic voltammetric measurements with thiophene and other monomers in ionic liquids, the results of which were published by Heinze et al. in 2007,<sup>77</sup> open quite a new view on this basic phenomenon. The analysis of the electrochemical data clearly demonstrates that the loop effect is based on a homogeneous comproportionation reaction from an intermediate  $\text{Oligo}^{n+}$  with the starting monomer  $\text{Mon}$  to  $\text{Oligo}^{(n-1)+}$  and  $\text{Mon}^+$  (Scheme 4).

It is an autocatalytic mechanism, which considerably facilitates the starting oxidation of the monomer. The charged oligomer  $\text{Oligo}^{n+}$ , e.g. in the case of thiophene probably a tri- or tetracationic hexa- or octathiophene, is generated during the first anodic oxidation cycle and reacts as a redox mediator with the starting monomer. In order to trigger such redox reactions, it is necessary that the redox potentials of the  $\text{Oligo}^{n+}/\text{Oligo}^{(n-1)+}$  pair and that of the starting monomer  $\text{Mon}/\text{Mon}^+$  are only weakly separated. Digital simulations, which have been carried out for a large number of different experimental parameters, confirm this mechanistic concept. It seems that this electrocatalytic effect is a general phenomenon characteristic of many chain-forming electropoly-

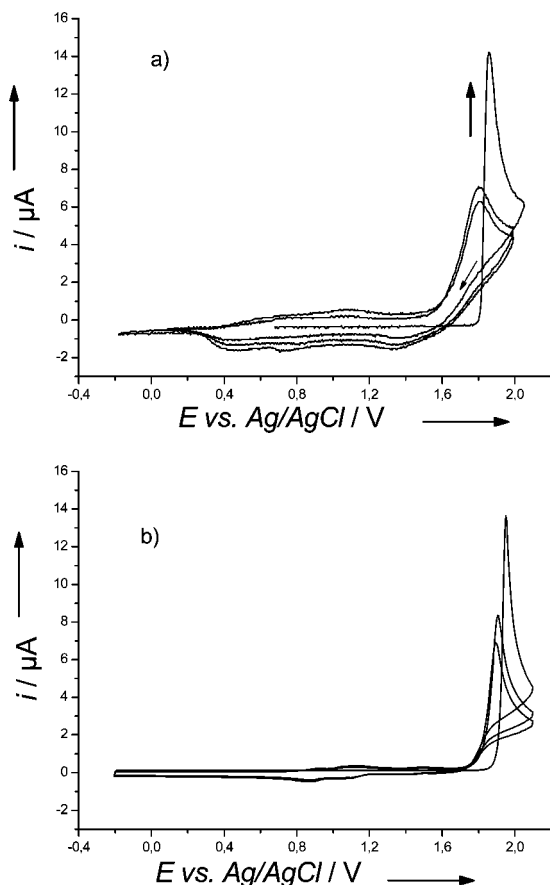
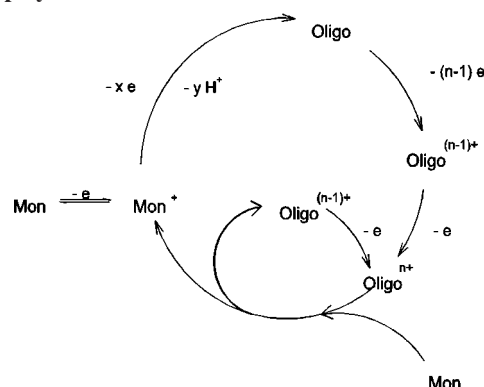


**Figure 3.** “Nucleation loop” of thiophene:  $v = 0.1$  V/s;  $c = 3 \times 10^{-3}$  M; (a) cyclic voltammetry in 1-hexyl-3-methyl-3H-imidazol-1-iumtris(pentafluoroethyl)trifluorophosphate = [HMIM][PF<sub>3</sub>(C<sub>2</sub>F<sub>5</sub>)<sub>3</sub>]; (b) simulation.<sup>77</sup>

**Scheme 4. General Reaction Scheme of the Autocatalytic Oxidation of Monomeric Starting Species during Electropolymerization<sup>77</sup>**



merization reactions. Studies of Zotti et al.<sup>78</sup> carried out with redox-active films of conducting polymers indicate similar electrocatalytic effects as observed during voltammetric multisweep experiments. Generally, this catalytic principle has been first described by Savéant and his group and is known as “redox catalysis”.<sup>79</sup>

### 2.1.3. Deposition, Growth, and Solid-State Processes

As described in the preceding section, polymerization starts with the formation of oligomers in solution. The next general step is the deposition, which includes nucleation, growth, and additional chemical steps under solid-state conditions. Potentiostatic, potentiodynamic, or galvanostatic techniques

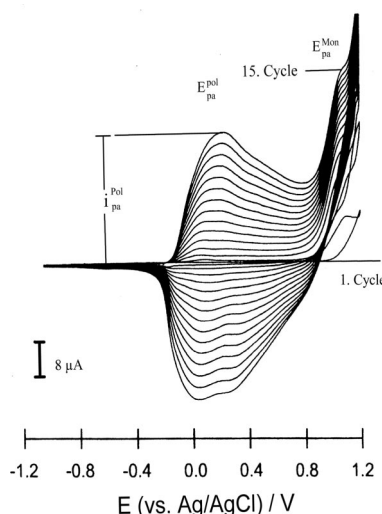


**Figure 4.** Typical potentiodynamic experiment of conducting polymer growth. Potentiodynamic growth of a polypyrrole film in acetonitrile (+1% H<sub>2</sub>O)/0.1 M TBAPF<sub>6</sub>,  $v = 100$  mV s<sup>-1</sup>,  $T = 298$  K.

can be used to generate and monitor these processes. The potentiodynamic experiment, in particular, provides simple information on the growth rate of CPs. The increase in current with each cycle of a multisweep cyclic voltammogram is a direct measure of the increase in accessible surface and the number of rechargeable redox sites (Figure 4).

Assuming a linear growth, the relative growth rate per cycle  $v_g$  (eq 2) can be calculated from the anodic peak current  $i_{pa}^{pol}$  of the respective polymer oxidation, where  $k$  is a proportionality constant and  $n$  is the cycle number ( $n \geq 2$ ).  $v_g$  depends on the scan rate, the concentration of the monomer, and other parameters.

$$v_g = k \frac{i_{pa}^{pol}}{(n - 1)} \quad (2)$$

The disadvantage of the potentiodynamic technique is that multisweep experiments indicate the growth of a polymeric film but almost no direct information on the nucleation and growth mechanism can be obtained. The reason is that, during potentiodynamic experiments, polymers are charged and discharged and growth processes are interrupted. Therefore, in the literature, potential step measurements have been used to analyze the deposition processes of CPs (Figure 5; also see section 4.2).<sup>80</sup>

In the electrodeposition of CPs, different models for layer formation have been discussed. They all refer to the deposition of metals.<sup>81,82</sup> There are two kinds of nucleation, namely instantaneous and progressive, and three types of growth involving one- (1D), two- (2D), and three-dimensional (3D) processes. In the case of instantaneous nucleation, the number of nuclei is constant and they grow without the formation of further nuclei. In the case of progressive nucleation, nuclei are generated at all times. 1D growth occurs only in one direction, e.g. perpendicular to the electrode. In the 2D growth, the nuclei preferably grow parallel to the electrode, and in the 3D growth, the rates for these processes perpendicular and parallel to the electrode are very similar. Based on these general features, two special models are presented in the literature that may describe the nucleation and growth process of CPs. The first one is related to the electropolymerization mechanism of Diaz<sup>6</sup> and as-

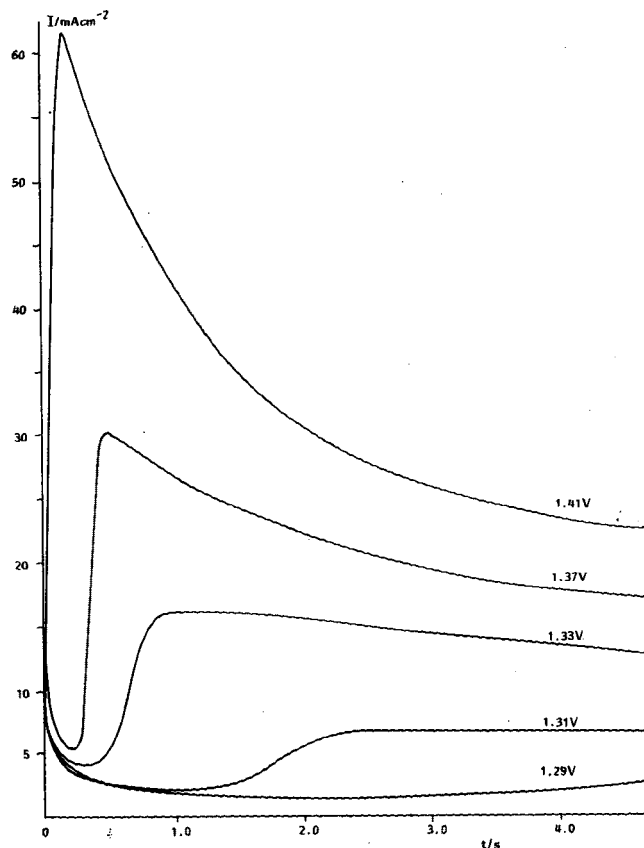


**Figure 5.** Current–time responses to potential steps from 0.0 V to the values shown in the figure. Solution contains thiophene (50 mM) in  $\text{CH}_3\text{CN} + \text{Bu}_4\text{NBF}_4$  (0.2 M) using a Pt electrode. Reprinted with permission from ref 80. Copyright 1986 Elsevier.

sumes the adsorption of the monomer onto the electrode surface followed by a chain propagation process where oxidized monomer units are coupling at the end of oligomeric surface-bound chains. As in particular in the short time domain only 3D or 2D mechanisms have been observed, this deposition route is unlikely.<sup>57</sup> The second model, which obviously is quite realistic, resembles the findings obtained in the course of potentiodynamic rotating ring-disk electrode (RRDE) and spectroscopic measurements.<sup>67,70,83</sup> It assumes that the starting compound is oxidized at the electrode and then forms soluble oligomers in the diffusion layer in front of the electrode. After oligomers saturate this interface, the CP's nucleation and growth starts. During the running deposition, the mechanism may change due to overlapping of the growing nuclei.

The analysis of the current–time responses has been carried out by the application of theoretical expressions developed for metal deposition.<sup>82</sup> However, two important details have made it difficult to present an unambiguous interpretation of the experimental data. First, the oxidation of the monomer and the successive soluble oligomers is not considered. Second, the model does not regard any solid state polymerization steps which take place after deposition and may involve additional charge transfer reactions. Therefore, it is not surprising that, in dependence on the experimental conditions and the selected time domain, different nucleation and growth mechanisms even for the same polymer have been detected.<sup>84,85</sup> In order to refine the modeling, in very recent publications, sophisticated items have been introduced which consider *inter alia* mass transport and charge transfer control.<sup>76,84,85</sup> The most prominent mechanisms for deposition

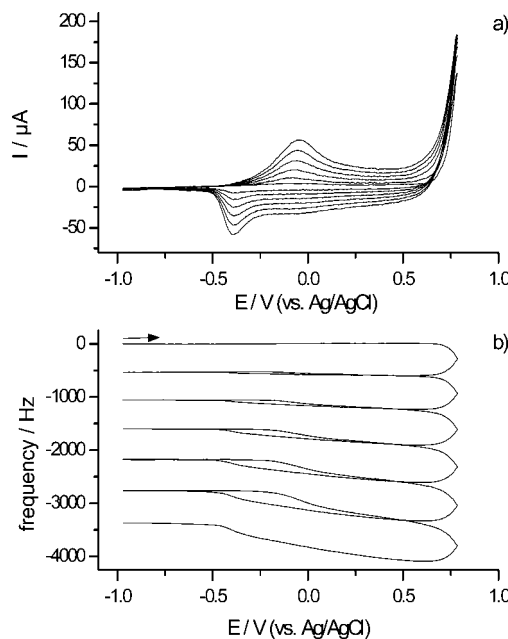


**Figure 6.** EQCM during potentiodynamic polymerization of 4,4'-dimethoxybithiophene in  $\text{CH}_2\text{Cl}_2$ , 0.1 M TBAPF<sub>6</sub>,  $v = 10 \text{ mV} \cdot \text{s}^{-1}$ : (a) cyclic voltammetry; (b) frequency–potential plot showing mass changes as a function of the applied potential.

of heterocycles such as thiophene or pyrrole are instantaneous (2D or 3D) nucleation and 3D growth,<sup>57,76,84</sup> in the case of aniline progressive nucleation, 3D growth, and layer by layer deposition.<sup>86,87</sup>

In addition to normal electrochemical pulse measurements, scanning probe techniques such as atomic force microscopy (AFM) have been very useful for obtaining information about the early stages of polymer deposition.<sup>87</sup> Surprisingly, in the case of polypyrrole and polybithiophene, AFM images unambiguously indicate progressive nucleation.<sup>88,89</sup>

Mass changes during the electrodeposition process can be monitored using electrochemical quartz crystal microbalance measurements (EQCM), where potential step techniques<sup>90,91</sup> and cyclic voltammetry<sup>92,93</sup> have been coupled to the QCM technique. They reveal that deposition occurs preferably in the potential range where the monomer and short oligomers are oxidized (Figure 6). In general, no deposition is observed outside of this range. Surprisingly, lowering the temperature raises the efficiency of deposition, owing to the fact that the solubility of the oligomers decreases.<sup>92</sup>

The potential step method is very helpful in exploring nucleation and growth mechanisms of CPs, but it delivers no direct information about chemical steps during deposition. These were obtained by voltammetric experiments with oligomeric films under solid-state conditions. For example, voltammetric measurements on hexaphenylene layers deposited on a Pt electrode revealed that the material “polymerizes” upon anodic oxidation.<sup>94</sup> It was shown that hexaphenylene dimerized at low oxidation potentials, yielding dodecaphenylene, while at higher potentials long chains were produced and cross-linking steps became more and more predominant.<sup>95</sup> Later on, further solid-state experiments with monodisperse oligo-thiophenes confirmed these results.<sup>96</sup> The application of low-temperature voltammetry to octathiophene, for instance, allowed the reversible generation of trications or even tetracations. This stability disappeared when the temperature was raised. If, in the case of octathiophene, the switching potential  $E_\lambda$  was set in the ascent of the anodic

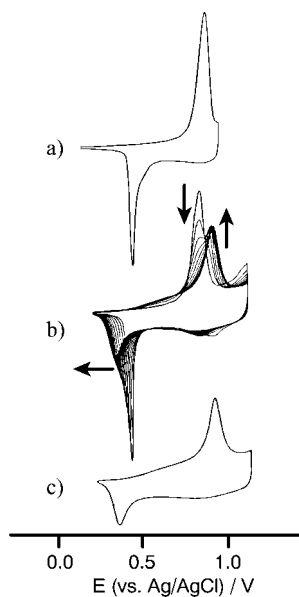


**Figure 7.** Potentiodynamically generated solid-state coupling of octathiophene,  $v = 10 \text{ mV} \cdot \text{s}^{-1}$ ,  $T = -5^\circ\text{C}$ : (a) cyclic voltammogram of octathiophene,  $E_\lambda = 1.07 \text{ V}$ ; (b) cyclic voltammetry during coupling,  $E_\lambda = 1.25 \text{ V}$ ; (c) cyclic voltammogram of sexidecithiophene,  $E_\lambda = 1.25 \text{ V}$ . The resulting sexidecithiophene forms a stable  $\sigma$ -interchain product after oxidation. Reprinted with permission from ref 96. Copyright 1996 Elsevier.

trication wave at 1.25 V, two new waves appeared—one in the anodic and the second one in the cathodic scan—and gradually increased, while the original signals for the redox processes of the starting material decreased (Figure 7). The resulting isopotential point confirmed that octathiophene reacted to produce a new electroactive species without side reactions. The optical absorption of the electrochemically generated product was red-shifted and its cathodic peak potentials upon discharging (reduction) lied negative to those of the educt, indicating that the product consists of larger molecules with a more extended redox system. If experiments were carried out at higher sweep rates ( $v > 100 \text{ mV} \cdot \text{s}^{-1}$ ), broad waves were observed during the cathodic reverse scan at potentials around 0 V. This is typical for the discharging of protons formed during the process. Coulometric analysis of the voltammograms showed that one charge is lost per molecule (by proton cleavage) in the condensation reaction. The average functionality of a monomer unit,  $f$ , was calculated from coulometric data. The resulting values of  $f < 2$ , together with all other observations, gave clear evidence that the short-chain octathiophene dimerized quantitatively in this solid-state reaction, forming an isomer of sexidecithiophene.<sup>96</sup> Using higher formation potentials, a cascade of solid-state coupling and proton elimination steps generated a typical conducting polymer.

In summary, all the recent findings published in the literature exclude a simple chain propagation mechanism for the formation of conducting polymers. Rather, electropolymerization involves three different stages:

- Oxidation of the monomer at the electrode and formation of soluble oligomers in the diffusion layer—preferably successive dimerization steps
- Deposition of oligomers, involving nucleation and growth processes
- Solid state polymerization, producing longer chains and cross-linked materials.

An important point in understanding the properties of CPs is the length of the conjugated chain, which can be achieved by electropolymerization. Already at the beginning of this research it was discovered that preferably short chains were generated; for example, in the case of polyphenylene, a chain length of 16 units was achieved.<sup>97</sup> As has been shown, the reactivities of the generated oligomeric intermediates depend on their charging level. Consequently, the applied formation potentials steer the chain length of the resulting product. Thus, low oxidation potentials produce “short” chain lengths. For example, using an extremely low oxidation potential, the electropolymerization of pyrrole leads to formation of an oligomer PPy II with a chain length between 8 and 16 units. At higher oxidation potentials, PPy I is generated with chain lengths between 32 and 64 units.<sup>98</sup> Lastly, at very high potentials, cross-linked networks are formed.<sup>99</sup> The mechanistic details of the electropolymerization process reveal that the material produced at the electrode consists of a mixture of species with different conjugation lengths.<sup>69</sup> Apart from the formation potential, additional factors such as the polymerization technique—potentiodynamic, potentiostatic, or galvanostatic—and the temperature influence the quality of the deposited material (see below).

## 2.2. Cathodic Electropolymerization

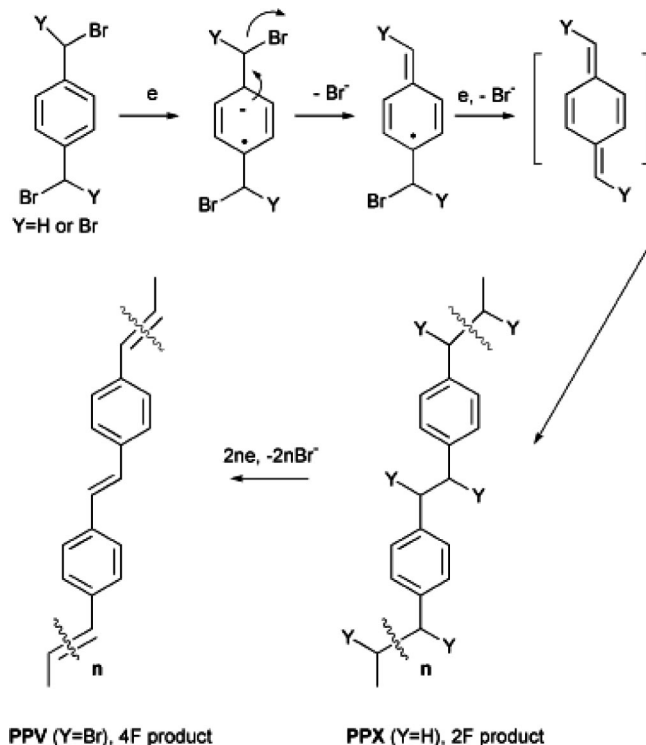
As it has been shown, oxidative electropolymerization is widely used for the preparation of conducting polymers. Of the large number of anodically electropolymerizable aromatic systems (Figure 1), polypyrroles, polythiophenes, and polyanilines are the most studied. Nevertheless, there are very few reductive electrosynthetic processes that yield conducting polymers. The best known conducting polymers produced by this method are the poly(*p*-phenylenevinylenes) (PPVs) *via* the poly(*p*-xylylenes) (PPXs). The current interest in these polymers results from the fact that they have been successfully used as materials for organic light emitting devices.<sup>99,100</sup> Chemical<sup>101–104</sup> and electrochemical<sup>105</sup> routes to obtain these conducting polymer families have been described in the literature, but here we will focus only on the electrochemical pathway.

### 2.2.1. Electropolymerization of PPXs and PPVs

In 2002 Utley and Gruber reviewed extensively this topic;<sup>105</sup> thus, we will discuss only the more recent literature. PPVs are obtained via the electrochemical reduction of readily available  $\alpha,\alpha,\alpha',\alpha'$ -tetrahalo-*p*-xylylenes, with the bromo-compounds being the most used due to their lower reduction potentials (Scheme 5). After the first two electron transfers, a quinodimethane intermediate is produced, which spontaneously polymerizes to obtain poly(*p*-xylylenes) (PPXs). The mechanism of polymerization is still not very clear.<sup>105</sup> It seems that radical anions of electrogenerated quinodimethanes initiate a chain propagation process resulting in poly(*p*-xylylenes). A second electroreductive step generates the vinylene unit on the polymeric backbone to yield the poly(*p*-phenylenevinylenes) (PPVs).<sup>106,107</sup>

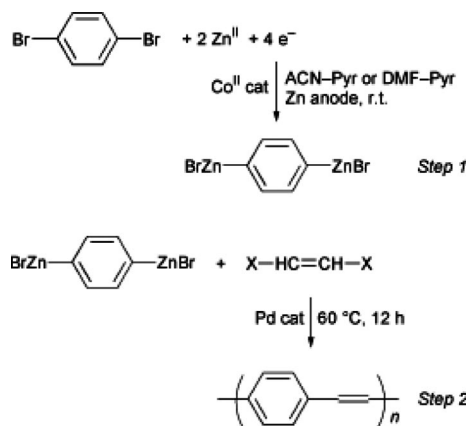
Due to the high reduction potential of the compounds ( $> -2.0 \text{ V}$  vs SCE), mercury electrodes are normally used for the electrosynthesis and DMF has been shown to be an appropriate solvent. Assisted electroreduction using cathodic mediators generates PPVs in good yields without reaching high potential values.<sup>105</sup> The mediator also facilitates the application of less lachrymatory and cheaper chlorinated

**Scheme 5. Electrochemical Reductive Electropolymerization of  $\alpha,\alpha,\alpha',\alpha'$ -Tetrabromo-*p*-xylene (TBPX) To Produce PPVs<sup>a</sup>**



<sup>a</sup> Reprinted with permission from ref 105. Copyright 2002 Royal Society of Chemistry.

**Scheme 6. Electrosynthesis of PPVs Using as Key Step a Paired Electrolysis Process<sup>a</sup>**



<sup>a</sup> Reprinted with permission from ref 109. Copyright 2002 Royal Society of Chemistry.

derivatives instead of the brominated precursors. Among the proposed mediators, anthracene has been the most studied compound. When it is used, the yield of PPV rises to 134%, in comparison to the case of electrosynthesis without mediator.<sup>108</sup>

An alternative two-step procedure for the synthesis of PPVs has been developed using electrogenerated arylzinc compounds as key intermediates. Using 1,4-dibromophenylanes as starting materials, their cobalt-catalyzed electroreduction is conducted in an undivided cell fitted with a zinc sacrificial anode. The second step is a palladium-catalyzed coupling of the obtained zinc species with vinyl or aryl dihalides (Scheme 6).<sup>109</sup>

The electrochemical preparation of PPV was followed by *in situ* internal reflection FTIR, and the behavior of the film was analyzed by EQCM experiments. It was possible to demonstrate by IR that traces of water have a negative effect on the quality of the PPV film (even if some reports<sup>110</sup> suggest the use of 0.2% water during the electropolymerization process).<sup>111</sup> As previously mentioned, DMF was an adequate solvent for the electropolymerization. Moreover, the same technique demonstrated that the polymerization and charging of PPV was easier using tosylate than  $\text{BF}_4^-$  ions. EQCM showed that, during the cathodic charging–discharging process of PPV films, the mass of the material changes due to cation insertion and release in order to maintain electro-neutrality.<sup>112</sup>

In order to gain more insight into the formation mechanism proposed by several groups, *in situ* spectroelectrochemical UV–vis and RRDE (rotating ring disk electrode) studies of the initial stages in the reductive polymerization of PPV in DMF were carried out using as starting material tetrabromo-*p*-xylene (TBPX).<sup>113</sup> These experiments revealed the oxidation of  $\text{Br}^-$  at +1.2 V on the ring electrode, with the associated oxidation currents dependent on the negative potential used for reduction of TBPX. The results obtained from electrochemical and UV–vis experiments led to the conclusion that splitting of bromine from TBPX occurs in two reduction steps in the range between −1.4 and −1.6 V. Two bromide ions were cathodically removed, producing the proposed brominated quinonidemethane intermediates, whose presence was confirmed in the UV–vis spectrum. Beyond −1.6 V, PPV oligomeric chains were formed and precipitated at the electrode surface, giving the typical UV–vis response of the PPV polymer.

PPV films deposited on Pt electrodes by electrochemical polymerization were studied during the p- and n-doping process in different electrolytes with *in situ* resonant Raman, optical absorption, and ESR spectroscopy (Figure 8). The experiments clearly demonstrate the possibility of having mobile radical species as the charge carriers in both types of doping.<sup>114</sup> The Raman spectra obtained were very similar in all the n-doping and p-doping experiments, even with different electrolyte salts. These results indicate that the reversible Raman responses of PPV originate mainly from perturbations within the polymer chains and that the same structural modification occurs in both charged states. These changes were attributed to the reversible change of benzenoid (undoped) to quinoid (doped) structures of the aromatic moiety.<sup>115</sup>

### 3. Charging–Discharging of Conducting Polymers

#### 3.1. Redox Properties of Oligomers and Polymers

Doping processes typically lead to charging of conducting polymers. As already mentioned, this doping corresponds to an electrochemical oxidation in the case of p-doping and to a reduction in the case of n-doping. Suitable redox reagents are either chemical electron acceptors, such as iodine and  $\text{FeCl}_3$ , or electron donors, such as potassium naphthalide; or the process may be electrochemically induced, using an electrochemical cell. Analogously to redox reactions in solution, polymeric chains in a film are negatively charged in the case of reduction and positively charged in the case of oxidation. To maintain electroneutrality, in the simplest

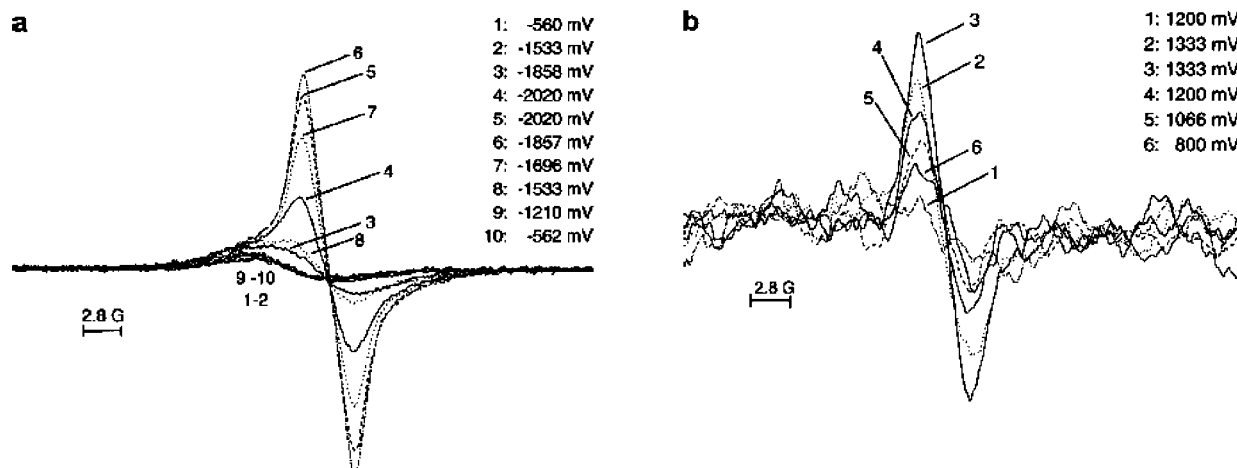


**Figure 8.** *In situ* ESR signals obtained during doping and undoping of PPV film: (a) n-doping; (b) p-doping. Reprinted with permission from ref 114. Copyright 2002 Springer.

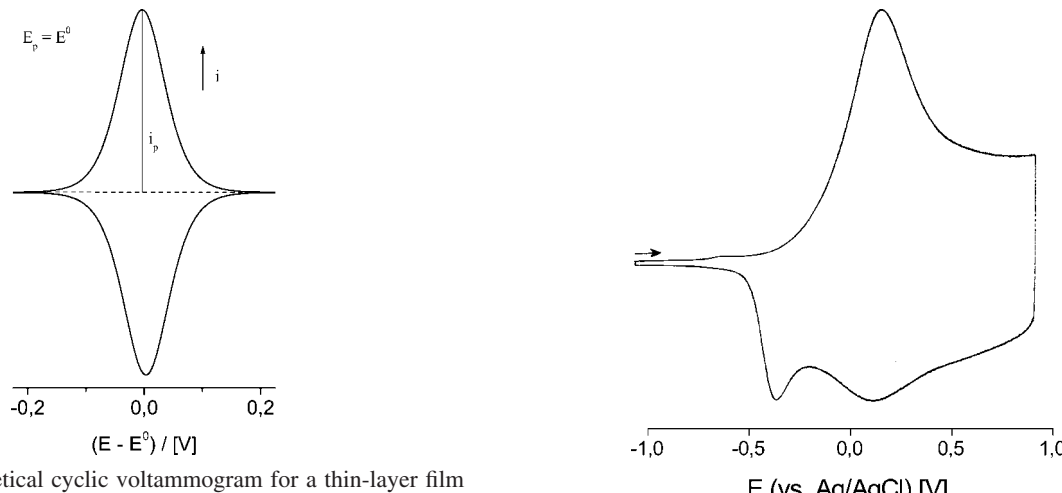


**Figure 9.** Theoretical cyclic voltammogram for a thin-layer film with one redox center.

case, counterions diffuse into the film during charging and out of the polymer during discharging.

The most popular electrochemical technique used to monitor such charging processes is cyclic voltammetry. Theoretical concepts that describe the voltammetric response during charging and discharging of redox-active thin films were developed more than three decades ago.<sup>116,117</sup> In the case of a simple one-electron transfer, reversible cyclic voltammograms (CV<sub>S</sub>) should show completely symmetrical and mirror-image anodic and cathodic waves with identical peak potentials and current levels (Figure 9).

The current in the reversible case is then (eq 3):

$$i = \frac{n^2 F^2 A \Gamma_T \nu \exp \theta}{RT(1 + \exp \theta)^2} \quad (3)$$

where  $\theta = (nF/RT)(E - E^0)$  and  $\Gamma_T = \Gamma_0 + \Gamma_R$  correspond to the total surface covered with reduced and oxidized states. Apart from the mirror symmetry of the waves it is also characteristic that, in contrast to measurements obtained with soluble redox systems, the current  $i$  and the scan rate  $\nu$  are directly proportional to each other. In principle, the above rules are valid only for monomolecular layers. With a large increase of film thickness, diffusion sets in during electrochemical charging/discharging and as a consequence the voltammetric response gradually shifts from mirror symmetrical diagrams to the classic, asymmetrical shape with  $i$

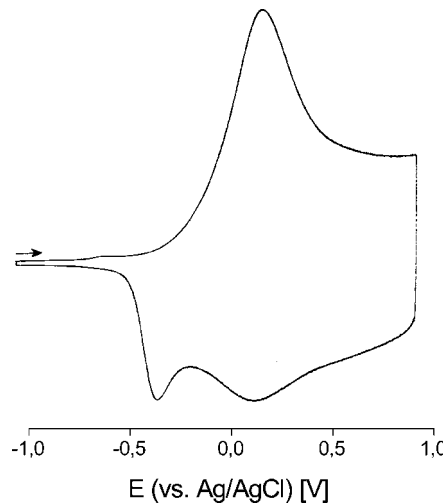


**Figure 10.** Cyclic voltammogram of the oxidation of poly(4,4'-dimethoxybithiophene) in  $\text{CH}_2\text{Cl}_2/0.1 \text{ M TBAPF}_6$ ,  $T = 273 \text{ K}$ ,  $\nu = 200 \text{ mV} \cdot \text{s}^{-1}$ .

proportional to  $\nu^{1/2}$ . Generally, there are fundamental differences between simple one-electron redox processes of redox polymers and those of conducting polymers. Characteristic features of voltammetry of conducting polymers are a steep anodic wave at the start of charging, followed by a broad and flat plateau as potential increases. In the reverse scan a potential-shifted cathodic wave appears at the negative end of the capacity-like plateau (Figure 10).<sup>118,119</sup>

Detailed information about the correlation between redox states and structure was obtained by measurements of charging/discharging properties of well-defined, monodisperse oligo(*p*-phenylenevinylenes) in solution and under solid-state conditions (Figure 11).<sup>21,120</sup> The analysis of the reduction data showed that the number of accessible redox states increases with increasing chain length of the system, resulting in the superposition of redox states over a broad potential range for long chain lengths. Therefore, the controversial capacity-like plateau which generally appears in voltammograms of CPs can be shown to refer to faradaic redox processes. Moreover, the voltammetric signal of the steep anodic wave at the beginning of the charging certainly belongs to a close superposition of several redox states, probably up to a level of tetracations or even more for longer chains. In the case of oligo(*p*-phenylenevinylene) with six phenylenevinylene units, at least seven redox states can be

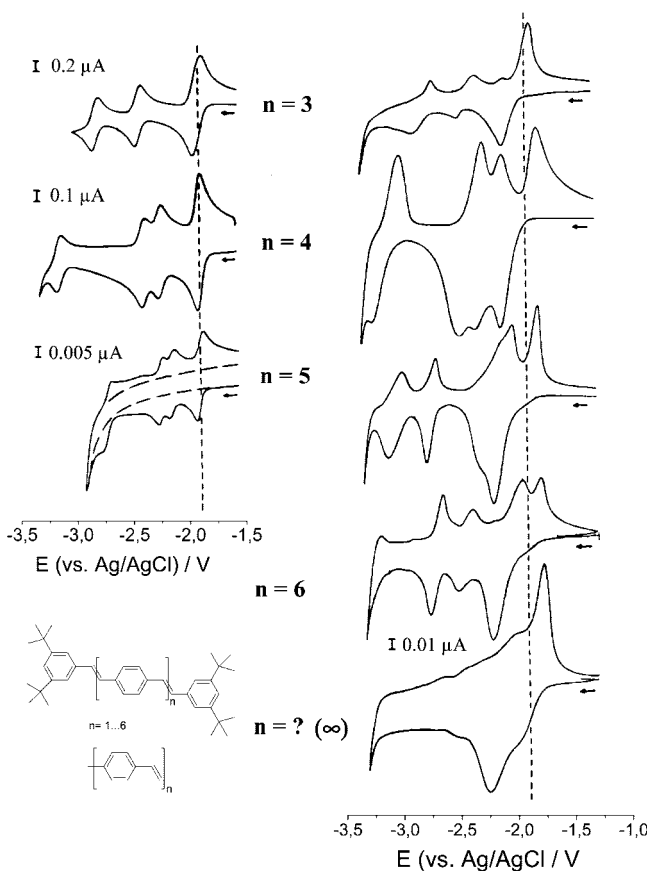
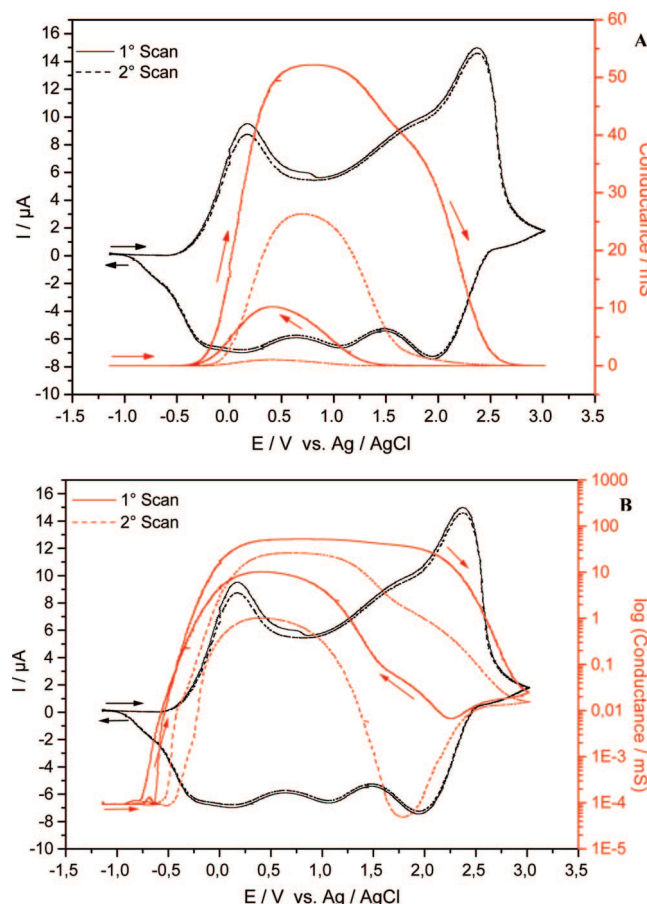


**Figure 11.** Cyclic voltammograms of the reduction of (left) oligo(*p*-phenylenenevinylene)s in solution ( $T = -65\text{ }^\circ\text{C}$ ,  $v = 100\text{ mV}\cdot\text{s}^{-1}$ ) in THF/TBAPF<sub>6</sub>, and (right) under solid state conditions ( $T = -65\text{ }^\circ\text{C}$ ,  $v$  between 10 and 50  $\text{mV}\cdot\text{s}^{-1}$ ) in DMA/TBABr. Reprinted with permission from ref 120. Copyright 1994 Wiley-VCH.

found in the potential range between  $-2.0$  and  $-3.0$  V. The fact that the polymeric material is normally polydisperse additionally favors the superposition of redox states.

These findings clarify that the electrochemical charging process of conducting polymers should be described by a sequence of discrete but overlapping redox steps. This implies that a model at the molecular level fits best the redox properties of conjugated materials. A band model (Figure 14), as favored by physicists, seems to be unlikely.

An approved method to describe the charging or doping level of CPs is the mole fraction of the corresponding monomers that are charged. The optimum doping level for PPy or PTh is about 0.33 but can have very much lower values. This depends, *inter alia*, on the structure and the applied charging potential but is also influenced by environmental parameters such as the solvent or supporting electrolyte.<sup>33,121</sup> From the respective doping levels, one can deduce that, upon oxidation of PPy, and often on that of PTh as well, every third or fourth heterocycle is charged, whereas in the case of PPP, provided that the experiments take place in common solvents such as propylene carbonate, only every sixth monomeric unit is charged.<sup>122</sup> Moving to a higher doping level, e.g. 0.5, a charge is forced in every second monomeric subunit, which, of course, induces a Coulombic repulsion. Therefore, to achieve this, a higher electrode potential must be applied, normally resulting in overoxidation effects.<sup>123</sup> Through the overoxidation process, a degradation of the polymer occurs, often induced by nucleophilic solvents such as water or nitriles. Therefore,

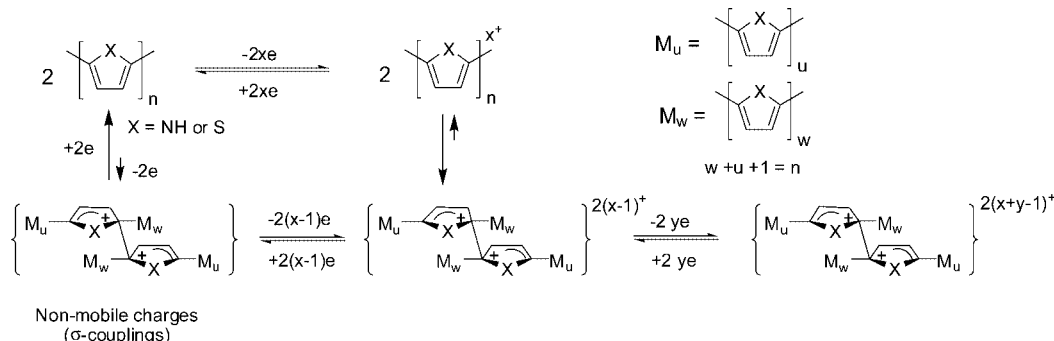


**Figure 12.** Cyclic voltammetry and *in situ* conductance measurements of poly(4,4'-dimethoxybithiophene) in  $\text{CH}_2\text{Cl}_2$ , 0.1 M TBAPF<sub>6</sub>,  $v = 5\text{ mV}\cdot\text{s}^{-1}$ ,  $T = 273\text{ K}$ . Black line, cyclic voltammogram; red line, conductance as function of potential measured during the potentiodynamic cycling; (A) linear scale representation of conductance; (B) logarithmic scale representation of conductance.<sup>125</sup>

overoxidized materials can be discharged only to a limited extent, which is a serious drawback for applications. In principle, a doping level of 1 should be possible, such that every monomeric unit bears a positive charge after doping. Up to now, only the very stable poly(4,4'-dimethoxybithiophene) system<sup>124</sup> has been charged up to this doping level. A characteristic feature of such a perfectly charged system is that the faradaic current drops to zero after passing the highest available redox state (Figure 12). This gives evidence that the capacity-like plateau results from a faradaic process.

All these data complement experimental and theoretical results already presented in the older literature.<sup>126,127</sup> The following general trends have been established for chainlike conjugated oligomers and polymers as a function of increasing chain length.<sup>128,129</sup>

- Redox states of identical charge (e.g., mono- or di-ion) shift toward lower energies. For long chains, the energies of low redox states gradually approach a common convergence limit.
- Adding successive monomeric subunits in the molecular chain enlarges the number of accessible redox states.
- The energy gap widens considerably between the lowest and the highest charged states.
- The number of redox states is limited and does not exceed the number of monomeric subunits in a chain.

**Scheme 7. Charging–Discharging of Conducting Polymers with Formation of Interchain  $\sigma$ -Couplings<sup>a</sup>**

<sup>a</sup> The exact position where the  $\sigma$ -coupling occurs has not been determined with precision.

- The chemical stability of charged species related to the same redox states increases, and therefore, the tendency for follow-up reactions decreases.<sup>130</sup>

A further characteristic of voltammetric experiments with CPs is the conspicuous separation between the wave of anodic charging and cathodic discharging (hysteresis) (Figures 6, 7, and 10 vs Figure 9). It was initially interpreted as a kinetic effect of slow heterogeneous charge transfer<sup>9,131</sup> or conformational changes during charging.<sup>132</sup> As the potentials of the anodic and cathodic peaks are virtually independent of the scan rate, Feldberg and Rubinstein<sup>133</sup> offered another explanation. In their opinion, the hysteresis is not due to a classical square scheme involving heterogeneous and homogeneous kinetics but due to N-shaped free energy curves as a consequence of phase transitions in the polymer. Recently, another concept has been developed based on the existence and stability of charged  $\sigma$ -dimers.<sup>33,98,134</sup> As already shown, these intermediates are formed within each coupling step during polymerization and their stability increases as a function of chain length (Scheme 2). Finally, depending on the structure of the (chainlike) system, the proton elimination stops and the  $\sigma$ -coupled chains remain as part of the charged polymer. The key hypothesis is that the charged interchain structure slowly decays at the end of discharging and forms again during charging. However, the coupling step between the chains does not exclusively take place at the radical cation level, but also at a higher charging level where the reactivity of the system is sufficiently high. The significant hysteresis between charging and discharging results from the fact that the interchain  $\sigma$ -dimeric carbocations (or carbanions) are energetically stabilized and decay at more negative (or positive) potentials than that at which the oxidation (or reduction) of the neutral polymers occurs (Scheme 7). The structure of these interchain  $\sigma$ -dimers is unclear. Recent studies have shown that dimerization reactions may take place even at positions that are blocked by substituents and do not contain any protons.<sup>135</sup> Sterical factors such as bulky substituents may confine coupling reactions during charging.<sup>136,137</sup>

In the literature, the  $\sigma$ -model has been controversially discussed.<sup>138</sup> It seems that dimerizations ( $\sigma$  or  $\pi$ ) are more or less accepted for oligomers up to chain lengths of 10 units. For longer oligomers and “real” polymers such as PPy or PTh, it has been proposed that the probability of the formation of interchain ( $\sigma$  or  $\pi$ ) dimers, especially in solution, decreases and that during charging an intrachain coupling may take place.<sup>138</sup> These previous studies totally neglect that the reactivity of CPs increases at higher redox states<sup>96</sup> and that intermolecular dimerizations are second-order reactions and are favored under solid state conditions.

In the electrochemical literature the description of charging conducting polymers is still dominated by the bipolaron model which has been introduced by Brédas in the field of CPs in the 1980s.<sup>139,140</sup> The model was originally constructed to characterize defects in inorganic crystalline solids. In chemical terminology, bipolarons are equivalent to diionic states of a system ( $S = 0$ ) after oxidation or reduction from the neutral state. The transition from the neutral state to the bipolaron takes place via the polaron state (= monocation,  $S = 1/2$ , ESR signal) and, thus, corresponds sequentially as well to redox transitions observed in two-step redox systems. In contrast to normal redox processes, however, additional local distortions occur in the chain during the charging of the polymer. Already in the first step, the formation of polarons, there is a gain of relaxation energy  $E_{\text{rel}}$ . This is released by structural relaxation after ionization, for which a vertical Franck–Condon-like ionization energy  $E_{\text{IP-V}}$  is necessary.  $E_{\text{rel}}$  corresponds to the bonding energy of the polaron. The structural relaxation causes a local distortion of the chain in the vicinity of the charge, whereby the twisted benzoid-like structure of the affected segments transforms into a quinoid-like structure in which the single bonds between the monomeric units shorten and assume double-bonding character. Removing a second electron from the polymer segment results not in two polarons but in the bipolaron, which is predicted to be energetically more favored than the polaron (Figure 13). The reason for this lies in the respective structural relaxations: that for the bipolaron is considerably greater than that for the polaron. The ionization energy required to remove a second electron decreases, or the electron affinity for taking up a second electron increases. In addition, it is assumed that the locally distorted bipolaron state comprises only four or five units of a chain segment. The energy gain of the bipolaron compared to two polarons is said to be about 0.4 eV.<sup>140</sup> In terms of redox energies, this means that the redox potentials  $E^\circ_2$  for bipolaron formation should be significantly lower than the potential  $E^\circ_1$  for polaron formation. The model is based on the ideal assumption that the length of a chainlike well-ordered polymer is infinite, which results, as far as electronic properties are concerned, in a band structure. During charging, polaron and bipolaron states develop in the band gap region, which leads to characteristic optical transitions. It should be noted that a fully developed bipolaron state in a real polymer with approximately 60 units should comprise up to 16 energetically equivalent bipolarons, which corresponds to a charging level of 0.26. Experimental evidence of the validity of the bipolaron model is mainly based on optical findings. Theoretical calculations suggest three

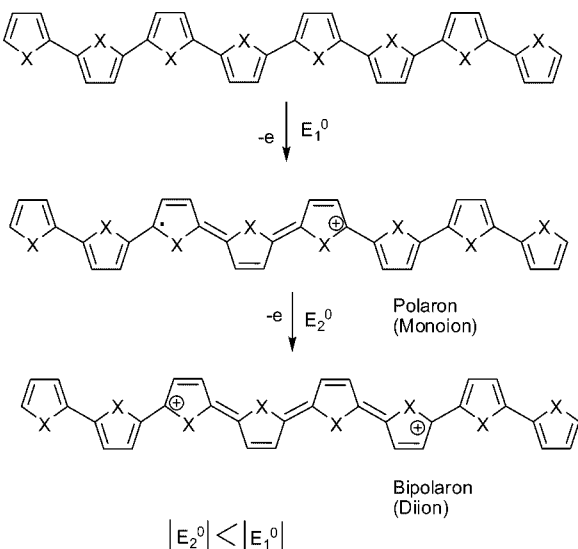


**Figure 13.** Formation of the bipolaron state in PPy or PTh upon oxidation: During charging of the polymer chain, the ionized states are stabilized by a local geometrical distortion from a benzoid-like to a quinoid-like structure. According to theoretical predictions, one bipolaron is thermodynamically more stable than two polarons despite the Coulombic repulsion between two similar charges.

absorption bands for the polaron and two for the bipolaron state<sup>141</sup> (Figure 14). These transitions have been experimentally observed in numerous absorption spectra of CPs.<sup>142</sup> On the other hand, it should be emphasized that the optical properties of extended mono- and dionic conjugated systems<sup>143</sup> can be described by simple quantum mechanical MO calculations at the molecular level.<sup>144</sup>

Studies of soluble oligomeric systems have shown that the bipolaron model is not universally valid. Therefore, new hypotheses, such as *two polarons (diradicals) in a singlet ground state*, have been introduced, which try to interpret phenomena outside of the classical approach.<sup>145,146</sup> An especially remarkable point is that this new interpretation is related to molecular systems but not to solid state phenomena. Additionally, real chain lengths lie between 30 and 60 units, conjugation lengths are rather short (5–20 units), and electrochemical as well as ESR studies<sup>120,147</sup> do not indicate any energetic stabilization of higher redox states. Thus, the reductive charging of oligomeric PPVs shows that tetraionic redox states can be generated which correspond to two “bipolaron states” (Figure 11), but a stabilization of these redox states has not been detected. Another argument against the validity of the bipolaron model is the fact that conductivity in highly doped polymers decreases drastically (Figure 12A).<sup>22,33</sup> A logarithmic plot of the conductivity (Figure 12B) accurately shows that its drop at high potentials coincides with the end of the faradaic charging process of the conducting polymer. According to the predictions of the model, the conductivity should increase at higher doping levels,<sup>140</sup> owing to a better overlap between the bipolaron and the valence band. Moreover, it is noticeable that the UV-vis spectra of short oligomers of thiophenes are very similar to those of polymers.<sup>148,149</sup> The long-wavelength transitions of oligomers are continuously shifted to lower energies as a function of increasing chain length. Only the intensities of the band increase, but the band shapes do not change on going from oligomers to polymers. This supports the view that CPs should be handled as molecular systems. Finally, the fact that solid state layers of electropolymerized conducting polymers are normally not crystalline but gener-

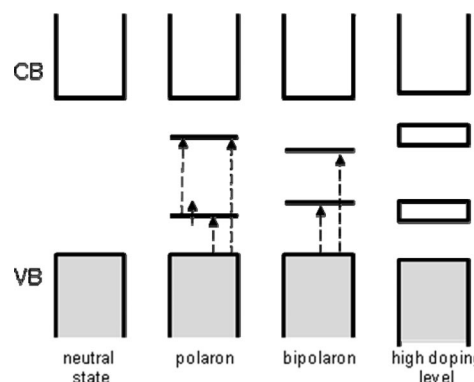


**Figure 14.** Band structures in conjugated polymers upon doping as proposed in the bipolaron model, and optical transitions for the polaron and the bipolaron state.

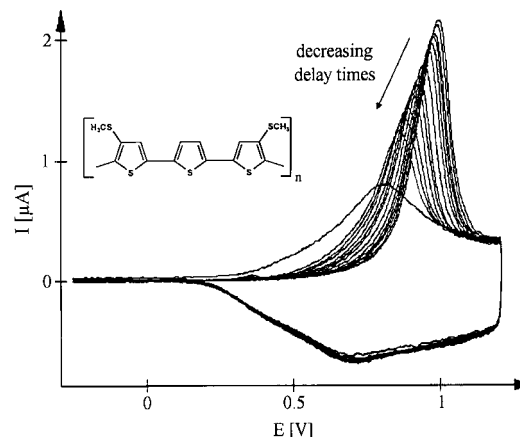


**Figure 15.** Memory effect of poly(4,4''-dithiomethyl-2,2',2''-terthiophene) in acetonitrile (0.1 M TBAPF<sub>6</sub>) for different waiting times  $\tau$  (top down): 30, 15, 10, 8, 6, 4, 2, and 1 min; 45, 30, 15, 10, and 5 s;  $v = 60 \text{ V} \cdot \text{s}^{-1}$ ,  $T = 298 \text{ K}$ , Pt disk electrode ( $r = 12.5 \mu\text{m}$ ).

ally form disordered amorphous structures also gives evidence of systems with small inner interactions. Theoreticians have, therefore, now suggested the application of a molecular picture for the description of optical and electronic properties of CPs.<sup>150</sup> A similar prior approach has been presented by Tolbert.<sup>151</sup>

A very unusual phenomenon that is often observed during charging/discharging of CPs is the so-called memory<sup>152,153</sup> or first cycle effect.<sup>154</sup> It implies that after a waiting time in the discharged state of a polymeric film the first voltammetric cycle differs markedly in shape and peak position from subsequent cycles. While the anodic wave of the very first cycle appears at relatively positive potentials and is normally both steep and sharp, all subsequent anodic scans show broadened waves which are significantly shifted toward negative potentials (Figure 15). Characteristically, the shape and position of the cathodic discharging waves remain unchanged during all cycles. Nechtschein et al.<sup>152</sup> were one of the first who described this phenomenon in the case of CPs. They also coined the phrase “memory effect” because the electrochemical response during charging of polymeric films depends on the history of foregoing electrochemical events. They initially assumed that, during charging/discharging of CPs, a rearrangement of the chain configuration took place, which was followed by the incorporation and extraction of counterions. Thus, during reduction, expulsion of counterions occurs from opened channels that get closed slowly as a function of waiting time. As a

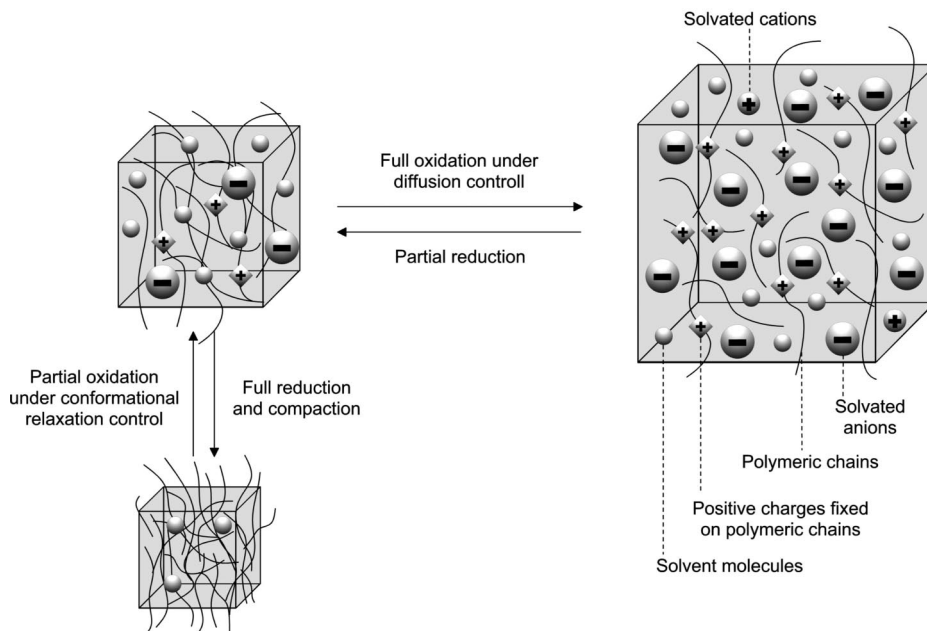


**Figure 16.** Schematic representation of the ESCR model; change of the matrix volume during charging/discharging of CPs. Adapted from ref 159.

consequence of this relaxation, the reoxidation requires increasing extra energy to reopen the channels. The relaxation processes can be extremely fast. Hapiot et al. have shown that, in the case of polyaniline, even after a very short waiting time of only 200 ms, a significant decrease of a high electron transfer rate between the film and the electrode occurs and disappears again within a few microseconds.<sup>155</sup>

The measurements showed that the shift of the first oxidation peak  $V_r(\tau)$  as a function of waiting time  $\tau$  toward more positive potentials can be described according to a logarithmic law (eq 4), where  $V_0$  is a constant potential at a given scan rate and  $a$  the slope of relaxation of the peak potential shift.<sup>155</sup>

$$V_r(\tau) = V_0 + a \log \tau \quad (4)$$

Memory effects have been observed in different materials, for example PPy, PTh, and PANI. They are a very general property of conducting polymers. In the meantime, several additional models have been developed which try to explain the effects. Zotti et al.<sup>156</sup> suggested an expulsion of solvent leading to shrinkage of the polymeric matrix. Several authors have proposed ionic effects of the electrolyte. Aoki introduced a percolation model,<sup>157</sup> showing that redox switching includes the propagation of a conductive front within the polymer film perpendicularly to the electrode, segregating the polymer in a conducting and insulating phase. At a well-characterized potential, a percolation threshold occurs at which the conversion rate from the insulating to the conducting phase reaches its maximum. Simulations reveal that this threshold approximately corresponds to the peak potential of the first cycle.

Based on the ideas of Nechtschein, Otero et al.<sup>158,159</sup> have developed the so-called ESCR model (electrochemically stimulated conformational relaxation). It assumes that application of an anodic overpotential to a neutral conjugated polymer causes, as a first step, an expansion of the closed polymeric structure. In this way, partial oxidation takes place and counterions from the solution enter under the influence of an electrical field the solid polymer at those points of the

polymer/electrolyte interface where the structure is less compact. This is the nucleation process. Then the oxidized sphere expands from these points toward the polymer/metal interface and grows parallel to the metal surface. The rate of this part of the overall reaction is controlled by a structural relaxation involving conformational changes of polymer segments and a swelling of the polymer due to electrostatic repulsions between the chains and to incorporations of counterions (see Figure 16).<sup>160</sup> The oxidation process is completed by diffusion of counterions through the already opened structure of the polymer. During reduction, opposite processes occur. The positive charges on the polymers are neutralized and counterions are expelled. Reverse conformational changes lead to a shrinking of the polymer. Diffusion of the counterions becomes more and more difficult, as the structure closes. The compaction of this closing step depends on the cathodic potential applied to the polymer and will be more efficient at more negative potentials. The compact structure hinders counterion exchange with the solution.

A quantitative expression for the relaxation time  $\tau$  needed to open the closed polymer structure is given by the following expression (eq 5):

$$\tau = \tau_0 \exp[\Delta H^* + z_c(E_s - E_c) - z_r(E - E_0)] \quad (5)$$

where  $\Delta H^*$  is the conformational energy consumed per mole of polymeric segments in the absence of any external electrical field, the second term  $z_c(E_s - E_c)$  is the energy to reduce, close, and compact one mole of polymeric segments with  $E_s$  = the experimental potential of closure and  $E_c$  = the compaction potential, and, finally, the last term  $z_r(E - E_0)$  represents the energy required to open the closed structure. ( $z_r$  = charge consumed to relax one mole of polymeric segments;  $\tau_0$  = relaxation time in the absence of any polarization effects). At first sight, the ESCR model seems to be reliable. However, a very important criticism is that according to this model the partial oxidation should start at the solution/polymer interface where no direct connection

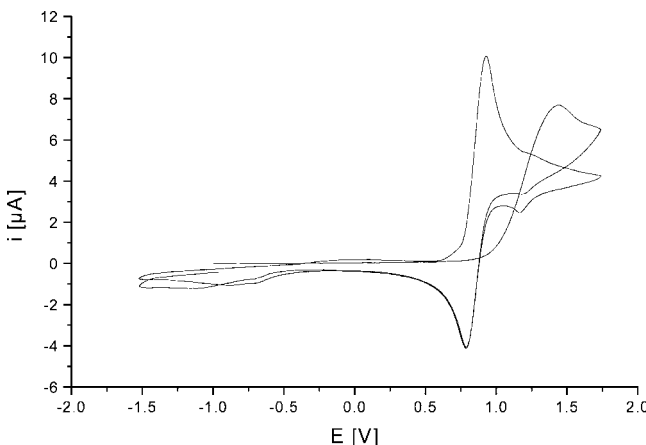


**Figure 17.** Cyclic voltammogram of the oxidation of *N,N*-dimethyl-*p*-toluidine ( $c = 1.5 \times 10^{-2}$  M) in acetonitrile ( $\text{CH}_3\text{CN}$ )/0.1 M TBAPF<sub>6</sub>,  $v = 10$  V s<sup>-1</sup>,  $T = 303$  K, 2,6-di-*tert*-butyl-4-methylpyridine  $c = 1.5 \times 10^{-2}$  M, showing the typical memory effect. Reprinted with permission from ref 161. Copyright 2006 Springer.

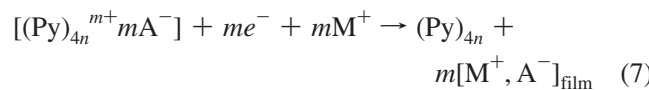
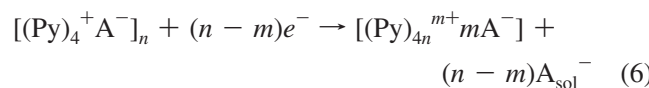
with the metallic electrode exists. That means that the actual electrode potential cannot be operative at the solution/polymer interface, which obviously excludes a driving force in that domain of the film. The work of Hapiot et al.<sup>155</sup> also contradicts the ESCR model because they have observed the memory effect in the “charged” state of polyaniline.

Very recently, Heinze reported<sup>161</sup> voltammetric experiments in which electroactive species, e.g. toluidine, in solution showed the phenomenon of a memory effect. After a waiting time of a few minutes in an acetonitrile solution, the first anodic wave of the oxidation of toluidine and other aromatic compounds was shifted to positive potentials whereas after passing the switching potential, all the succeeding anodic and cathodic waves indicated a normal reversible or quasireversible response (Figure 17).

According to the hypothesis of Heinze, during the negative polarization of the electrode, a passivating layer of polymeric acetonitrile is formed at the electrode surface, which hinders the heterogeneous electron transfer between electrode and electroactive species. During electrooxidation of the compound, this passivating layer is rapidly destroyed so that the electron transfer accelerates up to a normal rate. A similar scan dependence of the first cycle is observed in the case of conducting polymers after a long waiting time at negative potentials. Using ionic liquids as solvents, no memory effect has been observed.<sup>162,163</sup> This could also suggest that only specific solvents such as acetonitrile induce the memory effect.

An important point is that during charging and discharging of CPs, the principle of electroneutrality must be fulfilled. Consequently, in charged polymers that have been freshly anodically prepared using a potentiostatic or galvanostatic technique, anions must compensate the positive charges within the polymeric chains. However, spectroelectrochemical studies,<sup>164</sup> electrochemical quartz crystal microbalance (EQCM) measurements,<sup>165–168</sup> and SIMS and XPS measurements<sup>169,170</sup> on the mechanism of ion transport during charging and discharging of conducting polymers prove that discharging involves not only the expulsion of anions but also the incorporation of cations (eqs 6 and 7). In the case of small anions, this cation exchange mechanism is surprising. In the literature, one can find different explanations for this effect. Bruckenstein and Hillman<sup>171</sup> suppose that the mass exchanges

influenced by the mobility of the ions are kinetically controlled and that, on short time scales during reduction, cation entry competes effectively with anion expulsions as a means of satisfying film electroneutrality. In a recent paper, they hold the view that in permselective CPs, such as PEDOT, solvent is ejected during the initial phase of charging and incorporated at the end of discharging.<sup>172</sup> They assume changes in the polymer structure as reason for these processes. Heinze et al.<sup>33,173</sup> propose that the anion mobility depends on the structural peculiarities of doped polymers.  $\sigma$ -Dimers, which are formed at the beginning of charging, initiate immobile, localized charges that, in turn, impede the movement of anionic counterions. As a consequence, during the first part of discharging, mobile anions slowly diffuse out of the film; in the second part, cations are incorporated into the polymer, forming ion pairs with the immobile anions.



Using polymeric or large anions during electropolymerization, a pure cation transport generally results at a low charging level. This has been confirmed by *in situ* monitoring of the mass change during electrochemical switching using a quartz crystal microbalance.<sup>174</sup>

### 3.2. Specific Phenomena of n-Doping

In principle, electrochemical reduction (n-doping) of CPs is similar to that of oxidation (p-doping). However, there are only a few examples such as polyacetylene<sup>175</sup> or polyphenylenevinylene<sup>120</sup> systems (Figure 11), which present the characteristic charging/discharging behavior involving a peak-shaped reduction wave and a current plateau during cathodic reduction. At least two factors contribute to this situation. First, anodic charging of many CPs starts at potentials lower than +0.5 V vs Ag/AgCl. As the gap between oxidation and reduction of neutral CPs normally amounts to more than 2.5 eV, their reduction processes occur at potentials more negative than -2.0 V. Thus, the reduction of PPy with a first oxidation potential of approximately -0.9 V has never been observed, and the reduction of PTh and its derivatives starts at potentials lower than -1.7 V.<sup>176</sup> Second, the very negative reduction potentials of CPs exclude the application of many solvents as electrochemical reaction medium. Therefore, it is not surprising that typical voltammetric measurements show only the beginning of reduction, predominantly observed in the case of thiophene-based films.<sup>177–179</sup> A characteristic phenomenon that very often appears in the case of n-doping (after a preceding p-doping cycle) is so-called *charge* or *ion trapping*. It implies that the charge injected at a given potential is recovered, at least in part, at a different potential in the reverse scan (Figure 18). Zotti et al.<sup>180</sup> suggested that this effect could be related to irreversible chemical modifications of the polymers, such as the generation of quinone-like redox states. Zanelli et al.<sup>181</sup> assume that the negative charge injected in the polymer delocalizes in a wider region of the material.

In the case of PEDOT charging, Hillman et al. could show that ion trapping occurs during consecutive p- and n-doping

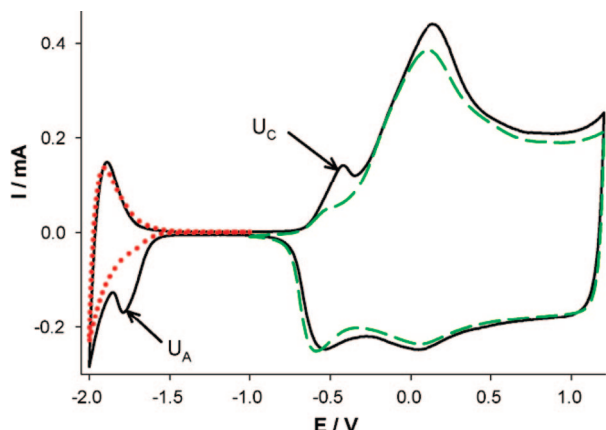


**Figure 18.** Cyclic voltammetry of a PEDOT film in 0.1 M TEABF<sub>4</sub>/CH<sub>3</sub>CN: responses of film cycled through both n- and p-doping regions (black line); through the p-doping region (green line); and through the n-doping region (red line). Reprinted with permission from ref 182. Copyright 2008 Elsevier.

cycles (Figure 18).<sup>182</sup> They present the plausible hypothesis that the discharging processes of this polymer are incomplete and regions of conducting material and associated anions/cations are isolated within an insulating matrix of undoped polymer. Using this model, kinetic control at the completion of the undoping process must be assumed, which may be caused by changes in the polymer structure.

### 3.3. Conductivity in Charged Systems

The most prominent feature of conjugated polymers is their conductivity in the *highly doped* state. The neutral form of CPs is insulating. Conductivity develops during charging of a polymeric film. Under *in situ* conditions, it increases sigmoidally as a function of the potential and reaches a plateau where very often, up to doping levels of 0.4, no further changes are observed (Figure 19).<sup>33,183</sup> Conducting polymers are semiconductors. Maximum conductivities lie in the range between 100 and 300 S·cm<sup>-1</sup> but may reach values higher than 1000 S·cm<sup>-1</sup>.<sup>184,185</sup> These values have been obtained using a four probe technique. In electrochemistry, the potential dependence of the conductivity of polymers can be measured using a microarray electrode

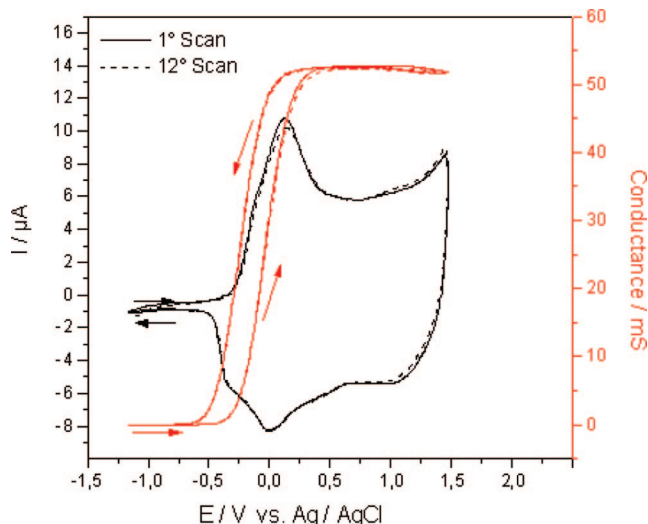


**Figure 19.** Cyclic voltammogram and typical sigmoidal change of the relative conductivity of poly(4,4'-bithiophene) in CH<sub>2</sub>Cl<sub>2</sub>, 0.1 M TBAPF<sub>6</sub>,  $v = 5$  mV·s<sup>-1</sup>.<sup>125</sup>

covered with conducting polymers and operated in a transistor-like configuration.<sup>22</sup> The maximum conductivities obtained under these conditions range between 10<sup>-2</sup> and 10<sup>-4</sup> S·cm<sup>-1</sup>. A disadvantage of these *in situ* experiments is that the conductivities are measured via the drain current, and their absolute values are not known and must be determined using an imprecise standard.

The mechanism of charge transport in electroactive polymers is still a matter of controversial debate. In the case of simple redox polymers, a mixed-valence conduction has been generally accepted, which is based on electron hopping between oxidized and reduced sites of a redox state.<sup>186,187</sup> The maximum conductivity should be observed when the amount of oxidized and reduced sites of a redox state is equal, which normally implies that a strong ESR signal appears. By contrast, conductivity measurements of CPs reveal that maximum conductivity arises at high doping, indicating that the charge carriers in that regime are spinless. At first sight, these findings are in excellent agreement with the predictions of the bipolaron model<sup>140,188</sup> (see section 3.1). It ideally assumes that spinless bipolarons could become mobile at high dopant concentrations, where the Coulomb attraction with counterions is largely screened. At very high charging levels, the bipolaron model predicts that the broadening of the bipolaron states in the gap leads to the merging of the lower and upper bipolaron bands with the valence band (VB) and the conduction band (CB), respectively. This effect produces a new unfilled VB band and, therefore, a transition to metallic-like transport properties. However, many experiments reveal that at “high” charging levels conductivity decreases (Figure 12). This may be due to degradation phenomena, but cyclic voltammetry indicates that almost all polymers which have been studied in a conventional potential range are stable during multisweep experiments.<sup>22</sup> In the literature, different explanations are presented. Wrighton assumes that in the very positive potential region localized charges are generated which minimize conductivity.<sup>22</sup> Zotti postulates that mixed valence conductivity operates between polaron and bipolaron states.<sup>189</sup> In addition, the influence of steric factors on the conductivity of CPs has been discussed.<sup>190</sup>

A very important point that has been often overlooked in the past concerns the question of whether the charge transport occurs intra- or intermolecularly. Within the original predictions of the bipolaron model, it has been assumed that charge transport takes place along single infinite long chains. However, the knowledge that the chain lengths of conjugated “polymers” are relatively short, ranging on average between 30 and 60 units, has led to the conclusion that the rate-determining transport step is intermolecular and should be described by a hopping process.<sup>191,192</sup> The bipolaron model is very popular within the community of (electro)chemists. A reason for this may be that it is based on chemical structures and the application of localized monoionic (= polarons) and diionic (= bipolarons) redox states. From the viewpoint of physicists, CPs may be considered as strongly disordered semiconducting materials. Their transport properties can be described by the variable range hopping model (VHR), where conduction occurs by hopping between electronically localized states in the band gap.<sup>193</sup>

A very helpful trendsetting experiment carried out by Heinze et al.<sup>194</sup> concerns conductivity measurements of a 3D hybrid network, in which hexathiophene oligomers form bridges between dendrimeric cores consisting of a polyphe-

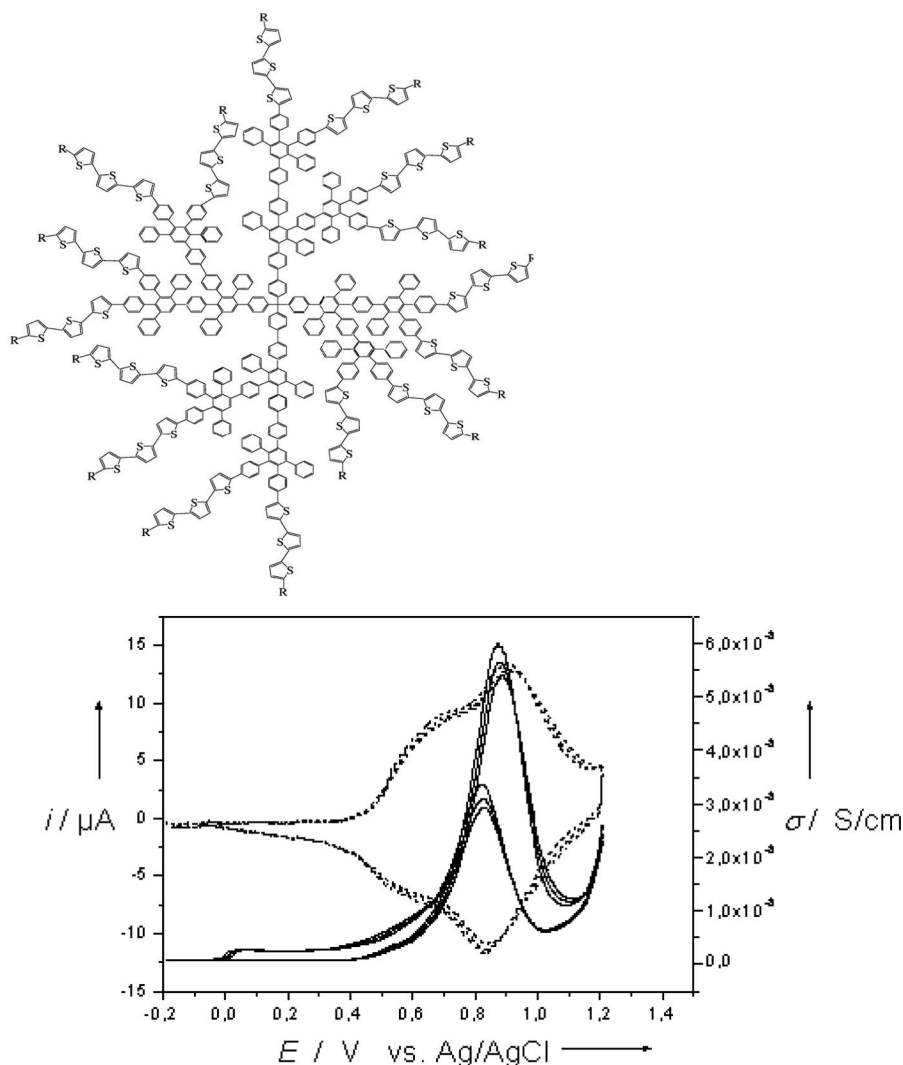


**Figure 20.** Terthiophene functionalized polyphenylene core dendrimer used as monomer,  $R = H$ . *In situ* conductivity measurement in the potential range between  $-0.2$  and  $1.2$  V. The film was generated in a solution of the dendrimer by electropolymerization, leading to the formation of hexathiophene bridges between the dendrimers (2 cycles between  $0.0$  and  $1.5$  V,  $v = 50$  mV·s $^{-1}$ ,  $c = 10^{-3}$  mol·L $^{-1}$  in  $\text{CH}_2\text{Cl}_2/\text{TBAPF}_6$ ), and measured in a monomer-free cell ( $\text{CH}_2\text{Cl}_2/\text{TBAPF}_6$ ,  $v = 5$  mV·s $^{-1}$ , room temperature). Reprinted with permission from ref 194. Copyright 2005 Wiley-VCH.

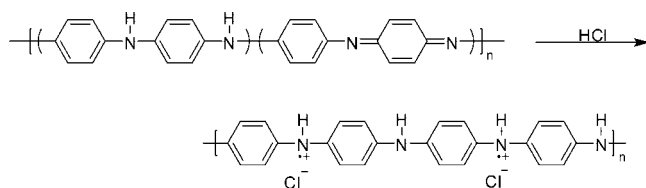
nylene system built around a tetraphenylmethane core. (For further discussion about special 3D structures, such as dendrimers, we refer to section 6.1). The monomeric dendrimer in the present example was a terthiophene functionalized polyphenylene (Figure 20). The *in situ* conductivity measurements of this network, obtained using an interdigital array<sup>195</sup> covered with the electrodeposited film, show an increase of the conductivity during voltammetric charging of the thiophene chains in the deposited material. However, this conductivity passes a maximum approximately at the half-charged level and drops to low values at higher potentials when all dicationic states in the hexathiophene chains are occupied.

In view of the bipolaron model, this finding is surprising, since bipolaron motion should exhibit a maximum of conductivity.<sup>140,188</sup> Better understanding of this behavior results when hopping processes are assumed similar to those observed in molecular organic radical ion salts<sup>196</sup> or in redox polymers. All experimental data obtained from conductivity measurements with radical ion salts reveal that a maximum of conductivity will be reached when only half the sites of a redox state are charged. In that case, the number of mobile charge carriers hopping intermolecularly between isoener-

getic sites approaches its highest value. The striking similarity between the increase and decrease of conductivity of these thiophene oligomers and those of radical ion stacks as a function of the charging level supports the assumption of identical conductivity mechanisms. The only difference is that radical ion salts are well-ordered crystalline materials in which the hopping processes of charges preferably take place along the stacks, while the dendritic networks are amorphous, leading to a three-dimensional charge transport. These results are also in perfect agreement with the model of Murray developed for redox polymers, that postulates maximum conductivity only in mixed valence states.<sup>187</sup> It seems that this principle is also valid in the case of many conventional conducting polymers.

During the initial period of charging, the number of mobile charge carriers increases drastically, but the formation of  $\sigma$ -dimers producing localized charges slows down this process. Within the plateau region of conductivity, successive and overlapping redox states are passed one by one. This means that the system always stands in a mixed valence state where electron hopping occurs between occupied and unoccupied sites of one redox state and the number of charge carriers remains almost constant. At the end of the charging

**Scheme 8. Proposed Mechanism of Protionic Doping of Emeraldine Base**



process (p-doping), all sites of the *last* redox state become empty and consequently conductivity drops down. Moreover, the hopping mechanism at half charging unequivocally proves that the rate determining step is the interchain electron exchange but not an intrachain mobility of polarons or bipolarons. Very recent studies of polymeric tetraphenylbenzidine systems have shown that the charge transport at both the monocationic and dicationic levels corresponds to one-electron interchain hopping processes.<sup>197</sup> All these findings favor the description of CPs on the basis of molecular systems.

It should be noted that the application of a linear scale for the evaluation of conductivity can be misleading because small changes are overestimated. It is advisable to use a logarithmic scale, which clearly reflects significant changes. In the case of voltammetric charging of poly(4,4'-dimethoxybithiophene), the logarithmic plot unequivocally documents that a very broad potential range of a high conductivity exists (Figure 12B) and that at the end of faradaic charging this conductivity strongly decreases, indicating the transition from a semiconducting to a nonconducting state. Surprisingly, the comparison of relative conductivities between p- and n-doped forms reveals that the values obtained during reductive doping are always considerably lower than those of oxidized forms.<sup>198–200</sup> A consistent explanation of this phenomenon is not available. Ahonen et al.<sup>201</sup> suggest that charge transport in the p-doping range occurs via polarons and bipolarons and free carriers, whereas the only charge carriers in the n-doping range are the negative polarons. Wrighton et al.<sup>199</sup> suppose that the higher conductivity of oxidized forms is associated with greater delocalization in broader bands. An additional reason for smaller conductivities during reduction may be the fact that bulky tetralkylammonium cations are incorporated into the polymer, which increases the hopping distance between the chains and, therefore, induces a lower conductivity.

Typical doping processes involve the partial oxidation or reduction of extended conjugated  $\pi$ -systems, leading to the generation of mobile charge carriers. However, in the case of polyaniline, the conductivity behavior is more complex and a new type of doping process has been introduced in the literature.<sup>14,202,203</sup> This is based on treating the emeraldine base of PANI with aqueous protonic acids (Scheme 8). It has been suggested that the complete protonation of the imine nitrogen atoms in emeraldine base results in the formation of a delocalized polysemiquinone radical cation and is accompanied by an increase in conductivity of about  $10^{10}$ . The most striking point is that the number of electrons associated with the polymer undergoes no change during the protonation. This process is known as “proton doping” of polyaniline.<sup>13,14</sup> Therefore, it has been postulated that the energy levels are rearranged during the *doping* process. However, in view of the discussion presented above, it is difficult to understand this conduction mechanism. All available redox states are fully occupied in the emeraldine

base. The only electrochemical change that occurs via protonation is a shift of the redox potentials to more positive values. Under these conditions, a partial reduction of the probe cannot be excluded during experimental manipulations.

#### 4. Controlling the Electropolymerization Process

A phenomenon that is typical of the electrosynthesis of CPs is the fact that the reproducible generation of materials exhibiting identical electrochemical and structural properties is difficult. Even small variations of experimental parameters such as temperature, formation potential, or concentration of the starting monomer creates significant changes of physical and chemical characteristics. At meetings and discussions, the slogan of the *challenging diversity* of CPs has been circulated again and again. The essential reason for this complex reaction pattern is based on the condition that each coupling step requires electrochemical activation (see section 2.1) and, moreover, the structure of the resulting polymer product depends on the selected experimental preparation method. Thus, both experimental parameters and the preparation technique determine the properties of the resulting polymers.

##### 4.1. Influence of the Polymerization Technique

Potentiodynamic (Figure 4), potentiostatic (Figure 5), and galvanostatic (Figure 21) polymerizations are the three most important techniques<sup>204</sup> that can be used to electrosynthesize a conducting polymer. Potentiodynamic polymerization (cyclic voltammetry) is characterized by a cyclic regular change of the electrode potential during the deposition of the conducting polymer onto the electrode. The growing polymer film—following the potential changes—continuously changes between its neutral (insulating) and its doped (conducting) states, which is accompanied by a continuous exchange of electrolyte and solvent through the freshly deposited polymer. This automatically provokes changes in the polymer matrix and favors the formation of disordered chains involving compaction and opening of the structure (Figure 16).<sup>159</sup> Moreover, during potentiodynamic cycling, conductivities of doped films decrease, which also indicates an increase of distances between chains.<sup>95</sup>

Conducting polymers made by potentiodynamic polymerization are generally obtained in their neutral state at the

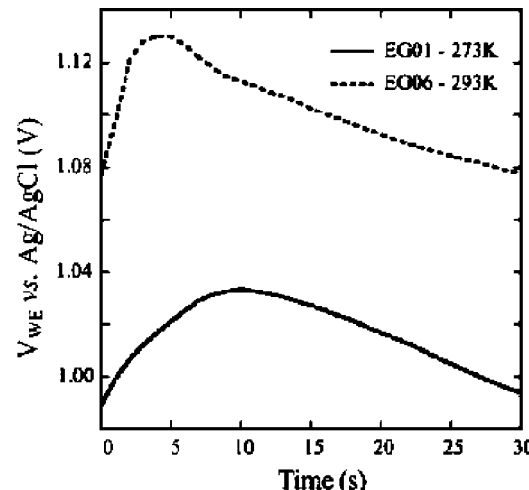


**Figure 21.** Galvanostatic electropolymerization of 0.5 M PPY at different temperatures in ACN and TPAPF<sub>6</sub> (0.5 M),  $J = 6.6$  mA/cm<sup>2</sup>,  $t = 30$  s.

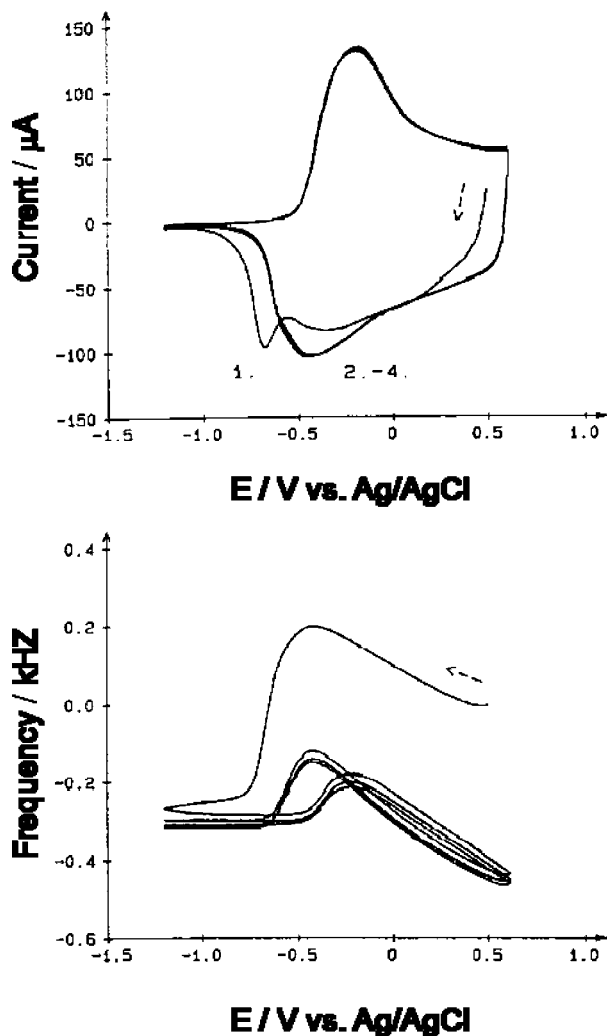


**Figure 22.** Multisweep cyclic voltammetry and EQCM measurements of a PPy film after potentiostatic polymerization ( $E_p = 0.8$  V) of pyrrole in propylene carbonate ( $c = 10$  mM,  $c(\text{LiClO}_4) = 0.1$  M,  $T = 298$  K); (a) CV,  $v = 20$   $\text{mV}\cdot\text{s}^{-1}$ , first cycle after polymerization; (b) frequency–potential plot.

end of the experiment, whereas potentiostatic and galvanostatic methods lead to polymers in their doped state. Their well-ordered polymer structures do not experience any changes after deposition and succeeding solid state reactions in both static methods. A characteristic example is polypyrrole, which has been galvano- or potentiostatically polymerized under mild conditions in PC/0.1 M LiClO<sub>4</sub>. Surprisingly, during the very first voltammetric discharge cycle, the reduction is significantly shifted to negative potentials and a strong mass increase proves an efficient cation insertion despite the fact that anions are small.<sup>166,205,206</sup> At low temperatures, this cation insertion completely dominates and is accompanied by a strong solvent insertion. In subsequent cycles, the cation effect and the correlated reduction shift significantly diminish (Figure 22). All these experimental findings support the mechanistic pattern developed by Heinze<sup>207</sup> for the formation of CPs. Using a potentiodynamic or galvanostatic preparation technique, the polymerization at low potentials ends in the formation of well-ordered  $\sigma$ -dimers, the first discharge of which occurs via an efficient cation insertion. In the case of a potentiodynamic polymerization, solvent molecules are incorporated into the polymer matrix during successive cycling and disordered structures involving defects and volume expansions are formed.

Due to the current control of the galvanostatic experiment, the overall polymerization rate is constant. However, at first glance, two phenomena are surprising (Figure 21). First, the resulting potential during the galvanostatic experiment is temperature dependent and shifts to lower values at decreasing temperatures. Second, at the beginning of the electropolymerization, the potential increases for a short period depending on the applied current density but decreases after a few seconds. In the case of the temperature dependence, the explanation is simple and is based on the fact that the solvent volume diminishes at lower temperatures and, therefore, the concentration of the starting monomer increases. The second phenomenon is more complex. As has been shown, the initial period of oligomerization involves the consumption of the starting polymer which leads to an increase of the potential. Almost simultaneously redox-active charged oligomers are formed in front of the electrode. They catalyze the oxidation of monomeric species which leads to a decrease of the potential after a few seconds.<sup>77</sup>

The potentiostatic method is characterized by strong changes in the current and the polymerization rate (Figure 5). Nevertheless, the results are in principle similar to those of the galvanostatic technique because the material that has been deposited is not discharged during polymerization.

Electropolymerization of PPy prepared by the galvanostatic or the potentiostatic technique leads to nonadhesive dendritic-type polymer films of low homogeneity. On the other hand, films obtained using cyclic voltammetry are shiny black and very adhesive and have a smooth and homogeneous surface.<sup>208</sup> This experimental observation can be related to a larger number of equivalent nucleation sites during the growth process present in the potentiodynamic approach.<sup>209</sup>

While the morphological properties of the obtained films may differ significantly upon change of the electrochemical preparation technique, the underlying mechanism of the electropolymerization remains the same. López-Palacios et al. have for example studied the mechanism in detail for poly[4,4'-bis(methylbuthylthio)-2,2'-bithiophenes] (poly-MB-TBT) electropolymerized by the potentiodynamic and the potentiostatic technique.<sup>210</sup> From the absorption spectra of the electrogenerated oligomers, they could deduce that the mechanism must be similar. Electronic properties such as conductivity, mobility, number of free carriers, and band gap showed differences and were dependent on the polymerization method. In this respect, poly(3-methylthiophene) showed, for example, a better performance when potentiostatically polymerized compared to a potentiodynamically prepared material.<sup>211</sup> Therefore, for each monomer system, the optimal electrochemical technique must be tested to carry out an efficient CP electrosynthesis.

## 4.2. Influence of Experimental Conditions

In addition to the electrochemical method applied during polymerization, experimental parameters such as potential, solvent, and temperature are also important for the quality and the properties of CPs. In particular, the formation potential in a potentiostatic/dynamic, or the corresponding current in a galvanostatic, experiment determines the chain length and structure of CPs. Very high oxidation potentials or currents, which imply the generation of highly charged and reactive intermediates, lead to defects and the formation of cross-linked materials.<sup>95</sup> At low potentials, the oligomeric intermediates are weakly charged, and consequently, the electropolymerization may end at an oligomeric level. Figure

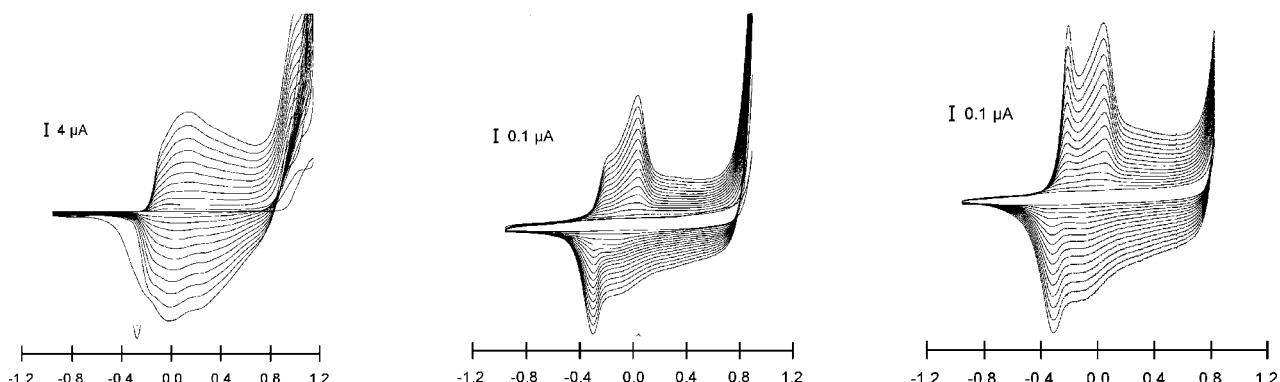


**Figure 23.** Potential dependence of potentiodynamic growth of PPy films. Nondegassed acetonitrile solution, 0.1 M pyrrole, 0.1 M TBAPF<sub>6</sub>, 1 wt % water,  $T = -20\text{ }^{\circ}\text{C}$ ,  $v = 100\text{ mV s}^{-1}$ . (Left)  $-1.12$  to  $1.13\text{ V}$ , 15 scans; (center)  $-1.12$  to  $0.88\text{ V}$ , 28 scans; (right)  $-1.12$  to  $0.83\text{ V}$ , 30 scans and scan range changed to  $-1.12$  to  $0.78\text{ V}$  for another 28 scans. Reprinted with permission from ref 212. Copyright 1999 Elsevier.

23 shows the cyclic voltammograms of the growth of PPy films, which differ only in the positive switching potential from  $1.13\text{ V}$  (left), to  $0.88\text{ V}$  (middle), to  $0.83\text{ V}$  (right).<sup>212,213</sup>

In addition to the normal wave of polypyrrole at  $E_p \sim 0.01\text{ V}$  vs Ag/AgCl, a new sharp oxidation wave emerged at potentials at about  $-0.23\text{ V}$  when the voltammetric switching potential was  $0.83\text{ V}$ . The same observations were made with polypyrrole synthesized at extremely low currents with the galvanostatic technique.<sup>173</sup> These data, in combination with spectroscopic results, provide evidence that at least two types of polypyrrole exist: the so-called PPy-I, with chain lengths up to 64 units, and PPy-II, with chain lengths between 12 and 16 units.<sup>98</sup> A cross-linked material referred to as Py-III is generated at potentials higher than  $1\text{ V}$  (Figure 23).

The second most important parameter during electropolymerization is the temperature. Its influence on the kinetics and the resulting properties of CPs is considerable. As already described, the polymerization is a multistep process in which each substep possesses its own activation energy. Therefore, at low temperatures, the rates of coupling steps and proton eliminations decrease. On the other hand, the thermodynamic equilibria between charged intermediates and corresponding dimers shift in favor of the coupling products due to entropic reasons and decreasing Coulombic repulsions between charged moieties.<sup>53</sup> Thus,  $\sigma$ -intermediates could be detected<sup>31</sup> and systems with shorter chain lengths are favored.<sup>98,212,213</sup> Obviously, low temperatures stabilize well-ordered structures and enhance conductivities of CPs.<sup>98,214–216</sup> For example, conductivities of PPy films generated at  $234\text{ K}$  reach conductivity values higher than  $1000\text{ S} \cdot \text{cm}^{-1}$ .<sup>217</sup> Moreover, despite the fact that the reaction rates slow down, the yield of deposited materials may increase because the solubility of oligomers decreases.<sup>92</sup>

Other factors that influence the polymerization process and the final properties of the generated CPs are solvents, additives (e.g., water, bases, acids), and electrolytes. In order to get an efficient polymer yield, solvents should possess a high polarity, which minimizes Coulombic repulsions during cationic coupling steps.<sup>61</sup> On the other hand, their nucleophilicity should be low. In the case of conventional solvents, it rises in the following order:  $\text{CH}_3\text{NO}_2 < \text{CH}_2\text{Cl}_2 < \text{PC} < \text{CH}_3\text{CN} < \text{H}_2\text{O}$ . Therefore, water can only be used for the generation of polymers for which the oxidation potentials of their monomers are low, e.g. pyrrole or ethylenedioxythiophene. Nevertheless, even for these systems, the electropolymerization process produces many defects due to nucleophilic attacks of water on the cationic intermediates.<sup>218</sup>

The most popular organic solvent is acetonitrile. However, it is not the best one for the preparation of CPs. Due to its low basicity—the  $pK_{\text{BH}}^+$  value of protonated acetonitrile<sup>219</sup> is about  $-10$ —superdry acetonitrile does not polymerize pyrrole. The reaction stops at the level of weakly acidic  $\sigma$ -intermediates of bipyrrole or, more likely, tetrapyrrole. A stronger base than acetonitrile must be used to initiate the elimination of protons. Water fulfills this condition. Pyrrole can be electropolymerized in acetonitrile in the presence of 1% water.<sup>32,33,220</sup> A similar effect results from the application of a sterically hindered base such as 2,6-di-*tert*-butylpyridine.<sup>46</sup> Solvents with a weak nucleophilicity, which can also be applied for monomers with high oxidation potentials such as benzene, are  $\text{CF}_3\text{COOH}$ , HF,  $\text{BF}_3$ -etherate,  $\text{SO}_2$ , and ionic liquids (see below). A disadvantage of these solvents may be that their handling is difficult or they are relatively expensive.

The influence of type and size of the electrolyte on the polymerization, the subsequent charging/discharging properties, and the morphology is considerable.<sup>221–224</sup> Thus, even the magnitude of conductivity of electrogenerated CPs is affected by counterions. For example, in the case of PEDOT and derivatives, the *in situ* conductivity decreases with the anion sequence  $\text{ClO}_4^- > \text{BF}_4^- > \text{CF}_3\text{SO}_3^- > \text{PF}_6^-$ .<sup>225</sup> Similarly, PEDOT films doped with monomeric (tosylate) or polymeric poly(4-styrenesulfonate) (PSS) counteranions, respectively, cover a wide range of conductivity values (4 orders of magnitude) from 450 (tosylate) to 0.03 (PSS)  $\text{S} \cdot \text{cm}^{-1}$ . Since their conjugated backbone is essentially the same and their optical and electrochemical properties are almost identical, the conducting behavior reflects the important role of counterions and proves dominant interchain processes.<sup>226</sup>

A detailed discussion of all these effects would go beyond the scope of this review. Nevertheless, one additional finding should be mentioned, because it principally highlights the complexity of counter- and co-ion movement in CPs during charging/discharging processes. The data concern polypyrrole films which have been electropolymerized under galvanostatic conditions in the presence of large poly(4-styrenesulfonate) (PSS) anions incorporated into the film to compensate the charges in the pyrrole chains.<sup>174</sup> Electrochemical quartz microbalance measurements conducted with these polypyrrole films during doping cycles in a normal electrolyte such as  $\text{NaClO}_4$  unambiguously show that at a low charging level only cations are inserted and released. By contrast, at a higher charging level in the so-called plateau region, only

anions ( $\text{ClO}_4^-$ ) are inserted/removed during potentiodynamic cycling.<sup>174</sup> This provides evidence that attractive interactions between polypyrrole chains and polymeric anions are very strong at a low charging level but weak at a higher level of more than 0.2. This result again supports the view that the charging/discharging processes in CPs are dominated by characteristic structural differences, which arise between the low and high redox states of the system. In our opinion, the  $\sigma$ -coupling model is strengthened by these observations.

### 4.3. Electropolymerization in Novel Electrolytic Media

#### 4.3.1. Electropolymerization in Microemulsion Media

Electropolymerization in aqueous media is an ongoing topic in the field of conducting polymers, because this solvent is ideal for nonpolluting large-scale applications. However, the low solubility of many of the organic starting monomers in water complicates their use in aqueous media. The application of microemulsions has opened a new way to solve this challenge. Microemulsions are systems that at least consist of three components: water, a hydrophobic organic material, and a surfactant.<sup>227</sup> They are generated by mixing the components, which then form a micellar solution thermodynamically stabilized by the amphiphilic surfactant. As the literature reveals, this solubilization procedure has been successfully applied to the electropolymerization of different CPs in aqueous media. Especially thiophene derivatives which are almost water-insoluble have been polymerized using the microemulsion technique,<sup>228–230</sup> but other monomers, such as pyrrole derivatives,<sup>231</sup> benzene,<sup>232</sup> or aniline,<sup>233</sup> have also been studied.

The most prominent material in this field is PEDOT,<sup>234–237</sup> which possesses extraordinary chemical and physical properties<sup>238</sup> and is commercially available. Due to the low solubility of its starting monomer in water ( $2.1 \text{ g} \cdot \text{L}^{-1}$  at  $20^\circ\text{C}$ ), an efficient oligomerization in aqueous solutions can only be achieved by the addition of surfactants. Thus, in the presence of nonionic polyoxyethylene-10-lauryl ether ( $\text{C}_{12}\text{E}_{10}$ ), a microemulsion system has been generated, in which the concentration of EDOT has been several times higher than that in an aqueous solution without surfactant.<sup>228</sup> Characteristic of all surfactants is the fact that the current density during electrooxidation increases markedly in the presence of micelles. In order to explain this behavior, a surfactant adsorption at the Pt electrode surface has been proposed. The opening of the micelles containing EDOT at the electrode surface during electropolymerization should speed up the rate of the reaction.

Another explanation of the catalytic effect is based on the observation that the monomer oxidation is shifted to lower values in micellar media. Systematic studies of the group of Lacaze have shown that the oxidation potential in anionic (sodium dodecylsulfate, SDS; sodium tetradecanesulfonate, STS) micellar solutions is lowered whereas no significant changes occur in cationic (cetyltrimethylammonium chloride, CTAC) as well nonionic (Triton X100) aqueous media.<sup>239</sup> According to Lacaze et al., this invariance of the monomer oxidation potential indicates that no or repulsive interactions took place between cationic or nonionic surfactants and the radical cations formed during the first step of the polymerization. In contrast, the variation of the oxidation potential in anionic micellar solutions demonstrates the existence of specific stabilizing interactions between anionic surfactants

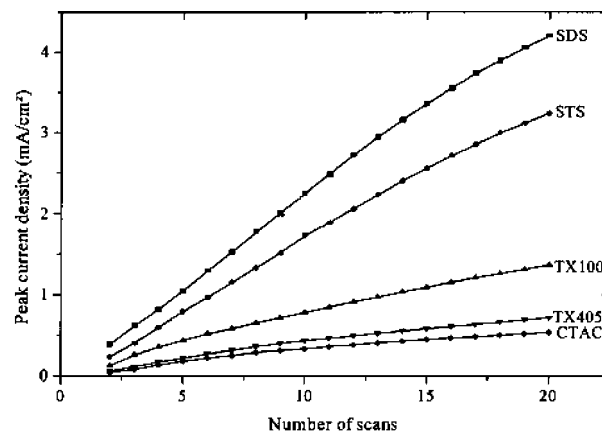


**Figure 24.** Electrochemical polymerization efficiency of 3-methoxythiophene in different micellar media (SDS, STS, TX100, TX405, CTAC). Reprinted with permission from ref 230. Copyright 2001 Elsevier.

and the reacting radical cations.<sup>230,234</sup> For example, the significant influence of different surfactants on the electrodeposition rate of 3-methoxythiophene has been analyzed via multisweep voltammetry. The plot of the anodic current density against the number of cycles (Figure 24) shows that the polymerization rate is considerably higher for anionic micellar media than for neutral and cationic ones. A general feature of polymer films generated in micellar solutions is that they are mechanically compact and are more stable than those obtained in organic media.

In addition to the microemulsion technique, acoustic emulsification has been used for the electropolymerization of suitable monomers in aqueous media. Ultrasonication of an immiscible mixture of the EDOT monomer and aqueous electrolyte produced stable surfactant-free emulsions, in which the generated microdroplets contain  $\text{LiClO}_4$ .<sup>240</sup> It was proposed that the electron transfer takes place between the electrode and monomer droplets, but not with the monomer dissolved in an aqueous phase. The polymerization proceeded smoothly, and the conductivity of the obtained films was in the typical range for PEDOT obtained by classical methodologies.

#### 4.3.2. Boron Trifluoride Etherate Catalyzed Electropolymerizations

During the past decade, boron trifluoride diethyl ether (BFEE)<sup>241</sup> has been used as a novel solvent–electrolyte system for electropolymerizing suitable monomers into CPs. Its main characteristic is the considerable lowering of the oxidation potential that is necessary for a successful electropolymerization. Pure BFEE is a strong Lewis acid which normally induces an additive polymerization resulting in a nonconjugated polymer. Hence, its acidity must be lowered by dissolving it in a coordinating solvent with a high donor number, such as acetonitrile (DN 14.1) or diethyl ether (DN 19.2).<sup>242</sup> It has been proposed<sup>242</sup> that in these solutions the weak interaction between the Lewis acid and an aromatic hetero- or carbocyclic monomer system reduces the aromaticity of the latter, facilitating its oxidation. The conductivity of BFEE in diethyl ether is relatively low and ranges between  $3 \times 10^{-4}$  and  $9 \times 10^{-4} \text{ S} \cdot \text{cm}^{-1}$ .<sup>241,243</sup> It is assumed that the conductivity in this electrolyte is based on the existence of polar molecules  $[(\text{C}_2\text{H}_5)_3\text{O}^+]\text{BF}_4^-$ ,<sup>244</sup> providing enough ions to produce a conducting medium. Another explanation for the conductivity of this medium is related to the complexation

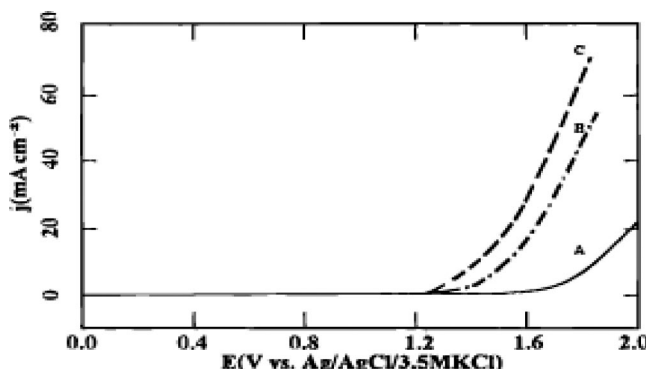


**Figure 25.** Voltammetric curves for the oxidation of thiophene (0.1 M) in (A)  $\text{CH}_3\text{CN}/\text{NEt}_4\text{ClO}_4$ , (B)  $\text{CH}_3\text{CN}/\text{AlCl}_3$ , and (C) BFEE;  $v = 10 \text{ mV}\cdot\text{s}^{-1}$ . Reprinted with permission from ref 242. Copyright 1997 American Chemical Society.

of low quantities of water, which generate  $\text{H}^+\text{BF}_3\text{OH}^-$  species that behave as electrolyte.<sup>245</sup>

The first polymer synthesized using BFEE as solvent–electrolyte system was polythiophene.<sup>246</sup> Thiophene and derivatives substituted with electron-withdrawing groups require high oxidation potentials in organic solvents up to 1.8 V vs Ag/AgCl, which lead to low quality polymers due to side reactions between cationic intermediates and residual water, the solvent, and/or the electrolyte anions. In addition, irreversible overoxidation of the electrodeposited conducting polymer may occur at these high potentials. This phenomenon is called the “thiophene paradox”: at the high potential necessary for the formation of the polymer, the material is overoxidized concurrently with its deposition.<sup>247</sup> The use of BFEE eliminates this problem by a shift of the onset of oxidation of thiophene from 1.65 to about 1.1 V vs Ag/AgCl (Figure 25).<sup>242,246</sup> Using this electrolytic medium, PTh can be electrochemically electropolymerized onto various noble and non-noble metallic substrates such as platinum, stainless steel, aluminum, titanium, nickel, zinc,<sup>248</sup> and p- or n-type silicon<sup>249</sup> without corrosion of the metallic support. A further advantage of this procedure seems to be that mechanically stable free-standing films can be easily generated.

In addition to thiophene-based polymers such as poly(bromo-thiophene)<sup>250,251</sup> or poly(chlorothiophene),<sup>243</sup> numerous other CPs have been prepared in the presence of BFEE. In particular, this strategy has been applied to many of those monomers that are difficult to oxidize, e.g. benzene,<sup>248</sup> furan,<sup>252–254</sup> benzofuran,<sup>255</sup> anthracene,<sup>256</sup> or 5-bromoin-dole.<sup>257</sup>

An interesting point is that the application of mixed electrolytes, e.g. BFEE and trifluoroacetic acid (TFA), increases the conductivity of the electrolyte significantly from  $1 \times 10^{-3}$  to  $5 \times 10^{-3} \text{ S}\cdot\text{cm}^{-1}$  and, additionally, shifts the onset of oxidation about several hundred millivolts to lower values.<sup>243</sup> Thus, the oxidation of 3-chlorothiophene begins in acetonitrile at 2.18 V vs SCE, in BFEE at 1.54 V, and in a mixture of BFEE and TFA at 1.16 V. Simultaneously, the charging/discharging behavior becomes more reversible (Figure 26) and the mechanical properties of free-standing films, e.g. the tensile strength, approach those of metals (Al foil).<sup>248</sup>

#### 4.3.3. Electropolymerization in Ionic Liquids

Electropolymerization using ionic liquids (IL) as electrolytes is a very promising method for preparing conducting polymers with enhanced optical and electrical properties. ILs

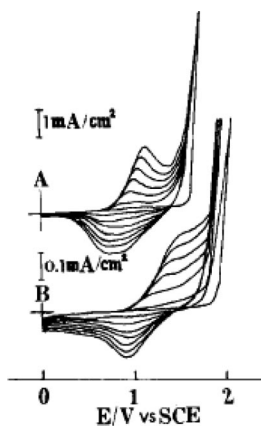


**Figure 26.** Potentiodynamic polymerization of benzene in (A) BFEE + TFA 2:1 and (B) pure BFEE on a SS electrode at  $100 \text{ mV}\cdot\text{s}^{-1}$ . Reprinted with permission from ref 248. Copyright 1999 Wiley-VCH.

(Figure 27) offer a unique combination of chemical and physical properties that make them very useful as electrolytes and solvents at the same time.<sup>258–262</sup> They exhibit great advantages; for example, their nucleophilicity is extremely low. Therefore, even highly charged cations of organic species are stable in these media. In addition, they are electrochemically stable in a very wide potential window (4–6 V). However, mass transport is slow; the high viscosity of these solvents diminishes the diffusion of electroactive species to the electrode, a factor that can be important to control the properties of electrogenerated films.<sup>1</sup> Thanks to the extraordinarily low vapor pressures even at elevated temperatures, it is possible to obtain water-free ILs by means of relatively easy purification procedures. Thus, very reactive intermediates such as radical cations generated during the monomer electrolysis can be stabilized. Finally, the possibility of analysis in potential regions normally not available with the classical solvent–electrolyte mixtures is an additional advantage of these media.

All the classic CPs have been prepared in ILs. The corresponding electrosyntheses involve *inter alia* the formation of PPY,<sup>263–265</sup> PEDOT,<sup>266,267</sup> PTh,<sup>268,269</sup> PPP,<sup>270,271</sup> and PANI.<sup>272</sup> Mechanistic studies of the electropolymerization process in ILs reveal that at least the initial phase of oligomerization is identical to that observed in conventional organic media (e.g., ACN/TBAPF<sub>6</sub> or PC/LiClO<sub>4</sub>).<sup>77</sup> The same applies to the electrochemical properties of polymers synthesized in ILs. However, many characteristics show quantitative changes. Thus, an enhanced cycling stability<sup>263,273–275</sup> or an increase of conductivity<sup>276</sup> has been observed. Interestingly, as shown by EQCM and impedance measurements, during voltammetric charging/discharging experiments, a significant cation exchange takes place, which increases at higher scan rates.<sup>267,271</sup> The cation expulsion and incorporation during charging/discharging cycles is more pronounced at the beginning of the polymer doping. Randriamahazaka et al. suggest that this effect is a consequence of different polymer zones of different lengths and/or various morphologies.<sup>267</sup> By contrast, findings obtained in conventional solvents support the view that  $\sigma$ -dimerization causes these effects.<sup>33,98</sup> A peculiar phenomenon is that in ILs no memory effect has been detected even after a long waiting time at negative potentials.<sup>162,163</sup> A clear explanation for this conspicuous difference between ionic liquids and conventional organic solvents is not available in the literature. It seems that, in the case of organic solvents, passivating surface effects slow

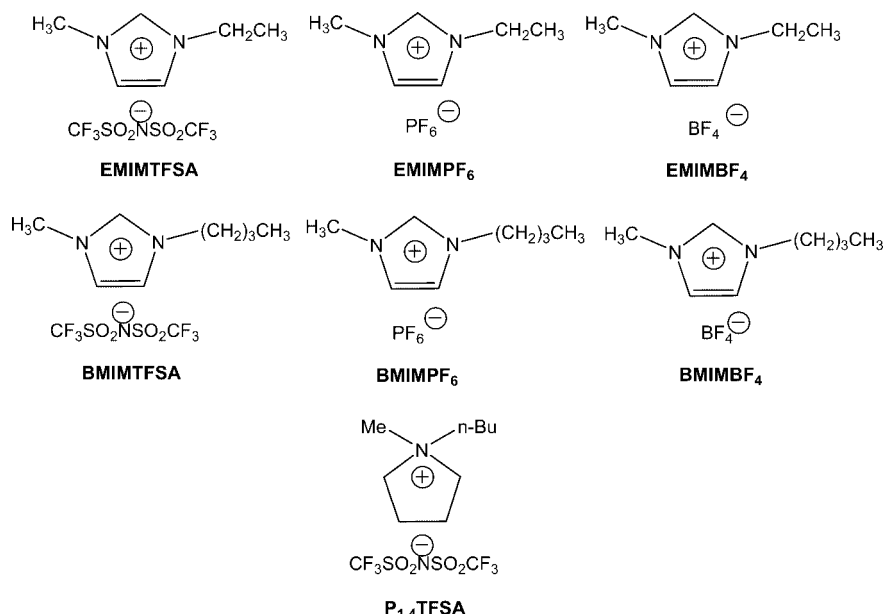


**Figure 27.** Examples of some ILs used in electropolymerization studies of CPs.

down the electron transfer kinetics,<sup>161</sup> whereas, using ILs, no surface changes occur.

Cation intercalation was also studied with the aid of solid state NMR techniques. PPy was analyzed in a phosphonium-based ionic liquid [tri(hexyl)(tetradecyl) phosphonium bis(trifluoromethanesulfonyl) amide].<sup>277</sup> The high viscosity of the ionic liquid (277 cP) required slightly higher polymerization potentials (due to IR drop) and longer polymerization times. After electrosynthesis, the films were peeled off from the electrode, crushed, ground up, and NMR analyzed. <sup>13</sup>C NMR, <sup>31</sup>P NMR, and <sup>19</sup>F NMR spectra of films after potentiostatic growth indicated the incorporation of both cations and anions from the IL into the film during growth. However, complete expulsion of the phosphonium cations was observed when the film was oxidized. The successful intercalation and deintercalation process of IL cations is notable due to their large size and suggests that this ionic liquid may play a positive role in this exchange process.

Recently, a new method was reported for the electropolymerization of PPy without any added support electrolytes. The reaction is carried out using a pyrrole monomer aqueous solution and a viscous composite of polyelectrolyte-functionalized ionic liquid (PEFIL) between the aqueous solution and the electrodes.<sup>278</sup> PEFIL is a 1-methyl-3-methylene-imidazolium based polyelectrolyte that contains poly(4-styrene sulfonate sodium) (PSS) as counteranions. PEFIL is a positively charged polymeric ionic liquid, which can provide a high local ionic conductivity and fast ion mobility during electropolymerization, providing anions for the doping process.

Since ILs are expensive, new strategies have been developed to take advantage of them. Xu et al. suggested the use of IL microemulsions which are prepared from mixtures of surfactants, ILs and water.<sup>279</sup> The best results were obtained for an electrolyte medium of BMIMPF<sub>6</sub> in water (H<sub>2</sub>O% = 90 wt % + nonionic surfactant Tween 20) for the polymerization of PEDOT.

Electrochemical devices based on the conducting polymers PANI, PPy, and PTh were constructed using ILs as electrolytes. Actuators constructed with PANI fibers showed extremely high performance.<sup>280</sup> Electrochromic devices

constructed with PANI/BMIMBF<sub>4</sub>/PEDOT-POT also showed an exceptional stability up to 1,000,000 redox cycles.<sup>281</sup> Similar observations were reported for EDOT, Py, and aniline deposited onto ITO-coated glass electrodes using BMIMBF<sub>4</sub><sup>282</sup> or 1-ethyl-3-methylimidazolium-ethyl sulfate<sup>283</sup> as electrolyte. From a technological point of view, electropolymerization in ILs represents an easy way to enhance the CPs properties without the necessity of controlling the water amount that is troublesome in other solvents.

## 5. Electrosynthesis of Functionalized Conducting Polymers

Functionalization of CPs with groups or moieties providing specific physical and chemical properties in addition to the electronic properties of the conjugated polymer backbone has attracted increasing interest in the last few years due to a number of applications, such as sensors,<sup>284,285</sup> electrochromism,<sup>286,287</sup> electrocatalysis,<sup>288</sup> and optoelectronic devices.<sup>289</sup> Most studies report on monomer units of the electropolymerizable material bearing one additional functionality as a side group. The functionalities are therefore distributed throughout the whole CP film on the electrode in a three-dimensional fashion upon electropolymerization. Depending on the chemical nature of the functional group, these groups can also be modified in such a way that they are part of the monomeric or oligomeric units which can be electropolymerized.

There are in general two different strategies to incorporate additional functionality into a CP film: the first is the straightforward electropolymerization of functionalized CP monomers. Important issues which arise are (a) the potential distortion of the  $\pi$ -conjugated backbone by steric interactions with the additional functional groups, (b) direct interaction (inductive and/or mesomeric) of functional groups with the charged  $\pi$ -conjugated system which might influence the efficiency of the electropolymerization process, and (c) the presence of easily oxidizable groups in the monomer that can interfere with, or even completely inhibit, the polymerization process. From careful examination of electrochemical and spectroscopic data of electropolymerized products, one finds that mostly oligomeric materials are produced via

this approach. Coming from synthetic polymer science, postelectropolymerization or polymer-analogous reactions are the second pathway to produce functionalized CPs. Here, electropolymerization is first carried out with CP monomers that contain reactive groups such as active esters or protected amines, which can afterward be deprotected and functionalized with the functional moiety of choice. In this review we will mainly give examples of the direct electropolymerization of CP monomers bearing functional groups, which is more interesting from an electrochemist's point-of-view. We will further focus our literature review on redox-active substituents having potential applications in optoelectronic devices or electrocatalysis (section 5.1) and ionic substituents in so-called self-doped conjugated polymers (section 5.2).

## 5.1. Redox-Active Substituents

### 5.1.1. Organic Redox-Active Substituents

Conjugated polymers bearing redox-active substituents are highly attractive for applications in optoelectronic devices, such as organic solar cells and electrochromic devices, because the substituents introduce additional electronic properties.

Figure 28 shows the principle of an organic solar cell.<sup>290–292</sup> The cell is typically built in a sandwich assembly: the photoactive layer is embedded between two electrodes. The photoactive layer is composed of an electron-donor material (p-type) and an electron-acceptor, that can transport electrons (n-type), and both materials are in contact with the respective electrodes. As p-type materials, conjugated polymers have been successfully introduced, because they typically show good reversible oxidation properties, as discussed in the previous chapters. The most studied organic solar cells, with efficiencies of up to 5%, are made by simple mixing (blending) of the conjugated polymer poly(3-hexyl thiophene) as electron donor (p-type) and fullerene derivatives as electron acceptor (n-type).<sup>293,294</sup> Following light absorption in the solar cell, bound electron–hole pairs, so-called excitons, are created.<sup>295</sup> After successful separation of charge carriers at the donor–acceptor interface, the electrons move within the acceptor materials to the Al electrode, while the holes travel to the opposite electrode. Since the exciton diffusion length in organic materials is typically only 5–20 nm, one prerequisite for organic solar cells is the close interdispersion of donor and acceptor on this length scale such that charge separation can occur before charge recombination. An alternative to the pure mixing of the components is the tuning of the structure via smart design of the molecular architecture. The direct attachment of fullerene molecules to the CP backbone is, for example, expected to lead to materials with an intimate contact and

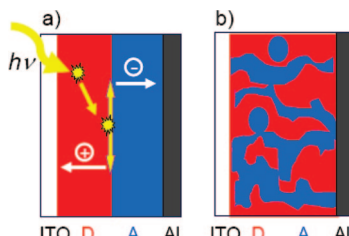


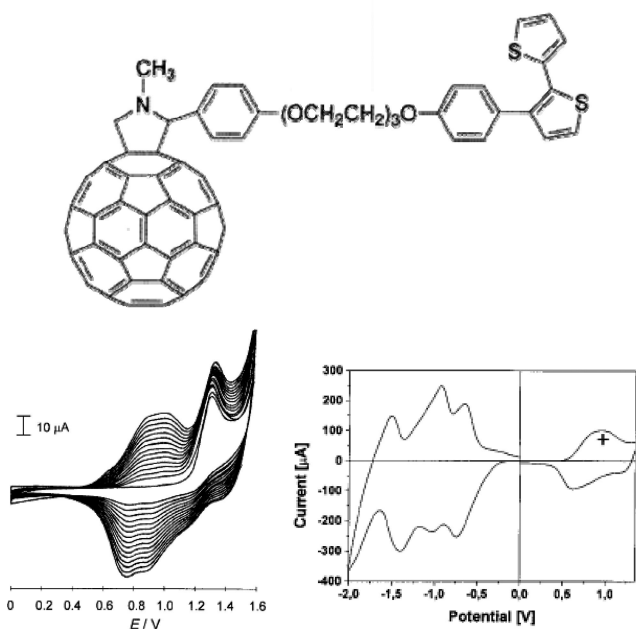
**Figure 28.** Schematic representation of the principal of organic solar cells: ITO, transparent indium tin oxide layer as electrode; D, donor; A, acceptor; Al, aluminum electrode. Different configurations of the photoactive layer: (a) bilayer; (b) interdispersed D and A phase made by mixing (blend).

continuous pathways of the donor and the acceptor. In this case, a high p-type charge carrier mobility along the CP backbone is present, in addition to the n-type behavior of the covalently linked acceptor moieties. In the literature, these architectures are often referred to as double-cable polymers because the conjugated polymer backbone ideally forms a chain bearing a number of closely spaced pearls represented by the electron acceptor.<sup>296,297</sup> However, the expression double-cable polymer seems to be misleading since the electropolymerization of polymers usually does not lead to ideal linear chains.

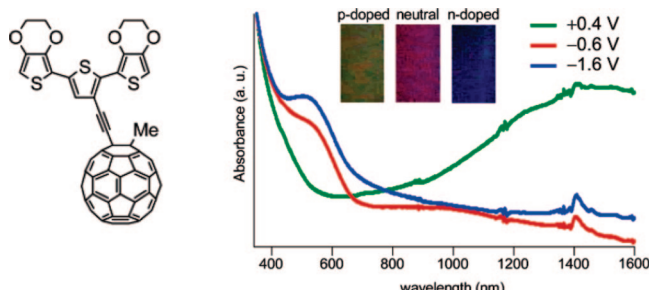
The first conjugated polymer material bearing fullerene side groups was reported by Benincori et al. in 1996.<sup>298</sup> They attached C<sub>60</sub> to the bridging carbon of cyclopentadithiophene, leading to a monomer which could be electropolymerized. The resulting polymers showed amphoteric redox behavior: Reversible anodic waves correspond to the electrochemical oxidation of the conjugated backbone, and reversible waves at negative potentials correspond to the reduction of the fullerene pendant groups. The anodic doping of the backbone was observed at more positive potentials than those for the polycyclopentadithiophene homopolymer. The absorption spectra of the undoped polymer showed a maximum at 440 nm, confirming a relatively short effective conjugation length characteristic for an oligomeric system. These results can be attributed to a combination of steric and electronic effects of the fullerene and/or to a low degree of polymerization due to the inherent low solubility of the system. Ferraris and co-workers reported one year later the electropolymerization of a bithiophene carrying a fullerene group via a flexible hexyl chain spacer.<sup>299</sup> Bithiophene was chosen as monomer since it allows easier electropolymerization at lower oxidation potentials than those for thiophene. The flexible alkyl chain both provided enhanced solubility of the monomer and minimized the electron-withdrawing effect of the fullerene on the electropolymerization process of the CP. Electrochemical and spectroscopic characterization of the electro-generated polymers revealed almost no electronic or steric perturbation of the conjugated chain. The neutral polymer had an absorption maximum of ~480 nm.

Figure 29 shows the structure of a bithiophene attached to a fulleropyrrolidine substituent through a large spacer and the CV of a successful electropolymerization in CH<sub>2</sub>Cl<sub>2</sub>.<sup>289</sup> Cyclic voltammetry in monomer-free solutions revealed one wave in the positive region corresponding to the reversible oxidation of the polythiophene backbone and several waves which can be correlated to the multiple reduction of fullerene. In addition to the electrochemical data, the authors showed for the first time that this kind of material is indeed applicable in organic solar cells: the donor backbone and the acceptor moieties do not interact in the ground state; that is, they show mutually independent electronic properties, whereas a photoinduced electron transfer occurs in the excited state. One indication of this phenomenon is the fluorescence quenching of the excitation of the polymer in the presence of C<sub>60</sub>.

Yamazaki and co-workers described the electropolymerization of ethylenedioxy-substituted terthiophene–fullerene molecules (Figure 30).<sup>300</sup> One main advantage of using ethylenedioxy thiophene monomers<sup>238</sup> is that the 3-position of the thiophene is blocked, resulting in exclusive electropolymerization of the 2-position, leading to regiochemically defined structures. The fullerene molecules were attached to the terthiophene unit by a triple bond, which apparently did not affect the electropolymerization process. This class



**Figure 29.** Electropolymerization of a bithiophene–fulleropyrrolidine. Left graph: CV in 0.1 M  $\text{Bu}_4\text{NPF}_6$  in  $\text{CH}_2\text{Cl}_2$ , against  $\text{Ag}/\text{AgCl}$ ,  $v = 100 \text{ mV}\cdot\text{s}^{-1}$ . Right graph: CV of the corresponding electrogenerated polymer, 1st cycle, in monomer-free acetonitrile solution. Reprinted with permission from ref 289. Copyright 2002 American Chemical Society.



**Figure 30.** Electronic absorption spectra of the polymer on an ITO electrode at three different potentials in acetonitrile (0.1 M  $\text{Bu}_4\text{NBF}_4$ ; potential vs  $\text{Fc}/\text{Fc}^+$ ). Reprinted with permission from ref 300. Copyright 2004 American Chemical Society.

of material is very interesting for electrochromic applications. Figure 30 shows the electronic absorption spectra of the polymer on an ITO electrode at three different potentials in acetonitrile.

Other interesting electron acceptor groups which can be attached to the backbone of conducting polymers are peryleneetracarboxylic diimide derivatives,<sup>301,302</sup> anthraquinone,<sup>303–306</sup> and tetracyanoanthraquinodimethane<sup>305,307</sup> moieties (Scheme 9). In addition to their properties as electron acceptors, they exhibit absorbance in the visible spectrum, giving a useful superimposition with the optical transitions of the conducting polymer backbone. In particular, peryleneetracarboxylic diimide (PTCDI) dyes could be a suitable replacement for fullerenes as electron acceptors in optoelectronic devices, since they show good electron mobility and good thermal and photostability.

One important feature and motivation for designing new materials for optoelectronic devices is engineering or tuning of the band gap, reflecting the difference between the HOMO (VB) and the LUMO (CB) level of a system. The optical band gap is correctly determined from the  $S_1 \leftarrow S_0$  absorption transition in UV-vis spectrometry. Nowadays, very often

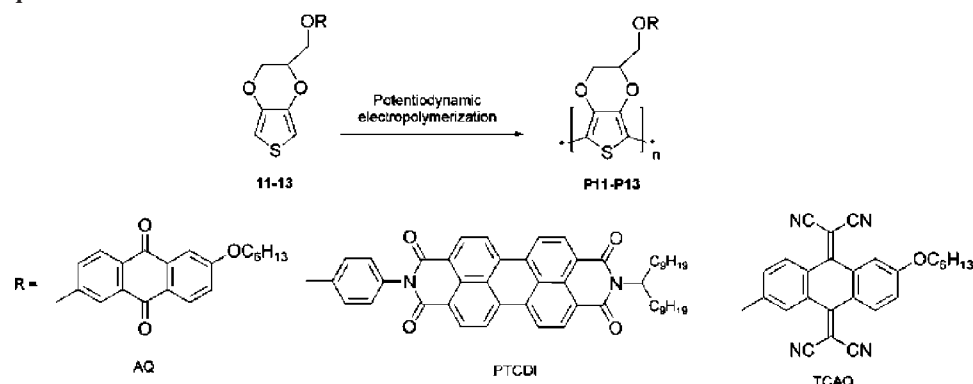
values of the absorption onset are used which may lead to errors because the onset of an absorption band energetically always lies below the exact value of the  $S_1 \leftarrow S_0$  transition ( $\sim 0.2$  to  $0.3$  eV).

The electrochemical band gap of an electroactive system is calculated as the difference between the respective oxidation and the reduction potentials, which are always measured against a reference electrode, e.g., the standard hydrogen electrode (SHE). In order to correlate these electrochemical data with the corresponding HOMO and LUMO levels, it is necessary to relate the respective redox potentials to the vacuum level. Using thermodynamic and extrathermodynamic assumptions, this (absolute) potential of the SHE has been determined as  $-4.6 \pm 0.1$  eV on the zero vacuum-level scale.<sup>204</sup> Other reference electrodes, such as the  $\text{Ag}/\text{AgCl}$  electrode or the  $\text{Fc}/\text{Fc}^+$  redox couple, as internal standard provide values which are calculated using the standard electrode potential series. Applying cyclic voltammetry, electrochemists usually determine the relevant redox potentials and the correlated band gap data from the first peak potential, the so-called midpeak potential, or the half-wave potential. In a paper published in 2002 by Hümmelgen et al., it was suggested to use onset potentials of oxidation and reduction in cyclic voltammograms for the determination of electrochemical band gaps.<sup>308</sup> Especially, in the literature concerning organic solar cells, this method has often been applied. However, from the viewpoint of electrochemistry, this strategy cannot be recommended. First, onset potentials (always lying outside of a current flow) are not standard potentials and do not possess thermodynamic significance. The error of the band gap estimation amounts at least to 0.3 eV. Second, kinetic, hysteresis, memory, dispersion, and *iR* effects may additionally influence the position of the onset potential, which enlarges the error.<sup>309</sup> Additionally, it should be noted that the optical and electrochemical band gaps are not identical. Optical excitation of an electron from the ground (HOMO) to the first excited (LUMO) state only involves small changes of solvation and Coulombic interaction terms. Electrochemical oxidation, on the other hand, produces cations and reduction anions, the solvation and Coulombic influences of which on the HOMO and LUMO levels are significant.

The levels of the HOMOs and LUMOs have a strong influence on an efficient charge separation and on the absorption behavior of the photoactive layer. The term low or narrow band gap materials refers to materials which exhibit a red-shifted absorption and therefore enhanced light-harvesting properties in organic solar cells. Yamashita and co-worker presented polymers with band gaps of as low as 0.5 eV by electropolymerization of precursors based on three-ring systems with a median acceptor such as benzo[1,2-*c*:3,4-*c'*]bis[1,2,5]thiadiazole and two external thiophene rings.<sup>310</sup> Roncali et al. electrogenerated poly(thiophenes) with narrow band gaps and high stability under n-doping cycling from dimers of EDOT and thieno[3,4-*b*]pyrazine.<sup>311</sup> The trick here is to mix monomer segments with higher HOMO and lower LUMO to reduce the band gap due to intrachain charge transfer.

The first example of a p-type conjugated polymer in direct conjugation with n-type perylene moieties exhibiting a narrow band gap of  $\sim 0.9$  eV was recently shown by Segura and Bäuerle.<sup>312</sup> They reported the successful electropolymerization of a peryleneeamidine-imide derivative fused with a terthiophene moiety through an imidazole unit (Figure

**Scheme 9.** Electropolymerization of EDOT Monomers Bearing Anthraquinone, Perylenetetracarboxylic Diimide, and Tetracyanoanthraquinodimethane Moieties<sup>a</sup>



<sup>a</sup> Reprinted from ref 302 with permission. Copyright 2006 American Chemical Society.

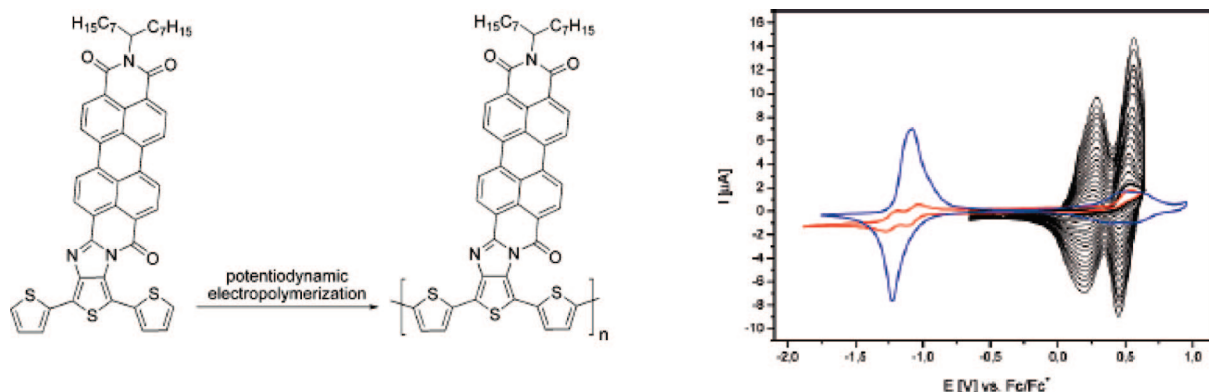


**Figure 31.** Electropolymerization of a peryleneamidine-fused polythiophene. CV of the monomer in  $\text{CH}_2\text{Cl}_2/\text{TBAPF}_6$  (0.1 M) (red line) and corresponding electrochemical polymerization (black curves). Blue line: Characterization of the polymer in monomer-free acetonitrile/TBAPF<sub>6</sub> (0.1 M) solution,  $v = 100 \text{ mV} \cdot \text{s}^{-1}$ ,  $T = 20^\circ\text{C}$ . Reprinted from ref 312 with permission. Copyright 2007 American Chemical Society.

31). Both an anodic shift of the reduction and a cathodic shift of the oxidation of the monomer compared to the case of a peryleneamidine-imide dye and a  $\alpha$ -tertiophene component can be attributed to the direct conjugation of the perylene to the thiophene backbone. The CV of the electro-generated polymer (blue line in Figure 31) exhibits a broad redox wave of the polythiophene backbone and an asymmetric redox wave at  $E_{pc} = -1.23 \text{ V}$  including the two redox waves of the perylene unit. The films are highly electroactive in both the p- and the n-doping process, which can be attributed to the direct conjugation of the polythiophene and peryleneimide moieties. The HOMO and LUMO were estimated to be  $-5.1 \text{ eV}$  and  $-4.2 \text{ eV}$ , respectively, leading to a band gap of  $0.9 \text{ eV}$ .

Further progress in the direction of combining perylenes with electropolymerizable thiophene monomers and oligomers was shown by Chen et al.<sup>313</sup> and Würthner et al.<sup>314</sup> These research groups attached electron-rich oligothiophenes at the bay positions of electron-poor perylene bisimides (Figure 32).<sup>314</sup> The absorption behavior of the perylene chromophore and the oligothiophene units was not influenced by the presence of the other, indicating negligible ground-state interaction. Upon electrochemical cross-linking of the thiophene moieties, polymeric networks were obtained.

Würthner et al. pointed out that the films are much more electroactive in the p-doping than in the n-doping process. A possible explanation can be found in the structure obtained during electropolymerization: the n-type perylene bisimides are probably embedded in the film in a rather disordered

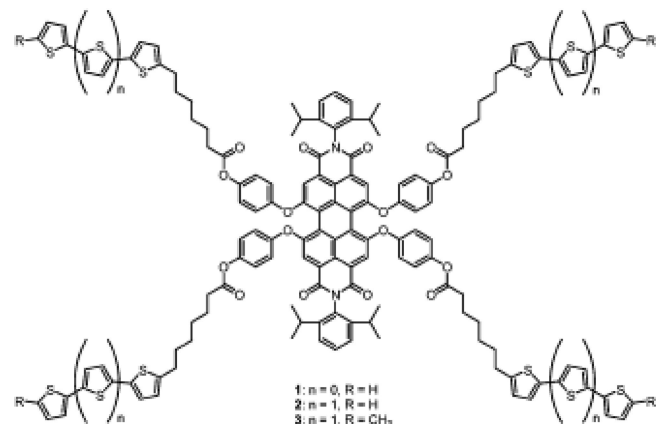


**Figure 32.** Oligothiophene-functionalized perylene bisimide. Reprinted with permission from ref 314. Copyright 2004 Royal Society of Chemistry.

fashion, while the oligothiophene units are regularly arranged, facilitating charging and discharging during p-doping. Since the conductivity mechanism of these materials can be directly compared to that of metallocopolymers, we refer to the discussion in section 5.1.2. A very recent publication by Würthner and Bäuerle reports on the synthesis of dendritic oligothiophene-perylene bisimide hybrids and their electropolymerization toward donor-acceptor networks.<sup>315</sup>

The characteristic colors of viologens (V), 1,1'-bis-substituted-4,4'-bipyridinium salts, in their different redox states make these redox systems highly interesting for

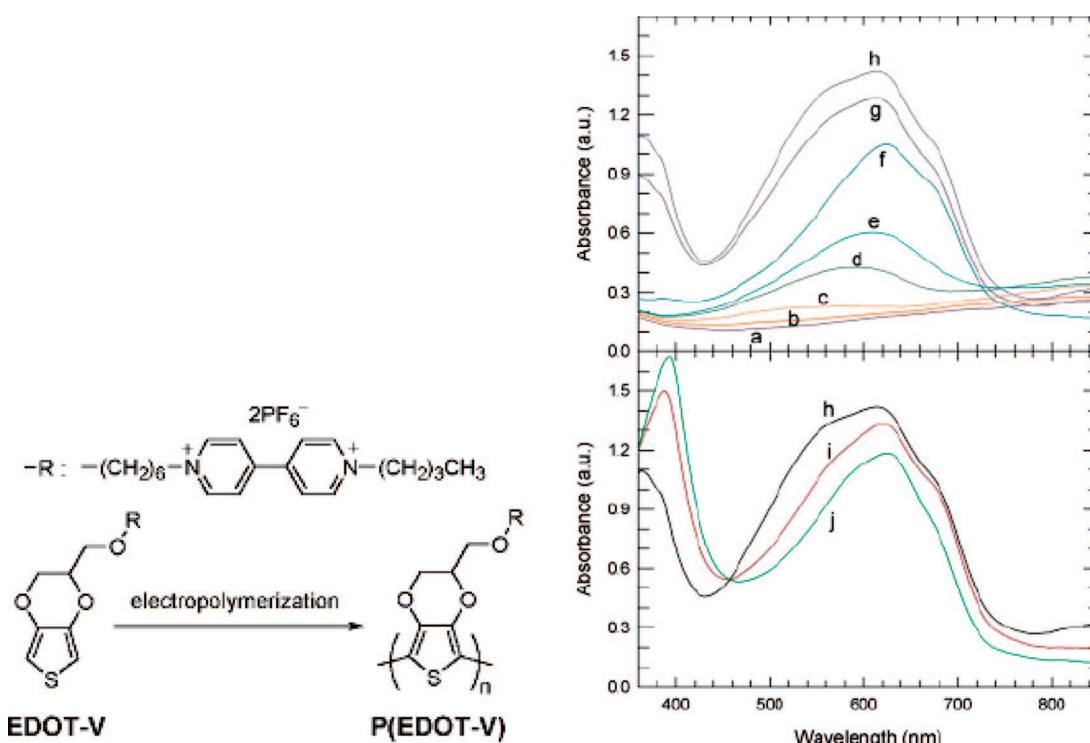


**Figure 33.** Electropolymerization of viologen-bearing PEDOT. Static spectroelectrochemistry of P(EDOT-V) on ITO glass at various potentials: (a) 0.5–1.2; (b) 0.2; (c) 0; (d) −0.2; (e) −0.4; (f) −0.6; (g) −0.7; (h) −0.8 to 1.0; (i) −1.2; (j) −1.4 to 1.6 V vs Ag/Ag<sup>+</sup>. The P(EDOT-V) film was prepared by potentiodynamic electropolymerization of 3 mM EDOT-V in the potential range 0–1.5 V for 5 cycles. Reprinted with permission from ref 287. Copyright 2004 Wiley-VCH.

electrochromic applications.<sup>316–320</sup> The dication V<sup>2+</sup> is generally colorless and is the most stable of the viologen redox states. Cycling toward negative potentials in a cyclic voltammogram leads to two typical redox waves: The first is assigned to the redox reaction dication/radical cation V<sup>2+</sup>/V<sup>0+</sup> and the second to that of the radical cation/neutral form couple V<sup>0+</sup>/V<sup>0</sup>. Both V<sup>0+</sup> and V<sup>0</sup> are colored. The colors can be tuned by introducing various substituents at the N-sites of the 4,4'-bipyridine. Viologens have first successfully been attached to the backbone of PPy<sup>321–324</sup> and PTh.<sup>325</sup> PEDOT derivatives containing pendant viologens have been investigated by Ko et al.<sup>287,326</sup> (Figure 33). Spectroelectrochemistry was used to study the potential of the electrogenerated polymers for electrochromic applications.

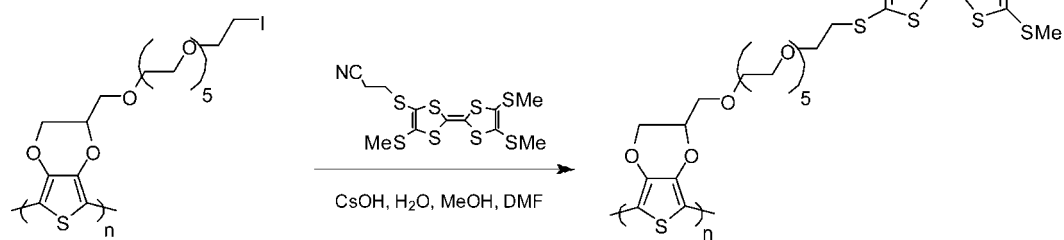
A polymer-analogous reaction was reported by Roncali et al. for the incorporation of tetrathiafulvalenes into CP films based on PEDOT.<sup>327</sup> Tetrathiafulvalenes show two well-defined reversible, one-electron oxidation processes, making them interesting for electrochemical sensors. The direct electropolymerization of tetrathiafulvalene (TTF) bearing

polythiophenes<sup>328,329</sup> had been reported as difficult due to steric and electronic hindrance. The reaction scheme is represented in Scheme 10. Lyskawa and co-workers followed a similar route by grafting TTF-podants onto a prepolymerized PEDOT film.<sup>330</sup> The modified films were proposed as sensors for the recognition of heavy metals in solution.

### 5.1.2. Conjugated Metallopolymers

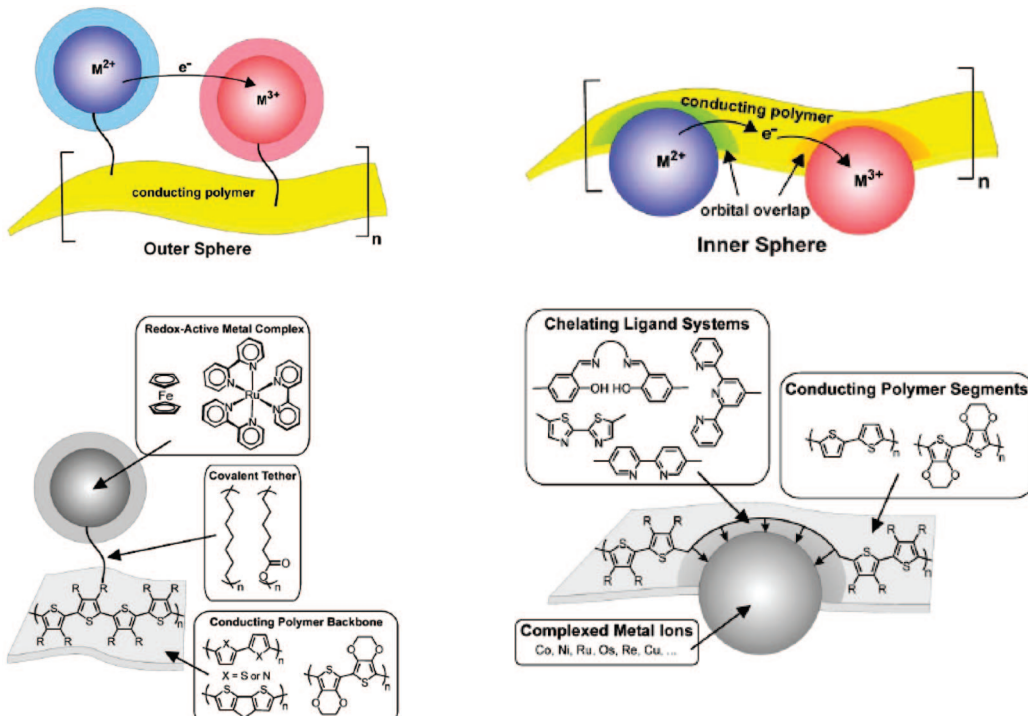
In the field of electrocatalysis and chemical and biosensors, electropolymerization of metallopolymers, that is, materials which combine the electronic conductivity of polymers and the properties of metal complexes, has become an active field of research.<sup>331–336</sup> Electropolymerization again offers an elegant and easy strategy for the immobilization of metal complexes on the surface of electrodes, since the metal complexes are incorporated in the CP film homogeneously in one experimental step. For electrocatalytic applications in particular, the electropolymerized film often offers advantages over the simple use of adsorbed electrocatalytic

**Scheme 10. Chemical Formula for a Polymer-Analogous Reaction of a Tetrathiafulvalene with a PEDOT Derivative Bearing an ω-Iodo-Polyether Chain<sup>a</sup>**



<sup>a</sup> Reprinted with permission from ref 327. Copyright 2001 Wiley-VCH.

**Scheme 11. Top:** Mechanisms of Electron Transfer in Conducting Polymer Systems. **Bottom left:** Exemplary Molecular Components of Outer Sphere Metallocopolymer Systems. **Bottom right:** Molecular Components of Inner Sphere Metallocopolymer Systems. Reprinted with Permission from Ref 340. Copyright 2005 Royal Society of Chemistry



mieties.<sup>337,288,338</sup> In the literature, different models describing the influence of the conjugated backbone on electron transport between metal centers are discussed.<sup>339,340</sup>

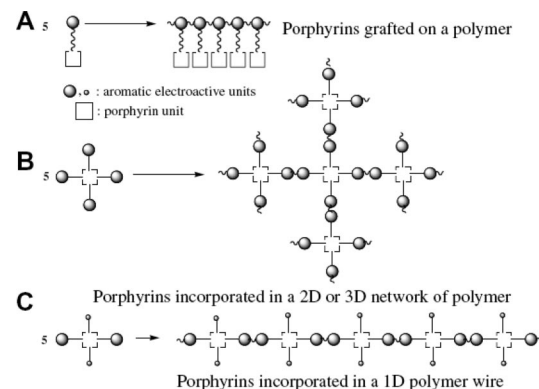
Scheme 11 shows a schematic of the so-called outer sphere and inner sphere mechanism and exemplary materials, as presented by Holliday and Swager.<sup>340</sup>

The two mechanisms depend on the mode of interaction of the transition metal centers with each other and the conducting polymer backbone. In the outer sphere systems (Scheme 11 bottom left), redox active metal centers or complexes are attached to the conducting polymer backbone but have no direct interaction with it. The outer sphere electron transfer between different metal sites is similar to the hopping mechanism described for conventional redox polymers<sup>186,187</sup> and can be applied to the functionalized conducting polymer systems bearing organic redox-active substituents. Inner sphere architectures (Scheme 11 bottom right) involve the incorporation of the metal centers into the conducting polymer backbone with strong coupling between the orbitals of the CP backbone and the metal orbitals. Studies by Zotti et al. show that electron transfer rates between metal sites in polythiophenes with pendant ferrocene moieties are enhanced when a conjugated linkage is used.<sup>341</sup> The authors suggest that electronic communication through a conjugated linkage via band transport is more effective than pure electron hopping. In our opinion, at the present state of knowledge, a decisive commitment in favor of molecular or band models as well as inner or outer sphere mechanisms is difficult. Anyway, it seems that all transport processes in CPs can be consistently described by hopping.

In the following we will discuss two representative conjugated metallocopolymer systems: metallocporphyrins and metallocene-containing CPs.

The incorporation of metallocporphyrins into conducting polymers is of special interest for electronic and optical

**Scheme 12. Different Possibilities of Electrode Modification Using Porphyrin Units by Electrochemical Polymerization<sup>a</sup>**



<sup>a</sup> Reprinted with permission from ref 344. Copyright 2007 Elsevier.

devices because of their redox, photoactive, guest-binding, and catalytic properties.<sup>342,343</sup> Depending on the central metal ions, the porphyrin ligands can be reversibly oxidized to cationic or anionic radicals. The square-planar geometry of the porphyrin core makes it possible to tailor-make substituted porphyrins that control the supramolecular structure of the CPs. Scheme 12 shows several architectures which can be obtained by electrochemical polymerization.<sup>344</sup>

In Scheme 12A porphyrin units are covalently linked to the electroactive monomer and electropolymerization yields a “double-cable” polymer. The electrochemical polymerization of monomers containing porphyrins has been reported for a number of CP monomers, such as thiophene,<sup>345,346</sup> bithiophene,<sup>347</sup> terthiophene,<sup>348–351</sup> pyrrole,<sup>352–356</sup> ethynylaniline,<sup>357</sup> EDOT,<sup>358</sup> and fluorene monomers.<sup>359</sup> Since the precursor porphyrin can be substituted by four electroactive units, electropolymerization can further lead to 2D or 3D networks upon electropolymerization, as depicted in Scheme 12B.<sup>360,361</sup> Porphyrins incorporated in 1D polymer wires

(Scheme 12C) have also been reported: fibers were obtained, for example, by electropolymerization of zinc-5,15-dichloro-10-[4,4'-bipyridinium-hexafluorophosphate]porphyrinate.<sup>362</sup> Porphyrin-acetylene-thiophene polymer wires were synthesized having a height of 2.5 nm and a length of up to 3  $\mu\text{m}$  as measured by atomic force microscopy.<sup>363</sup>

Vorotynsev has very recently published an extensive review of conducting polymers incorporating metallocene complexes and their derivatives;<sup>364</sup> therefore, in the present review only a few examples will be discussed. Figure 34 shows an example of a monomer synthesis of titanocene dichloride derivatives functionalized with pyrrole<sup>365,366</sup> (TC-Py) and EDOT<sup>367</sup> (TC-EDOT).

Both potentiodynamic and potentiostatic electropolymerization techniques produced TC-Py and TC-EDOT electroactive films with the organometallic center covalently linked to the CP polymer chain. A comparison of these two polymer systems showed that the oxidation potentials of the poly(TC-EDOT) materials are located at less positive potentials and the reduction potentials of the titanocene system are less negative, in comparison to the respective modified poly(TC-Py) film (Figure 34 right graph). From this behavior the authors propose that—using PEDOT—the conductivity of the polymer matrix is higher in the electroactive range of the titanocene centers, which allows a more efficient reduction of the immobilized centers and a better reversibility of the redox process.

Roncali and co-workers reported that the electropolymerization of ferrocene-functionalized EDOT was very difficult because of the considerably lower oxidation potential of ferrocene compared to EDOT. Stable ferrocene-derivatized polymers could only be obtained by copolymerization with other EDOT derivatives.<sup>368</sup>

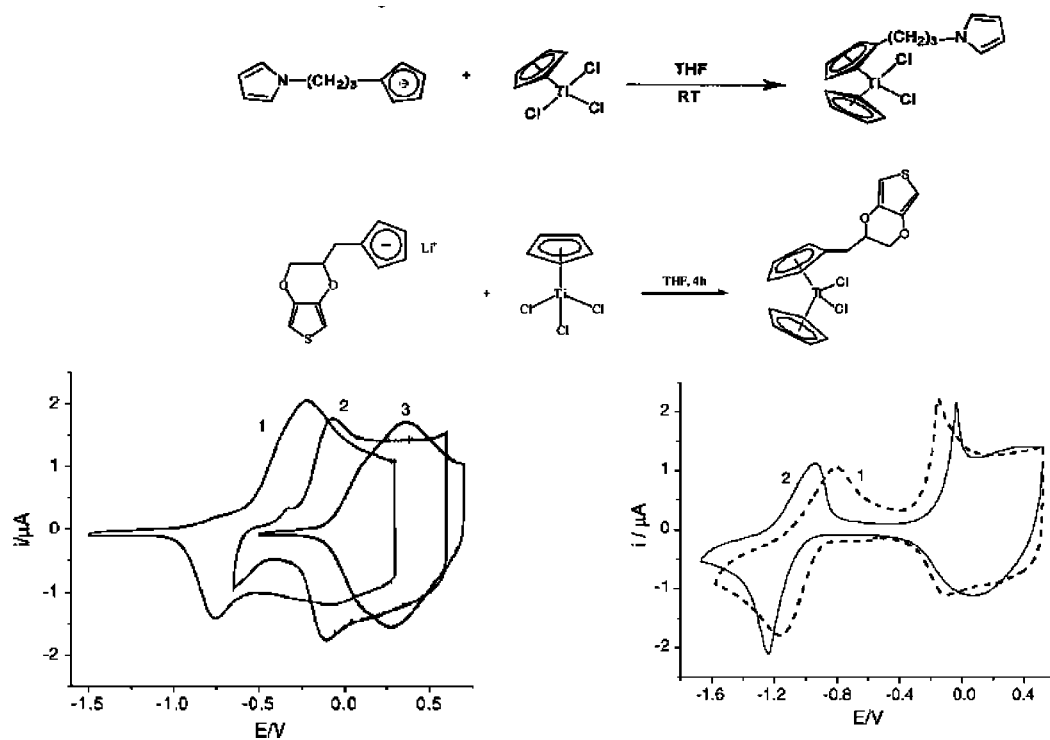


**Figure 34.** Monomers for CP bearing metalorganic units. Last reaction step of the synthesis of titanocene dichloride derivatives functionalized with Py (TC-Py) and EDOT (TC-EDOT). Left graph: Cyclic voltammogram of the p-doping of Pt modified electrodes with PEDOT, P(TC-EDOT) (2), and P(TC-Py) (3). Right graph: Comparison of the first cyclic voltammograms of P(TC-EDOT) (1) and P(TC-Py) (2). Reprinted with permission from refs 365 and 367. Copyright 2001 and 2006 Elsevier.

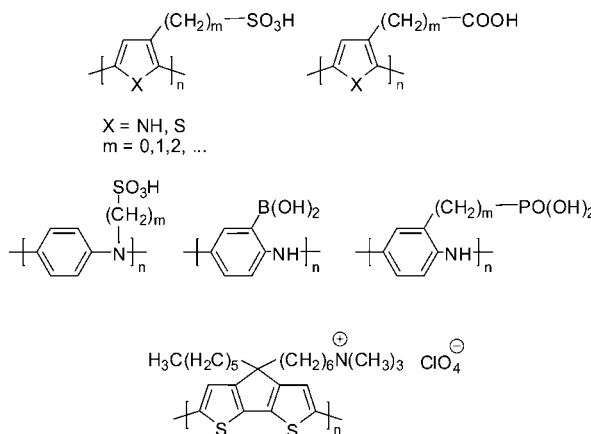


**Figure 35.** Examples of self-doped conducting polymers based on polypyrrole, polythiophene, and polyaniline.<sup>24</sup>

## 5.2. Self-doped Conducting Polymers

Self-doped conducting polymers are particularly interesting, since they combine electronic charge transport of conjugated polymer backbones with polyelectrolyte properties due to ionic moieties.<sup>369,370,24,371</sup> In the literature, the expression “self-doped conducting polymers” is used for conducting polymers which consist of typical CP repeating units bearing additional covalently linked ionizable (anionic and cationic) functional groups. The introduction of the ionic functionality can be achieved either by functionalizing the CP monomer and subsequent polymerization or by postpolymerization modification in so-called polymer-analogous reactions. A variety of different self-doped polymers are reported in the literature, and representative examples are shown in Figure 35. Typical ionizable organic groups are acidic functions, such as sulfonic,<sup>372–377</sup> boronic,<sup>378–380</sup> or phosphonic acids.<sup>381,382</sup> For further examples, we refer to

the book about self-doped conducting polymers by Freund and Diore which was published in 2007.<sup>24</sup>

The expression self-doped is a bit misleading, since it suggests that these conducting polymers are doped intrinsically and therefore conducting without any additional doping needed. This is not the case, since the ionic groups do not contribute to the electronic conductivity; the doping process still requires the diffusion of counterions into the structure to preserve electroneutrality. Therefore, the authors suggest the term “*self-ionized conjugated polymers*” as a description of this special class of conducting polymers. Figure 36 shows the process of oxidation (p-doping) for conducting polymers bearing a fixed anionic group ( $A^-$ ) with a free counterion ( $Y^+$ ). Upon oxidation of the conducting polymer to cationic species, the immobilized anions can screen the positive charge and maintain the electrical neutrality of the doped polymer. The excess free cations have to move away from the backbone into the electrolyte solution (e.g., protons in the case of acidic functions). Due to the higher mobility of the smaller cations, the rate of the charging process can be significantly increased in self-doped conducting polymers compared to classical CPs.

The concept of self-doped conducting polymers with n-doping properties was introduced by Wudl et al.<sup>383</sup> Analogous to the p-type materials, n-type CPs are conducting polymers which bear fixed cationic groups with free counteranions. Zotti and co-workers studied the behavior of polycationic polythiophenes bearing ammonium groups.<sup>384</sup> The materials exhibited well-defined reversible p- and n-doping characteristics. The n-doping process accompanied by the expulsion of the free counteranions was reported to be fast and independent of the cation size.

The water solubility of many self-doped polymers in the neutral (insulating) and doped (conducting) states<sup>385,386</sup> can be explained by the polyelectrolyte character of the polymers and makes these materials highly interesting for technological applications. Simple casting allows, for example, deposition of layers onto essentially any substrate. A remarkable property is that for some polymers the conductivity is independent of the pH of the solution. Self-doped polyaniline exhibits, for example, redox activity and electronic conductivity over an extended pH-range, making it interesting in biosensors.<sup>387–391</sup>

Since self-doped polymers exhibit faster electronic and optical responses upon changing the redox state compared to their parent polymers, especially the use in electrochromic devices has become an active area of research for self-doped conducting polymers.<sup>392–395</sup> Enhanced charge storage performance makes self-doped conducting polymers further attractive materials for polymer-based batteries.<sup>396,397</sup>

## 6. Controlling the Size and Form of Conducting Polymers

Though the potential of CPs for technological applications is immense, as shown in the last sections, their inherent

hardness and low solubility often complicate their manipulation and processing still remains very difficult. A fundamental challenge in the last few years has been to find ways to bring them into structures of well-defined shape. In this section, we present methods for how the morphology of CPs can be tuned both on the molecular level and on the mesoscopic scale.

### 6.1. Novel Architectures on the Molecular Scale

While most of the discussion in this review is based on conjugated chainlike polymers made from electropolymerizable monomeric units, in some cases also bearing additional functional groups (see section 5), much interest has been recently devoted to so-called 2D and 3D conjugated polymeric systems. As 2D structures, we refer to the special case of surface-confined (fixed) conjugated monomeric precursors, which are electropolymerized by coupling with their next neighbors on a surface. These conjugated systems form one-dimensional  $\pi$ -electron systems parallel to the surface with electrical and optical properties strongly influenced by interchain interactions. The surface immobilization is typically achieved by the concept of so-called self-assembled monolayers (SAMs). SAMs can be defined as organic molecules which are attached to substrates via chemical bonds; the most prominent examples are thiol-bearing molecules on gold surfaces. An in-depth discussion together with further types of SAMs will be given in section 6.2.1. The electropolymerization of pyrrole units anchored on gold surfaces by alkanethiols in propylene carbonate was first claimed by McCarley in 1994,<sup>398,399</sup> but the results were controversially discussed later on.<sup>400,401</sup> Göpel et al. claimed that electrooxidation of terthiophene–alkanethiols on gold is accompanied by desorption of the molecules.<sup>402</sup> Garnier and co-workers studied electrooxidation of SAMs of terthiophene–hexanethiols and proposed an electrochemically induced formation of covalent  $\beta-\beta'$  linkages between adjacent terthiophenes, leading to an oligomeric sexithiophene.<sup>403</sup>

Stable monolayers on ITO substrates were obtained by Zotti and co-workers, who studied carboxyalkylfunctionalized bi- and terthiophenes—depicted in Figure 37—bearing the thiophene chains either parallel (left sketch) or perpendicular (right sketch) to the surface.<sup>404</sup> Electrochemical oxidation of the layers of adsorbates containing moieties parallel to the substrate produced polymer layers consisting of thiophene hexamers, as proven by cyclic voltammetry and UV-vis spectroscopy.

The adsorbed linear terthiophene monolayers (Figure 37, right sketch) can only couple with terthiophenes from solution, producing one-end grafted sexithiophene monolayers. In agreement with preceding data, these experiments prove that in SAMs an alignment of reactive chainlike oligomers only parallel to the surface favors coupling steps with neighboring oligomeric moieties. Furthermore, the low reactivity of all these oligomers prevents the formation of long chains.

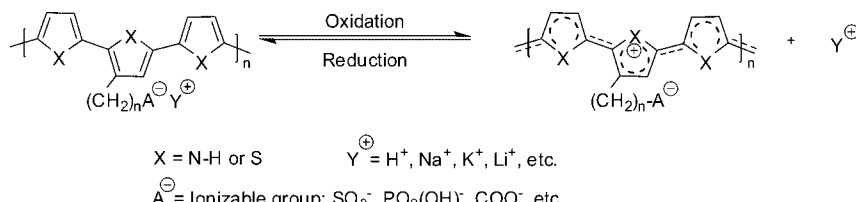
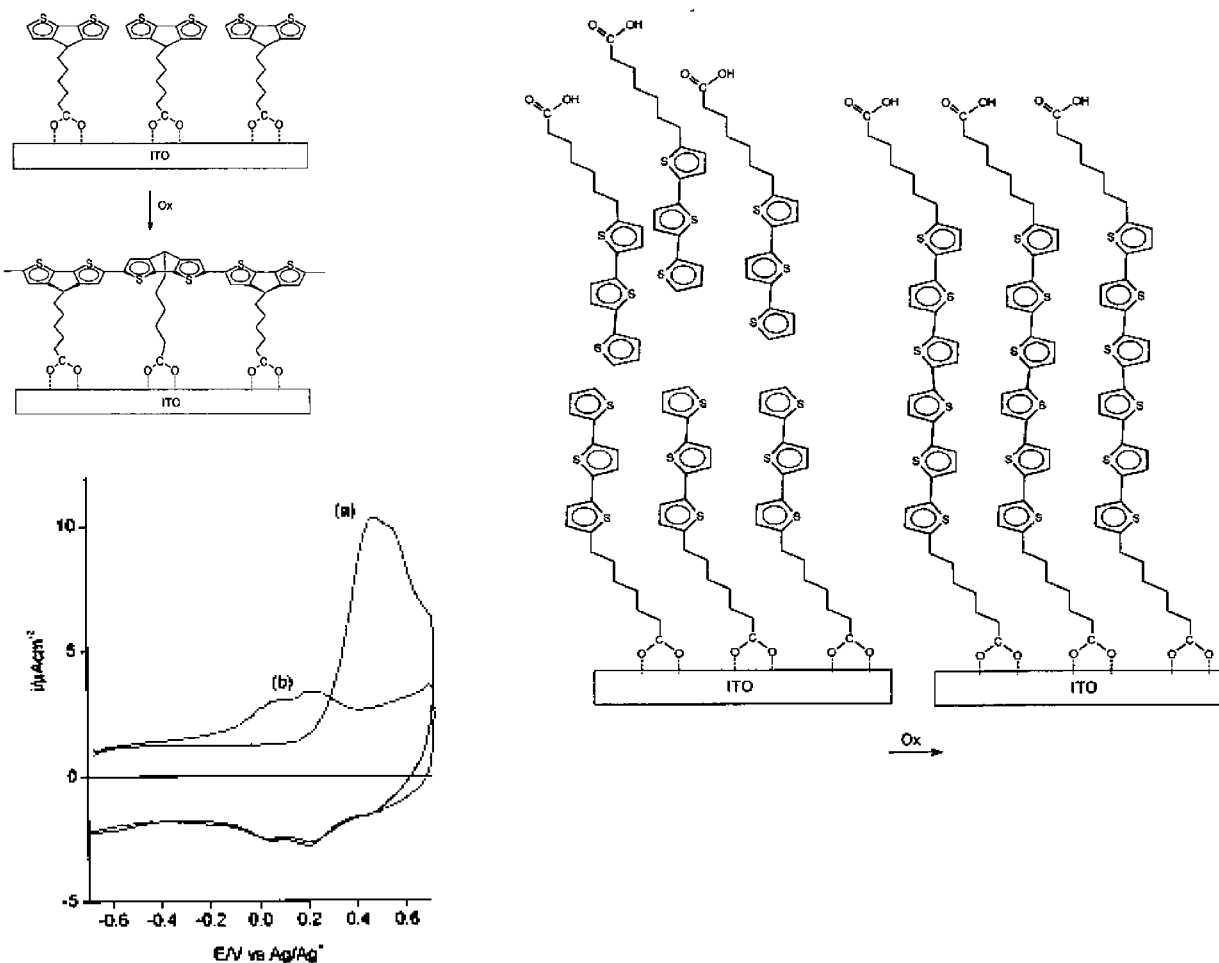


Figure 36. Charging and discharging processes occurring in a self-doped (ionized) conducting polymer during p-doping.



**Figure 37.** Proposed mechanism of electropolymerization of self-assembled carboxypentyl and carboxyhexyl bithiophenes and terthiophenes, in which the oligothiophene chain is either perpendicularly (left sketch) or linearly linked (right sketch) to the tethering carboxyalkyl chain. Cyclic voltammogram of the monolayer (left sketch) on ITO in acetonitrile/ $\text{Bu}_4\text{NClO}_4$  (0.1 M),  $v = 0.1 \text{ V} \cdot \text{s}^{-1}$ : (a) first scan; (b) last scan representing an oligomeric chain. Reprinted with permission from ref 404. Copyright 1998 American Chemical Society.

Jüttner et al. proposed the electrooxidation of bithiophene and thiophene monomer units in SAMs with phosphonic acids as head groups as novel protective coatings for steel.<sup>405</sup> Whereas cyclic voltammograms characteristic for conducting polymers were observed for bithiophene monomers, the thiophene head groups did not give any indication of a successful polymerization. A possible reason for this effect is the higher oxidation potential of thiophene compared to bithiophene.

Self-assembled monolayers of a conjugated bithiophenic system connected to an alkanethiol chain have been deposited and electropolymerized by Roncali and co-workers.<sup>406</sup> The bithiophenic system involved an EDOT unit and a thiophene ring which was attached to an alkanethiol at the internal  $\beta$ -position via a sulfide linkage. The CV of the electrooxidized monolayer revealed reversible redox waves characteristic for a stable electroactive extended conjugated system. Conducting atomic force microscopy before and after electrooxidation of the monolayer showed that the increase in the effective conjugation length upon coupling of the immobilized bithiophenic system leads to a smaller HOMO–LUMO gap and better transport properties.

In a further approach, McCarley et al. prepared polypropyleneimine dendrimers with a diaminobutane core and pyrrole termini which were adsorbed onto Au substrates.<sup>407</sup> Electrochemical oxidation of these monolayers was reported to lead to intramolecularly oligomerized pyrrole dendrimers.

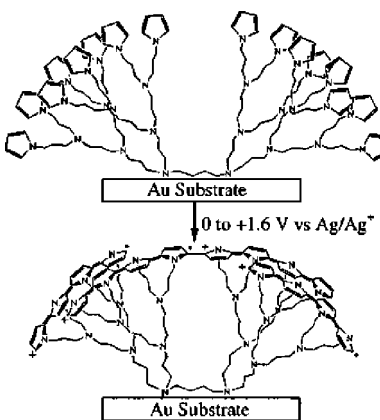


**Figure 38.** Sketch showing possible structures of surface-adhered poly(propyleneimine)dendrimers with pyrrole monomer termini before and after electrochemical oxidation. Reprinted with permission from ref 407. Copyright 2000 American Chemical Society.

A possible structure of these surface-confined oligomers is shown in Figure 38.

Dendrimers can be defined as monodisperse macromolecules with a well-defined branched structure.<sup>408</sup> Generally, these molecules are based on small 3D precursors that are synthesized (polymerized) sequentially to yield different sizes or generations. The electrochemical characterization of dumbbell-shaped dendrimers with 9-phenylcarbazole units

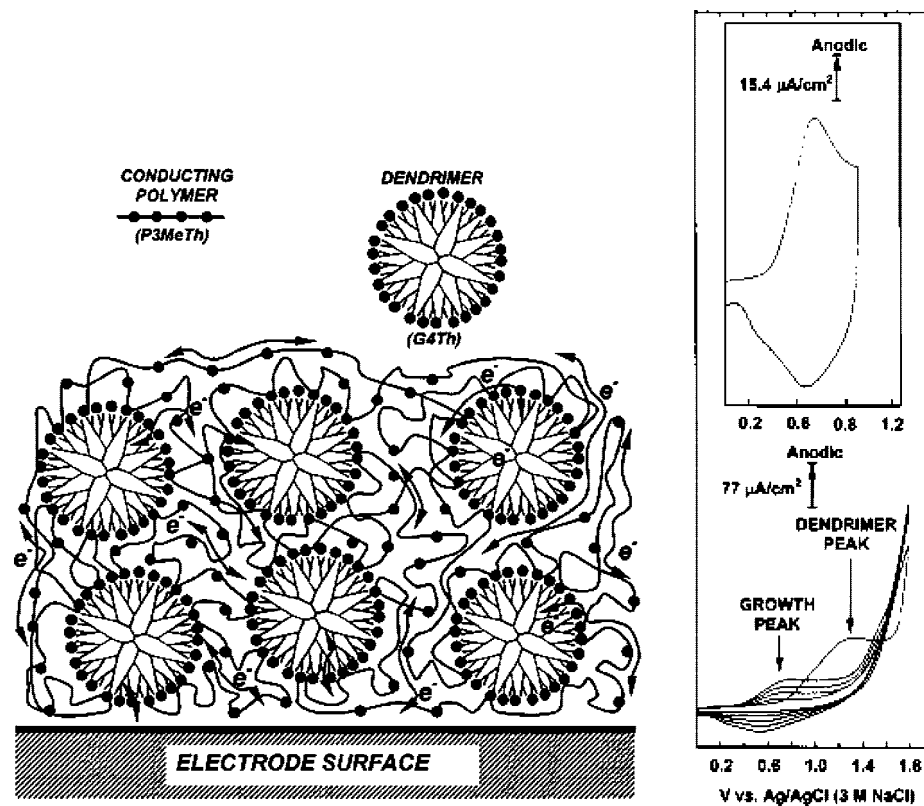


**Figure 39.** Schematic representation of a composite film containing thiophene-terminated poly(amidoamine) dendrimers cross-linked by poly(3-methyl thiophene). Bottom CV: Electropolymerization in  $\text{CH}_2\text{Cl}_2/\text{Bu}_4\text{NBF}_4$  (0.1 M) with 1 mM dendrimer and 200 mM 3-methyl thiophene at a scan rate of  $100 \text{ mV}\cdot\text{s}^{-1}$ . Top CV: CV of the resulting composite film in monomer-free electrolyte. Reprinted with permission from ref 411. Copyright 2002 American Chemical Society.

as dendrons showed that electropolymerization can occur via peripheral carbazole groups, leading to intradendrimer coupled oligomers.<sup>409</sup>

Electrogenerated poly(dendrimers) containing conjugated poly(thiophene) chains were presented by Roncali in 2000.<sup>410</sup> In a first step, neutral dendrimer cores with peripheral bithiophene (BT) groups were chemically prepared; the subsequent electropolymerization of these bithiophene groups lead to electroactive, electrogenerated poly(dendrimer) films. The electrochemical behavior of these films suggested a higher electropolymerization efficiency for higher generation dendrimers, an observation which was supported by an increased proximity of polymerizable bithiophene units for larger dendrimer cores. Polymer films based on copolymers of thiophene-end-functionalized poly(amidoamine) dendrimers and poly(3-methylthiophene) were successfully electropolymerized as novel electrochemically addressable composite thin films.<sup>411</sup> The conductivity of the films is comparable to that of pure poly(3-methylthiophene) films, and UV-vis absorption revealed lower conjugation lengths in the composites. One major gain of these dendrimeric structures is the possibility of incorporating Pt-ions into the polymer films (Figure 39). The authors present a “means for wiring together dendrimer-encapsulated metal nanoparticles”. This approach could be a first step toward the development of dendrimer-based battery materials and electrocatalytic polymers.<sup>412</sup>

Roncali and co-workers were the first to report about real three-dimensional  $\pi$ -conjugated systems. They presented tetrahedral structures involving four terthiophene branches attached to a silicon atom.<sup>413</sup> The electropolymerization of these dendrimer precursors resulted in polymer films in which discrete conjugated hexathiophene bridges were linked by

Si atoms. Similar, chemically synthesized materials were successfully implemented as donor materials in organic solar cells recently.<sup>414</sup> 3D hybrid networks, in which hexathiophene oligomers form bridges between dendrimERIC cores consisting of a polyphenylene system, were already discussed in section 3.3.<sup>194</sup> The monomeric dendrimer in this example was a terthiophene functionalized polyphenylene system built around a tetraphenylmethane core. The nice thing about this monomer is that not only can the terthiophene units couple together, but intraconnection of the polyphenylene cores can also take place.

A very recent publication by Roncali and co-workers showed a 3D conjugated structure based on four EDOT groups attached to a twisted bithiophenic structure.<sup>415</sup> This 3D precursor could be readily electropolymerized to an electroactive 3D  $\pi$ -conjugated material, as proven by electrochemical and optical characterization.

## 6.2. Organic Structure-Directing Agents

### 6.2.1. Self-assembled Monolayers

Self-assembled monolayers (SAMs) have attracted increasing interest during the last few years because they allow a straightforward preparation of chemically tailored surfaces with specific chemical and physical properties.<sup>416</sup> Typically, alkanethiols are used to modify metal surfaces, such as gold or silver. The modification of OH-bearing surfaces including  $\text{SiO}_x$  or ITO can be achieved with chlorosilanes and alkoxy silanes. SAMs of phosphonic acids or phosphonates on passivated iron or  $\text{Al}/\text{Al}_2\text{O}_3$  surfaces were also investigated.<sup>405</sup>

In the field of conducting polymers, a lot of work has been devoted to the study of electropolymerization on SAM-modified electrodes in comparison to nonmodified electrodes.

Publications from the 90s have shown that  $\omega$ -substituted alkanethiols are stable over wide potential ranges and that they attenuate the rate of electron transfer to redox probes in contacting solutions.<sup>417</sup> The current attributed to the ionic probes  $\text{Ru}(\text{NH}_3)_6^{2+/3+}$  and  $\text{Fe}(\text{CN})_6^{4-/3-}$  was significantly smaller in the presence of SAMs on the electrode, demonstrating the blocking capabilities of alkanethiols. Heinze and co-workers used scanning electrochemical microscopy and cyclic voltammetry to get local qualitative information about the status of SAM formation of *n*-alkanethiol SAMs with varying chain lengths [ $\text{CH}_3(\text{CH}_2)_n\text{SH}$ ;  $n = 7, 9, 11$ , and 15] on gold surfaces.<sup>418</sup> Additionally, the insulating properties after different immersion times were probed. The redox probe  $\text{Ru}(\text{NH}_3)_6^{3+}$  was used to study the inhibited long-range heterogeneous charge transfer through the SAM blocking layers. While the longer chain SAMs exhibit good blocking properties, especially the C8-SH-SAM seems to show a number of pinholes even after long immersion times, which might be explained by weaker Van-der-Waals interaction between the shorter alkyl chains.

Since the SAMs block the electron transfer from species in solution, they can also be successfully used to block the electropolymerization of conducting polymers. The influence of  $\omega$ -substituted alkanethiols on gold electrodes has been, for example, studied in detail for the electropolymerization of pyrrole as a function of the potential, pH value, and monomer concentration.<sup>419,420</sup> It was shown that though initially the alkanethiols retard the polymerization of pyrrole, as soon as polymerization is nucleated, polymer films are rapidly deposited. In addition, the thiols even seem to enhance the rate of polymer deposition. Possible explanations for the reduced blocking properties after repeated cycling are the development of defects or the partitioning of monomer into the SAMs where they can be oxidized successfully.<sup>419</sup> The kinetics are consistent with nucleation at isolated sites, so-called pinholes in the SAM film. The polymer seems to grow out from the monolayer and across the surface to form a coherent film. Mazur and Krysinski have used the effect of pinholes in thiol self-assembled monolayers to electrochemically prepare conducting polymer microelectrodes from aniline and derivatives.<sup>421</sup> Starting the growth from film defects, isolated conducting polymer microislands can be prepared which, upon doping, behave like microelectrodes, whereas, upon dedoping, these areas reveal blocking properties.

A combination of microcontact printing of an octadecanethiol SAM on gold electrodes and electropolymerization of pyrrole using these templates was, among other publications, shown by Baba and Knoll.<sup>422</sup> Microcontact printing typically involves the stamping of the SAM onto flat gold using micropatterned poly(dimethyl siloxane) stamps. The resulting electrodes consist of areas of clean gold and areas modified with the SAM. Again, the SAMs are used to block electron-transfer, whereas electropolymerization can start from the gold areas. The polypyrrole initially grown on the Au surface can further act as nodes for the generation of interconnected surface networks of PPy—dendritic conducting polymer networks—during the electropolymerization. The samples were characterized by *in situ* electrochemical surface plasmon spectroscopy (EC-SPS), cyclic voltammetry, and AFM.

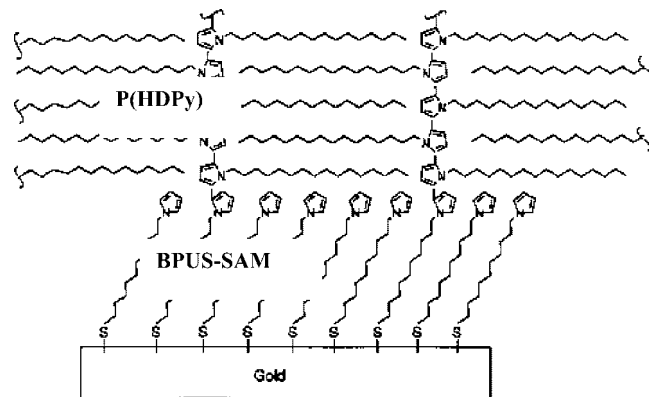


**Figure 40.** Representation of the chemical interaction between the surface confined pyrroles of bis( $\omega$ -(*N*-pyrrolyl)-*n*-undecyl)disulfide modified electrodes and *N*-hexadecylpyrrole monomers in solution. Reprinted with permission from ref 427. Copyright 2000 American Chemical Society.

The direct attachment of prepolymerized thiol-functionalized soluble polypyrrroles onto Au substrates was recently performed by Vercelli et al.<sup>423</sup> Polythiophene monolayers had been produced on gold before by adsorption of poly(3-alkylthiophenes)<sup>424</sup> and by sulfide linking of thiol-functionalized soluble polyalkylthiophenes.<sup>425</sup>

Several studies on SAMs bearing at least one electroactive monomer unit have been shown to fundamentally alter the nucleation and growth process of the following electropolymerization. Wrighton et al. used pyrrole attached to silicon with a silane group to promote the adhesion of subsequently electropolymerized poly(pyrrole).<sup>426</sup> EQCM and chronoamperometry were used to compare the electropolymerization of poly(*N*-hexadecylpyrrole) (P(HDPy)) on gold electrodes modified with a bis( $\omega$ -(*N*-pyrrolyl)-*n*-undecyl)disulfide BPUS-SAM and bare gold electrodes.<sup>427</sup> Films formed on BPUS-modified electrodes were more dense and grew in a more ordered manner than films prepared on the gold surface (Figure 40). The films were additionally more stable upon repeated cycling in a monomer-free electrolyte solution. The authors claim that the surface-confined pyrrole units of the SAM serve as specific nucleation sites for HDPy monomer species in solution by forming radical cations upon oxidation. When the oxidation potential of the monomer units in solution is reached, a reaction between surface confined pyrrole rings and monomers in solution can occur which leads to irreversible linkage of the polymer films to the underlying substrate.

SAMs bearing terminal amino groups were prepared by the adsorption of 4-aminothiophenol onto gold electrodes. After transformation of the amino groups into pyrrole rings, these surfaces were used as electrodes for the electrochemical polymerization of *N*-phenylpyrrole. Comparison of polymer films on modified and nonmodified Au electrodes by cyclic voltammetry again revealed significant differences in the growth characteristics of the films.<sup>428</sup>

The morphology of polythiophene films electrochemically grown on SAMs made from 11-(3-thienyl)undecyltrichlorosilane on indium tin-oxide (ITO) surfaces exhibits significantly lower roughness and higher density than PTh films directly grown on bare ITO surfaces.<sup>429</sup> Similar approaches have been recently exploited for carbazole,<sup>430</sup> thiophene, and oligothiophene derivatives.<sup>431,78</sup> Thin polyterthiophene films and oligothiophene-based self-assembled monolayers on ITO and gold were electrochemically coupled with different

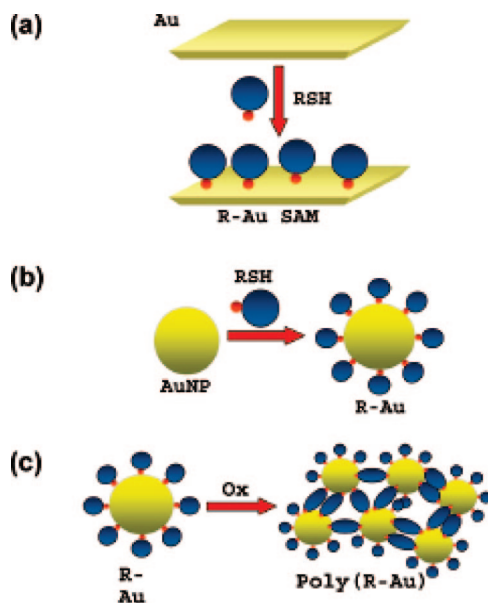


**Figure 41.** Pyrrolethiol- and thiophenethiol-capped Au nanoparticles linked together by electrochemical or chemical oxidation. Attachment of SAMs on a planar electrode (a) and on gold nanoparticles (b). (c) Electropolymerization leads to incorporation of gold nanoparticles in a conjugated polymer matrix. Reprinted with permission from ref 434. Copyright 2008 American Chemical Society.

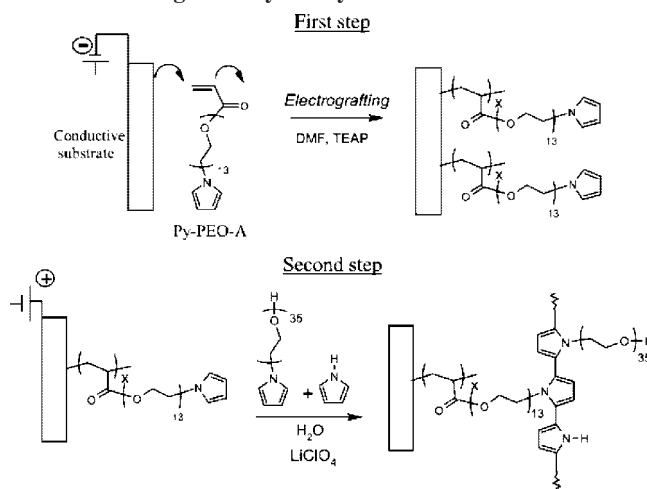
pyrrole- and thiophene-based monomers by anodic heterocoupling.<sup>78</sup> The nice thing in these investigations was that the corresponding homopolymers were soluble so that only surface-coupled polymers remained on the electrode and could be detected. This method allowed the formation of nanometer-size layers of polyconjugated polymers with nominally normal orientation of the chains to the surface, so-called polymer-brush electrodes.

So far, only planar electrodes have been discussed. Since thiol attachment on gold works on any geometry, gold nanoparticles can be incorporated into conducting polymer matrices, which provides a pathway to hybrid electrodes. Gold nanoparticles capped by ( $\omega$ -(*N*-pyrrolyl)decanepryrollyl)decanethiol were, for example, electropolymerized in methylene chloride at gold electrodes, yielding electrogenerated hybrid films of Au and poly(pyrrole).<sup>432,433</sup> A very recent publication by Zotti and Berlin includes a detailed study of gold nanoparticles linked by pyrrole- and thiophene-based thiols and their oxidative electrochemical coupling both as films and in solution (Figure 41).<sup>434</sup>

Electrografting provides a straightforward alternative to the use of SAMs to adhere redox-active units to the working electrode.

Lacroix and co-workers covalently attached ultrathin layers of thiophene derivatives to glassy carbon electrodes by electroreduction of diazonium salts.<sup>435</sup> The films were densely packed and were modeled as covalently grafted conducting oligomers (no pinholes could be observed by scanning electrochemical microscopy). Interestingly, these films were able to change their charge transfer characteristics upon doping (charge injection) from diode-like behavior to charge transfer transparency. Jérôme et al. studied  $\alpha$ -pyrrolyl- $\omega$ -acrylate-poly(ethylene oxide) (Py-PEO-A) as a dual macromonomer for electrografting:<sup>436</sup> the acrylate unit can be electrochemically grafted onto the electrode surface, leading to a hydrophilic coating of the electrode. Upon electrooxidation of a pyrrole and  $\alpha$ -pyrrole-PEO mixture, hydrophilic

**Scheme 13. Surface Modification of Electrically Conducting Substrates Using an Acrylate-Pyrrole Dual Monomer<sup>a</sup>**



<sup>a</sup> First step: Cathodic grafting of the monomer Py-PEO-A to the electrode. Second step: Anodic polymerization of Py monomers on the Py-PEO-A modified electrode. Reprinted with permission from ref 436. Copyright 2007 American Chemical Society.

and adherent polypyrrole films can be prepared (Scheme 13). The full, persistent adherence to the substrate and CV characteristics upon multicyclic voltammetry confirmed the electrochemical stability of the chemisorbed PPy films on the electrode.

Electrochemical growth of polypyrrole wires could be shown on electrografted electrodes of poly(ethylacrylate): first, cathodic electrografting of poly(ethylacrylate) films was performed to the electrode, followed by anodic electropolymerization of pyrrole using the modified electrode (Figure 42).<sup>437,438</sup> The grafted electrode actually behaves as a template for the PPy growth and triggers wire formation. The preparation of wires is strongly dependent on the experimental conditions: low conductivity for PPy is one of the prerequisites which can be addressed by using solvents with high donor number and low monomer concentrations. Further conditions are a high grafting density of the polyethylacrylate, a layer thickness of ~100 nm, and smooth substrates. Under these conditions, PPy nanowires were firmly attached to the electrode and the growth followed a columnar shape (Figure 42B).

### 6.2.2. Organic Supramolecular Arrays as Organic Templates

The morphology of conducting polymers can be drastically influenced by the presence of organic molecules forming superstructures in the electrolyte. Hatano and co-workers prepared anionic synthetic lipid assemblies as templates that exhibit helical superstructures in solution. Figure 43 shows an amphiphile bearing a L-glutamic segment, which forms a fibrous structure with a left-handed helical motif in methanol solution. Oxidative electropolymerization of EDOT and Py was carried out using this helical superstructure as template.<sup>439</sup> SEM images of the composite film showed that the resulting conducting polymers exhibit a left-handed helical structure, which is imposed by the amphiphile. *In situ* conductance experiments demonstrated the conductivity of the helical composites. The key step in this approach is the electrostatic attractive force between the cationic intermediates obtained during oxidation and the anionic assembly.

The presence of the polyanion poly(maleic acid-*co*-vinyl pyrrolidone) during the electropolymerization of pyrrole

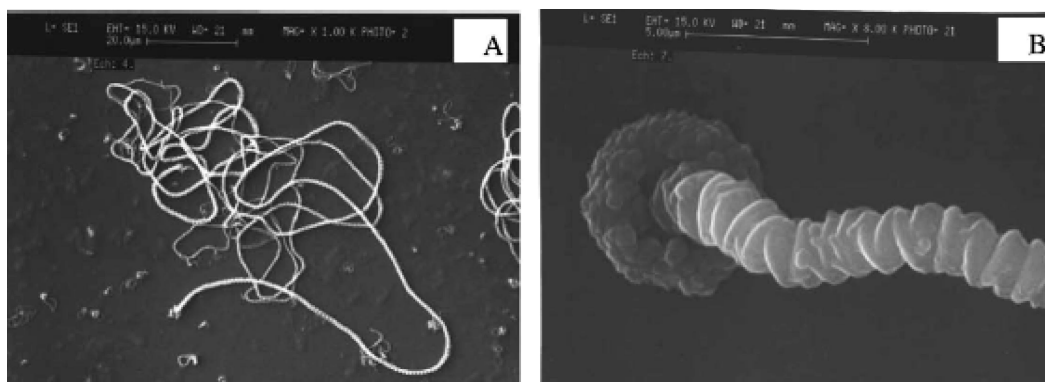


**Figure 42.** SEM micrographs of single fiber wires: (A) complete fiber, scale bar  $20\ \mu\text{m}$ ; (B) columnar microstructure of one fiber, scale bar  $5\ \mu\text{m}$ . Reprinted with permission from ref 438. Copyright 2004 Elsevier.

or aniline leads to CP nanowires.<sup>440</sup> In the absence of the polyanion under the same conditions, only nodular aggregates of the CP were obtained. Anionic porphyrin aggregates based on 5,10,15,20-tetrakis(4-sulfonatophenyl)porphyrin (TPPS) are also interesting templates, since it is well-known that porphyrins tend to aggregate into one-dimensional rodlike structures. They have been used as templates for electrochemical polymerization of EDOT, pyrrole,<sup>441</sup> and aniline<sup>442</sup> on ITO electrodes. Polymerization was carried out potentiodynamically in the presence of the porphyrin, resulting in rodlike structures 200–1000 nm in length and 30–50 nm in diameter. The films were characterized by UV-vis spectroscopy and *ex-situ* conductivity measurements. The aggregated TPPS molecules were entrapped in the CP matrix. Hatano and co-workers claim that, in principle, any superstructure can be created from CPs as long as the appropriate “anionic” assemblies suitable for the template exist.<sup>441</sup> In the few last years, a variety of biomolecules have been tested as morphology-directing agents for the elec-

tropolymerization of conducting polymers. Heparin, a highly sulfated, anionic polysaccharide composed of repeating glucosamine and uronic acid residues, could be used as template for the electrochemical growth of polypyrrole in a similar way.<sup>443</sup> In the approaches described above, the anionic assemblies function not only as a template but also as an anionic dopant. Water-soluble starch was recently shown to act only as structure-directing agent in the electrochemical synthesis of conducting polypyrrole (PPy) nanowires on a range of different substrates, e.g. ITO, stainless steel, titanium, gold, and graphite.<sup>444</sup> The synthesis of PPy nanowires involves two steps, as depicted in Figure 44. First, pyrrole monomers are spontaneously adsorbed onto starch molecules through hydrogen bonds in aqueous solutions. The adsorbed pyrrole monomers are subsequently electropolymerized along the starch chain. One advantage of this biomolecule approach is that the starch does not require removal from the final conducting polymer nanowire.

A novel way to control and lock-in molecular orientation in conducting polymers is to use a self-assembled medium of surfactant molecules. Poly(oxyethylene)<sub>n</sub>-oleyl ether ( $n = 10$ ) forms, for example, a hexagonal liquid crystalline (LC) self-supporting gel in water at concentrations between 35 and 60 wt %.<sup>445</sup> The aliphatic cores—which were measured to be 3 nm in diameter and 7.7 nm apart from each other—can incorporate hydrophobic molecules such as EDOT (which

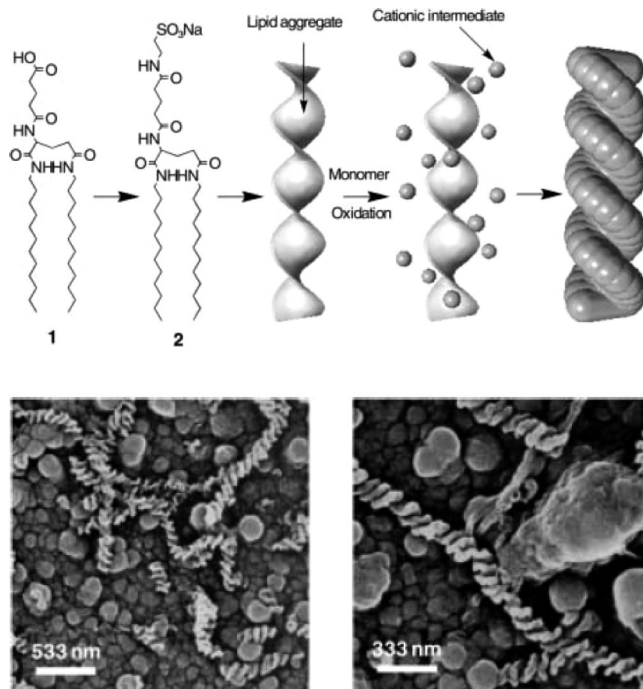


**Figure 43.** Top: Structure of (1) a synthetic lipid and (2) one bearing an L-glutamic segment, and schematic illustration of a templated oxidative electropolymerization. Bottom: SEM images of composite films of the synthetic lipid and PEDOT obtained by the templating method. Reprinted with permission from ref 439. Copyright 2004 Wiley-VCH.

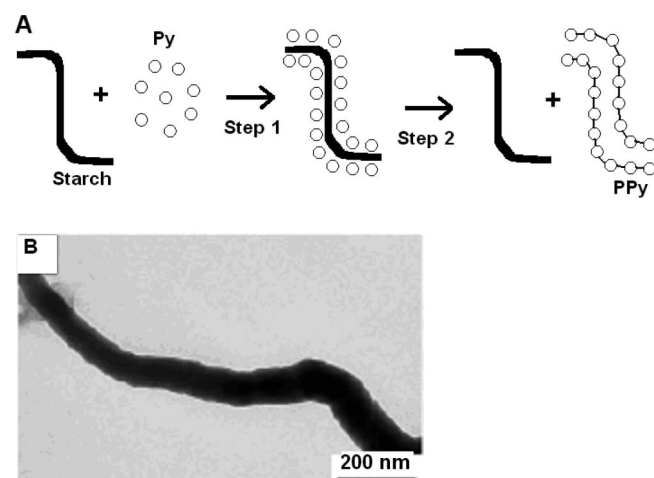


**Figure 44.** Simplified schematic representation of the synthetic procedure for the formation of PPy nanowires using starch as template: (A) Adsorption of Py on a starch surface in step 1; electropolymerization in step 2. (B) TEM image of a PPy nanowire. Reprinted with permission from ref 444. Copyright 2007 Royal Society of Chemistry.

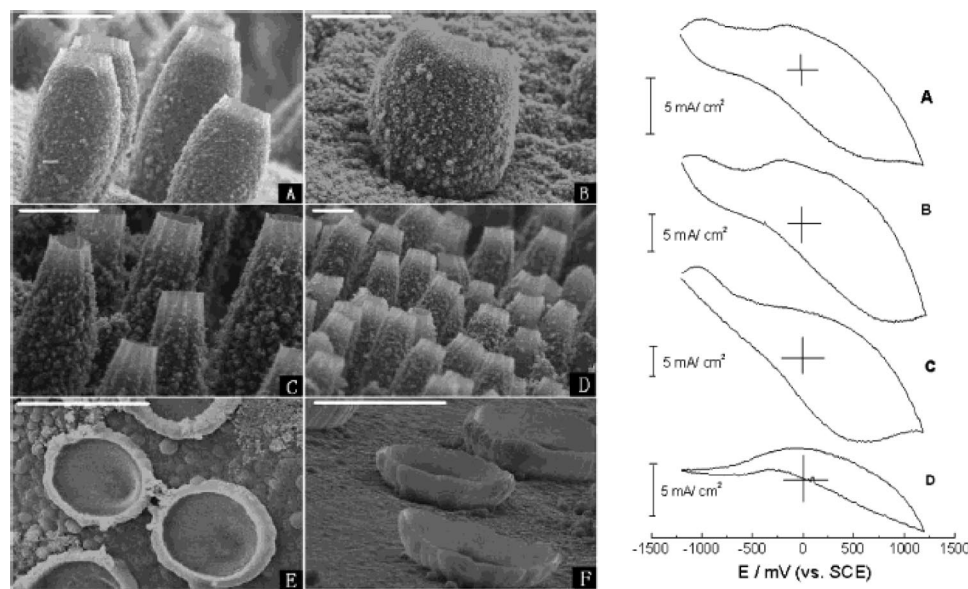


**Figure 45.** Left: Representative SEM images of PPy microstructures prepared by the gas bubble templating technique. Scale bars: 100  $\mu\text{m}$ . Right: CVs of PPy films showing microcups (A), microbowls (B), microgourds (C), and a flat film (D) in acetonitrile/tetrabutylammonium tetrafluoroborate at 100  $\text{mV}\cdot\text{s}^{-1}$ . Reprinted with permission from ref 452. Copyright 2003 American Chemical Society.

shows itself to have only a low solubility in water) up to a concentration of 0.25 M. These EDOT-doped gels could be successfully electropolymerized using tetraethylammonium perchlorate (TEAP) as a supporting electrolyte. Before performing the electropolymerization, the gels were exposed to a controlled temperature treatment in the sealed electrochemical cell to allow self-organization of the LCs into large, uniaxial domains,  $\sim 500 \mu\text{m}$  in size. After electropolymerization, the LC gel could be removed, leaving well-adhered PEDOT films, revealing birefringent domains matching those of the LC medium. The authors of this work propose that polymerization within the nanoscopic domains produces polymer chains oriented parallel to the LC director. The optical anisotropy of the template is apparently transferred to the PEDOT film during polymerization. The structure is locked-in due to the insolubility of the polymer.

Polyaniline nanowires in emeraldine form were electropolymerized in 1D aqueous channels formed by reverse hexagonal LC phases of the surfactant sodium bis(2-ethylhexyl) sulfosuccinate.<sup>446</sup>

Optically active, chiral conducting polymers were successfully electropolymerized in the group of Akagi.<sup>447–450</sup> Chiral conducting electrodes are particularly interesting for applications such as recognition of enantiomers or their use as chiral working electrodes in preparative electrosynthesis.<sup>451</sup> Both thermotropic LC phases based on (*R*)- or (*S*)-1'-binaphthyl-2,2'-bis-[*p*-(*trans*-4-pentylcyclohexyl)phenoxy-1-hexyl] ether (PCH506-Binol)<sup>447,448</sup> as well as lyotropic LC phases based on DNA<sup>449</sup> and hydroxypropyl cellulose<sup>450</sup> resulted in successful electropolymerizations of PEDOT and poly(bithiophene).

### 6.3. Tuning of Morphologies Using Templates and Patterning Techniques

#### 6.3.1. Soft Templates—The Gas Bubble Technique

Controlled electrochemical growth of CP microcontainers can be achieved by the so-called gas-bubble or soap-bubble technique. The oxidative electrolysis of slightly acidic water containing  $\beta$ -naphthalenesulfonic acid<sup>452,453</sup> (NSA) or cam-

phor sulfonic acid<sup>454,455</sup> (CSA) as electrolyte and surfactant was shown to generate small bubbles of  $\text{O}_2$  during the electropolymerization of pyrrole. The released  $\text{O}_2$ -bubbles are stabilized by the anionic surfactant molecules in the solution and assembled on the working electrode to act as “soap bubble” templates for the electropolymerization of the CP, leading to microstructures with a variety of different shapes. The size and shape can be modulated by the electrochemical conditions. Some scanning electron micrographs of representative PPy structures are shown in Figure 45.<sup>450</sup> The walls of the microstructures were confirmed to consist of PPy in the doped state. CV measurements of different structures reveal rather strong and broad redox waves in acetonitrile/tetrabutylammonium tetrafluoroborate due to their large surface area (Figure 45).

PPy microcontainers can also be obtained by direct oxidation of pyrrole monomer in an aqueous solution of poly(4-styrene sulfonic acid) (PSSA).<sup>456</sup> The microstructures consisted of PPy in the doped state with typical conductivity values ranging from  $10^{-2}$  to  $10 \text{ S}\cdot\text{cm}^{-1}$ . Good reproducibility and high densities (higher than 2000 units  $\text{cm}^{-2}$ ) were obtained. PSS doped PEDOT films exhibiting ring-, arrow-, and bubble-like microstructures have been generated by cyclic voltammetry in aqueous media; here again, the self-assembled “gas bubble” template mechanism has been proposed to explain the different shapes.<sup>457</sup> Microflowers<sup>458</sup> and microrings<sup>459</sup> could be electrochemically grown from self-doped polyanilines (Figure 46). The electroactivity of these structures can be kept at a very wide pH range, which is desirable for sensor design, especially in pH-neutral and base solutions.

Instead of using  $\text{O}_2$ -gas bubbles which might lead to overoxidation of the conducting polymers,  $\text{H}_2$  bubbles can also be used as templates. For this templating approach, an electroreduction step for the generation of  $\text{H}_2$  has to be performed before the electropolymerization of CPs, as demonstrated by Dai and co-workers.<sup>460</sup> For electropolymerization of PPy microstructures, naphthalenesulfonic acid aqueous solutions containing the pyrrole monomer were first cycled to negative potentials to generate  $\text{H}_2$  bubbles around

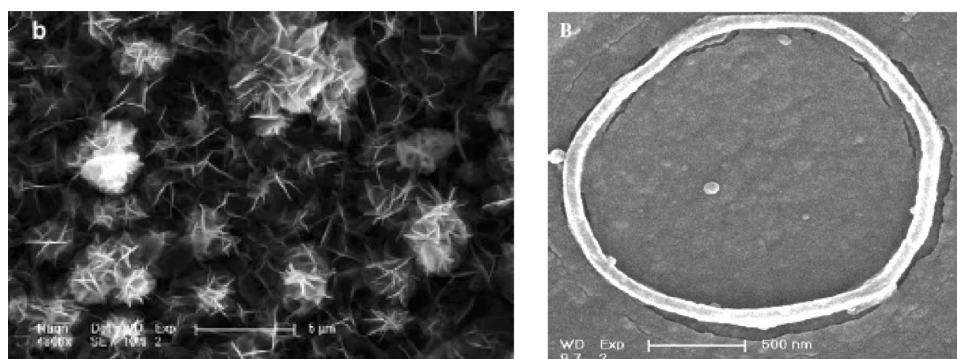


**Figure 46.** Microflowers and microrings of self-doped PANI. Reprinted with permission from refs 458 and 459. Copyright 2005 Elsevier and 2006 Institute of Physics.

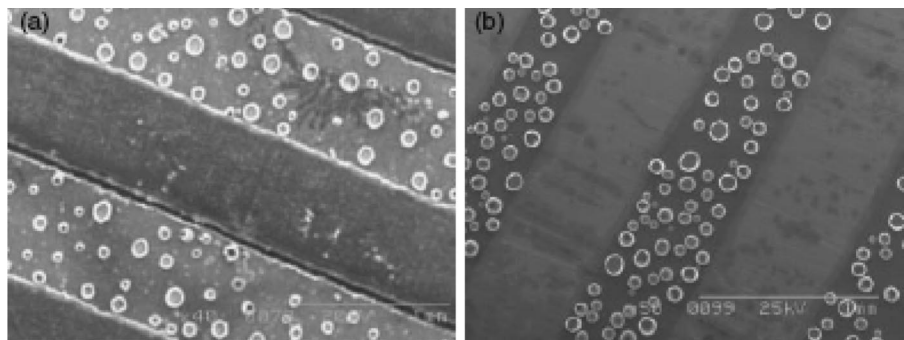


**Figure 47.** SEM images of polypyrrole microcontainer patterns using the gas bubble technique. Pattern induced by microcontact printing (a) and by plasma patterning (b). Scale bars 1 mm. Reprinted with permission from ref 460. Copyright 2004 Wiley-VCH.

the working electrode, followed by a change of the potential window to positive values to induce the pyrrole electropolymerization. The resulting microstructures showed good uniformity and exhibited high densities (2000–4000 units  $\text{cm}^{-2}$ ) on the surfaces. By prepatterning the working electrode with microcontact printing or plasma patterning, the CP microcontainers could be arranged in a controlled fashion (Figure 47). Hui and co-workers reported on the design of nanoporous PPy films using hydrogen bubbles as templates in a so-called template synthesis route.<sup>461</sup> They generated hydrogen bubbles on HOPG surfaces and electrodeposited polypyrrole onto these substrates. Electrochemical atomic force microscopy (EC-AFM) was conducted during the experiment and allowed *in situ* probing of the surface. After removal of the nanobubbles, nanoporous PPy films could be generated. This technique allows the preparation of a large variety of micro- and nanostructures by tuning of the electrochemical conditions.

### 6.3.2. Sacrificial Hard Template Methods

Electropolymerization in hard templates is a straightforward way to produce specific shapes of CPs on the micro- and nanometer scale. Template-assisted electropolymerization can be performed within channels, holes, or cavities of any porous template as long as it has a continuous pore structure from the top of the template down to the underlying electrode. The dimensions of the template determine the size of the CP replicated structure. Freestanding structures of CPs can be obtained when the templates are selectively removed after the electropolymerization. The most common templates used for nanotechnological applications are colloidal particles, anodized alumina membranes, track-etched membranes, and diblock copolymers. Structures obtained with these templates are inverse opals and nanotubes and nanow-

ires. Martin's group has pioneered the work of sacrificial template methods.<sup>462,463</sup>

**Colloidal Templates.** It is well-known that colloids made out of  $\text{SiO}_2$  or polymers, such as polystyrene (PS), can self-assemble into periodic three-dimensional structures, so-called colloidal crystals. These materials are thought to be ideal candidates for the construction of photonic band gap crystals with enhanced interaction with light. In principle, even nanometer-sized colloidal crystals can be formed. Braun and Wiltzius reviewed the use of these materials as templates for electrochemically grown semiconductors, polymers, and metals.<sup>464</sup> The electropolymerization procedure consists typically of three steps (Figure 48). First a highly ordered PS colloidal crystal is deposited on the electrode. Then a monomer/electrolyte solution is infiltrated into the interstitial spaces of the colloids and electropolymerization of the monomer is carried out. When the template is finally removed—in the case of PS with solvent—a microporous structure of the CP with inverse opal morphology is produced. Knoll et al. used this method to fabricate ordered honeycomb shaped PANI and its copolymers with poly(acrylic acid) and poly(styrene sulfonate) (Figure 48).<sup>465</sup> They claimed that the PANI grows first from the surface of the conducting substrate and then gradually covers the 3D templates from the bottom to the top. A similar growth mechanism was reported for 2D nanosphere templates; this methodology is known under the term nanosphere lithography.<sup>466</sup>

The inverse opal PANI films of Knoll et al.<sup>465</sup> exhibited high quality and remained electroactive in buffer solutions at neutral pH, which made them good candidates for biosensing applications. An application of these macroporous structures was presented in the electrocatalysis of the oxidation of reduced  $\beta$ -nicotinamide adenine dinucleotide

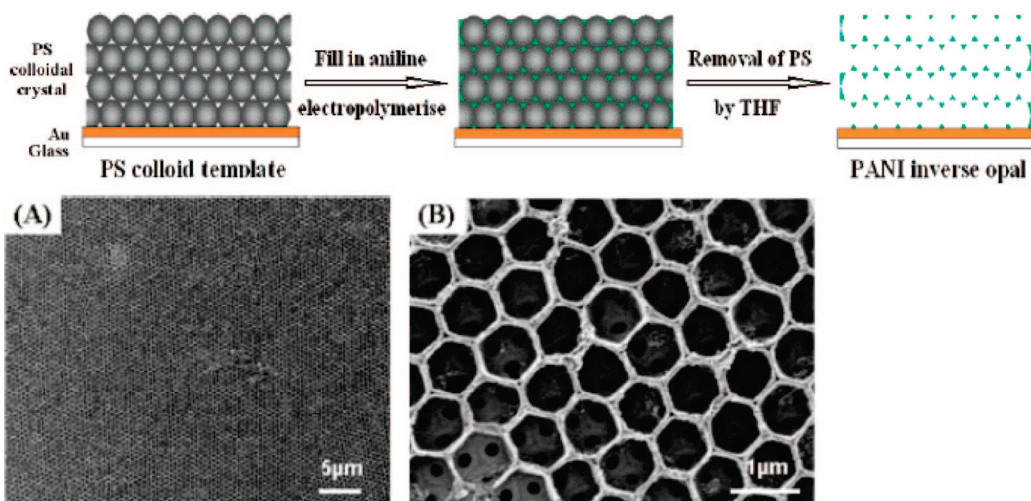


**Figure 48.** Schematic illustration of the procedure used for fabricating PANI inverse opal microstructures via electropolymerization within a PS colloidal crystal on top of a gold electrode. SEM-images of the PANI inverse opals with two different magnifications (A and B). Reprinted with permission from ref 465. Copyright 2005 American Chemical Society.

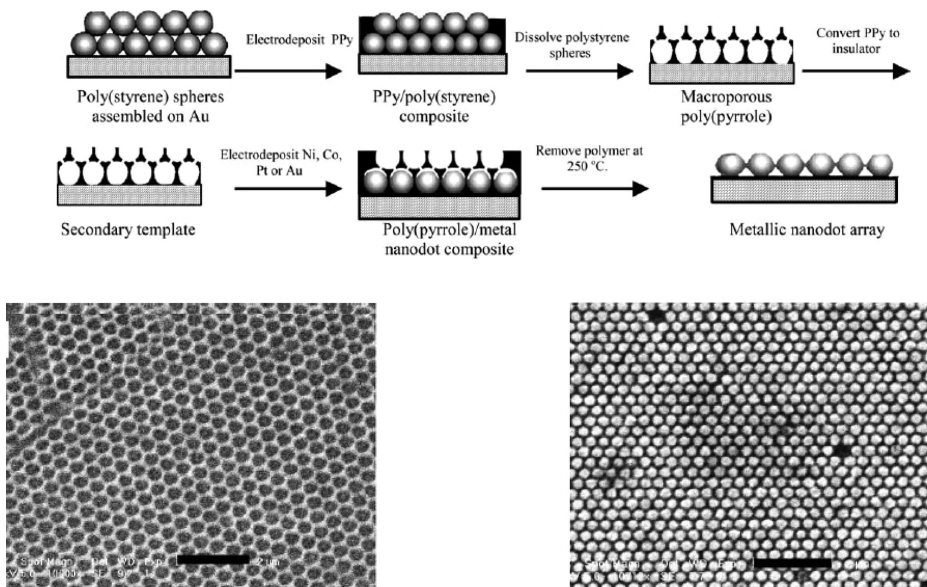


**Figure 49.** Schematic representation of the sequence of steps using a double templated electrodeposition method for the fabrication of arrays of metal nanodots. Left SEM image: PPy/dodecylbenzene sulfonate film electrodeposited within 500 nm PS spheres as a primary template. Right SEM image: array of Co nanodots after removal of the PPy secondary template. The scale bars amount to 2 μm. Reprinted with permission from ref 470. Copyright 2004 Elsevier.

(NADH). The structured films showed an increase of the electrocatalytic efficiency compared to the case of planar films. In another example, PPy based inverse opals were used as transducers for biosensors upon charging the CP matrix with an enzyme.<sup>467</sup> The sensing enhancement was found to be independent of the thickness of the films with up to a 7-fold increase of the analytical signal. This result was explained by an increase of the electroactive area that is controlled by the diameter of the original PS template<sup>468</sup> and the electrodeposition conditions. The conductivity values of PANI, PPy, and PBTh showing inverse opal structures are typically higher than those obtained for the planar films.<sup>469</sup> This result is consistent with early reports by Martin,<sup>462</sup> who demonstrated the increase of conductivity of conducting polymers upon an increase of the electroactive surface.

Ghanem et al. used the colloidal template method to produce polypyrrole and further refilled the CP inverse-opal structures with metals by electroreduction of the corresponding metallic salts.<sup>470</sup> Subsequent degradation of the conduct-

ing polymer by pyrolysis lead to well-ordered arrays of metallic nanodots (Figure 49). Platinum, gold, cobalt, and nickel have been successfully prepared in this way.

Surface charge control of nanoparticle templates can also be used to control the electrochemical preparation of CP nanostructures.<sup>466,471</sup> Smyth and co-workers used as model system 2-dimensional PS nanoparticle templates which were coated with either negatively charged poly(sodium 4-styrenesulfonate) or positively charged poly(diallyldimethylammonium chloride) (Figure 50).<sup>471</sup> Upon electrochemical deposition of PANI, PS/PANI-core-shell particles (Figure 50A) and PANI-PS nanocomposites (Figure 50B) were obtained for the negatively and positively charged PS templates, respectively, due to different growth mechanisms. For the negatively charged templates, the formation of core-shell particles was explained by the strong adhesion of the positively charged aniline monomers to the negative surface of the PS spheres, which lead to hollow PANI spheres after dissolution of the PS template. For the positively

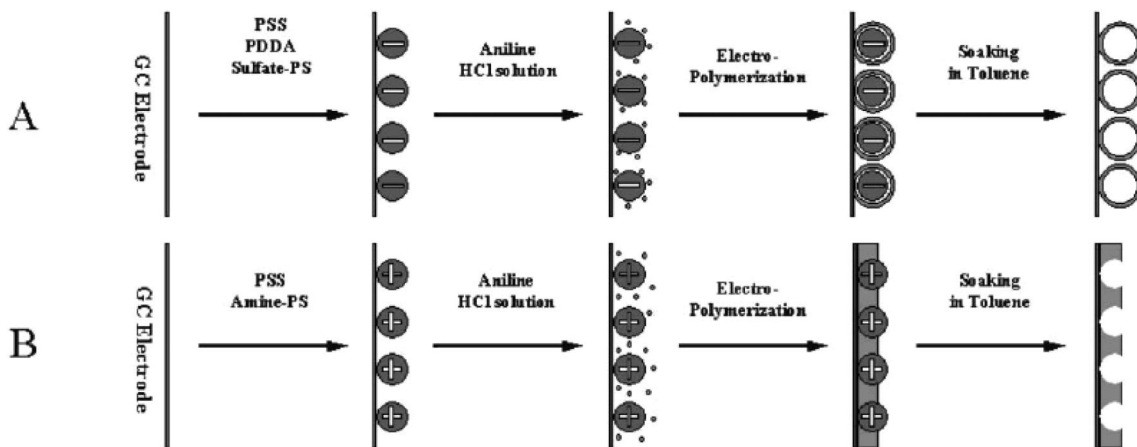


**Figure 50.** Schematic representation of nanostructured PANI-materials based on negatively (A) and positively (B) charged PS spheres on GC electrodes. Reprinted with permission from ref 471. Copyright 2007 Royal Society of Chemistry.

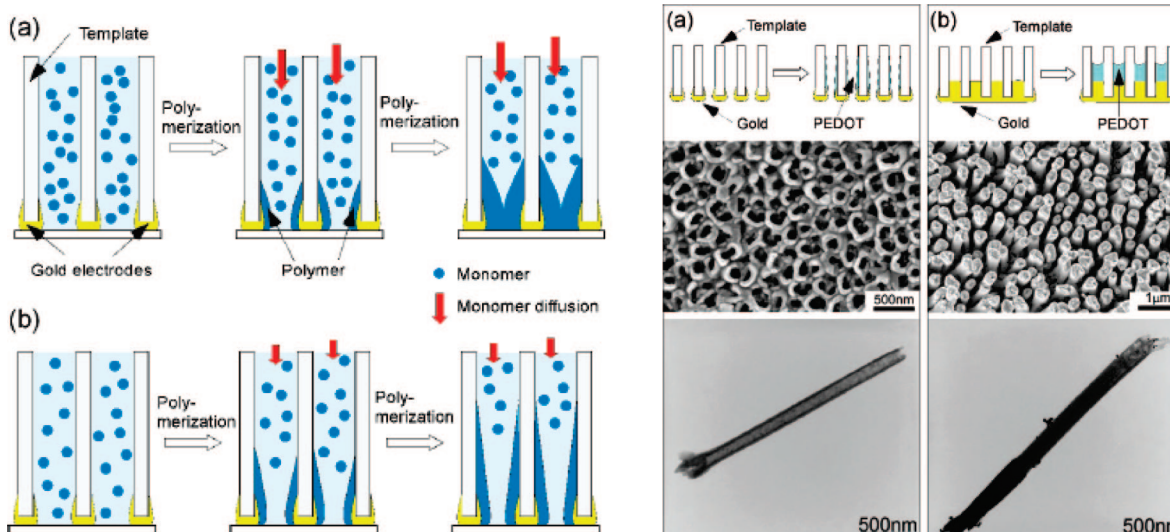


**Figure 51.** Left: Growth mechanism of PEDOT nanostructures based on diffusion and reaction kinetics for high oxidation potentials ( $\geq 1.4$  V). (a) Slow reaction rate under sufficient monomer supply; (b) fast reaction rate under insufficient monomer supply. Right: Growth mechanism of PEDOT nanostructures at very low oxidation potentials ( $< 1.4$  V) based on the predominance of electrochemically active sites on sharp electrode edges. Two cases: (a) annular and (b) flat-top electrodes together with SEM images of the electrodes and TEM images of the resulting PEDOT nanostructures. Reprinted with permission from ref 472. Copyright 2008 American Chemical Society.

charged templates, the formation of nanocomposite films was favored due to the preferential growth of PANI from the electrode. In this case, the positively charged aniline monomers are repelled by the template. SEM images showed nanoporous films after removal of the template.

**Nanoporous Membranes.** The synthesis of conducting polymer nanotubes and nanowires has recently been reviewed by Cho and Lee.<sup>472</sup> Conjugated polymers, such as PEDOT, PPy, PANI, and poly(3-hexylthiophene), can be successfully electropolymerized within nanoporous membrane templates, such as anodized aluminum oxide (AAO) membranes and track-etched polycarbonate membranes.<sup>473–478</sup> Electropolymerization was found to lead either to solid nanowires or to hollow nanotubes depending on the experimental conditions. A conclusive model has not been presented so far. Martin and co-workers proposed a model based on electrostatic and solvophobic interaction between the polymer and the pore walls to explain nanotube growth, which is thought to be applicable to chemical and electrochemical template synthesis.<sup>462</sup> Demoustier-Champagne made systematic investigations on the experimental parameters, such as electrolyte concentration, on PPy nanotubes.<sup>475,479</sup> Lee and co-workers

systematically investigated the electropolymerization of PEDOT within anodized alumina membranes (Figure 51).<sup>472,474</sup> The electropolymerization was performed potentiostatically with a Pt counterelectrode and an Ag/AgCl reference electrode using 0.1 M LiClO<sub>4</sub> in acetonitrile as electrolyte solution. At potentials below 1.4 V, electropolymerization is dominated by a mechanism based on the number of electrochemically active sites producing the nanowire structures of PEDOT and is strongly dependent on the base electrode shape. At high potentials ( $\geq 1.4$  V), the shape of the PEDOT nanotubes seems to be controlled by a mechanism based on diffusion and reaction kinetics. The interaction between pore wall and polymers has to be considered as well. This description has been shown to apply to other conducting polymers (PPy, P3HT).

Studies on the electrochemical synthesis of polyaniline in aqueous H<sub>2</sub>SO<sub>4</sub> solutions revealed a dependence of the growth of solid nanowires with tubular ends to open nanowires on the H<sub>2</sub>SO<sub>4</sub> concentration.<sup>480</sup> At high anodic potentials, the current transient data fitted a 3D diffusion-controlled nucleation and growth model, whereas a 1D branching model is applicable at lower potentials.

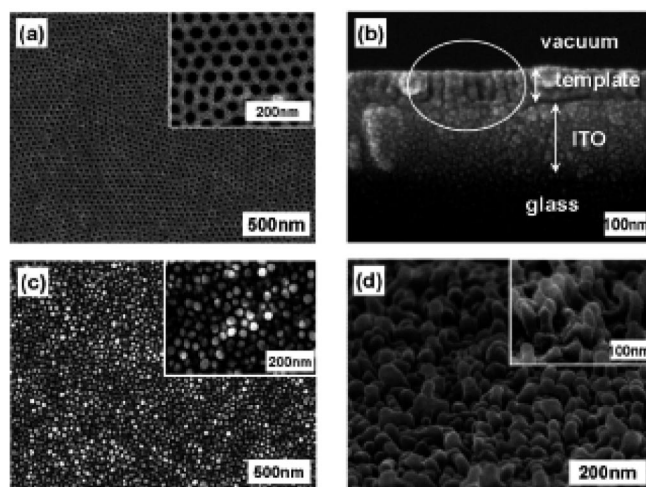


**Figure 52.** Growth of PPy nanorods in nanoporous block copolymer templates. Scanning electron micrographs of nanoporous templates prepared by films of polystyrene-*block*-poly(methyl methacrylate)/poly(methylmethacrylate) mixtures after degradation of poly(methyl methacrylate) on ITO glass: top (a) and cross-sectional (b) views. (c) Top and (d) cross-sectional images of PPy nanorods after removing the template. Reprinted with permission from ref 481. Copyright 2008 American Chemical Society.

Highly aligned ultrahigh density arrays of conducting polymer nanorods can also be prepared in block copolymer templates.<sup>481</sup> Block copolymers are promising materials for nanotechnology applications because they spontaneously microphase-separate into ordered structures with domain sizes ranging from 5 to 50 nm via self-assembly.<sup>482,483</sup> Large-area vertical orientation of cylindrical microdomain structures in a film can be achieved, for example using electrical fields.<sup>484–486</sup> Upon degradation of the minority block, these templates can be used for the growth of metal and semiconductor arrays. Similar templates were used for the electropolymerization of PPy and PEDOT (Figure 52).<sup>481</sup> The conductivity of individual nanorods was measured using current-sensing atomic force microscopy. High resolution transmission electron microscopy showed that the main chains of PPy are aligned along the nanorod direction. The measurements revealed high alignment of the polymer chains and an enhanced conductivity along the nanorod axes, i.e. along the growth direction of the electropolymerization.

It should be pointed out that template-synthesized CP materials typically have a higher conductivity than the bulk material, which can be explained by improved packing order and alignment of the polymer chains.<sup>487</sup> Martin and co-workers showed that polypyrrole nanofibers have higher charge transport rates than planar films under the same conditions.<sup>488</sup>

Variations of the light-emitting color and the photoluminescence intensity on the nanoscale were observed for the single strand of poly(3-butylthiophene) nanowires with different doping states when investigated with laser confocal microscopy.<sup>489</sup>

There are many applications where nanowires with their extremely high surface/volume ratio can be implemented. Fast color-switching electrochromic devices,<sup>490,491</sup> resistors, diodes, and field-effect transistors were, for example, demonstrated.<sup>492,493</sup> Lee and co-workers reported on the coelectrodeposition of MnO<sub>2</sub>/PEDOT coaxial wires in porous alumina membranes for electrochemical energy storage.<sup>494</sup> The coaxial wires were reported to have very high capaci-

tances at high current densities due to the hybrid character of the material.

### 6.3.3. Patterning with Scanning Probe Techniques (Direct Writing)

Direct writing of micro- and nanostructures with high spatial resolution can be achieved with scanning probe techniques.

Scanning electrochemical microscopy (SECM) is a surface analysis and modification technique in which an ultramicro-electrode (UME) is scanned across a surface immersed into an electrolyte solution. The faradaic current measured at the tip originates from a redox reaction of the electroactive species in the solution and depends strongly on the chemical nature of the substrate and the tip–sample distance. Scanning the UME at a constant height provides valuable information about local surface conductivity, morphology, concentration profiles, and maps of reactive sites. The first experiments on the deposition of CPs with SECM were performed in the direct mode where the substrate serves as counter electrode: Bard et al. showed the microdeposition of polyaniline on platinum,<sup>495</sup> and Schuhmann et al. deposited polypyrrole on gold-coated glass with a lateral resolution of 60 μm.<sup>496</sup> Zhou and Wipf then reported the electrodeposition of polyaniline micropatterns on gold, platinum, and carbon surfaces using pH shifts induced by the feedback mode of SECM.<sup>497</sup> In this so-called microreagent mode, a local pH increase at the SECM tip provides a condition necessary to polymerize aniline on the substrate. Turyan and Mandler studied polyaniline patterning on self-assembled monolayer modified electrodes,<sup>498</sup> and local electropolymerization of 2',5'-bis(1-methylpyrrol-2-yl)thiophene on poly(methyl methacrylate) substrates with a lateral resolution of 15 μm was reported by Heinze et al.<sup>499</sup>

Figure 53 shows the sketch of an electrode surface covered with a film of 4,4'-(dimethoxybithiophene) (DMBT) made by spin coating which is locally electropolymerized.<sup>500</sup> The UME locally oxidizes the mediator ruthenium (2,2'-bipyridine) (Ru(bipy)<sub>3</sub>Cl<sub>2</sub>) dissolved in water, which is reduced at the surface by the DMBT monomer, whereas the monomer is electropolymerized simultaneously. This approach takes advantage of the poor solubility of monomer and uncharged oligomers in aqueous solutions. Oxidation at constant current produced regular thin microstructures with a lateral resolution of 15 μm, proving the high resolution microstructuring possibility of the SECM technique.

Even smaller micropatterns of polythiophene with lateral resolution between 8 and 10 μm were prepared by electropolymerizing thiophene monomers dissolved in aqueous electrolytes onto immobilized MnO<sub>2</sub> substrates which can be locally activated by tip-generated protons. The galvanostatic oxidation of a mediator and the introduction of a chemical lens<sup>501</sup> produced well-defined, regular, and thin microstructures (Figure 54).<sup>502</sup> This approach is suitable for monomers with high solubilities in water.

Nanostructures in the subnanometer regime can be fabricated using electrochemical dip-pen nanolithography (E-DPN) which is an atomic force microscopy lithography technique.<sup>503</sup> The trick of DPN is that spontaneous condensation helps the transport of material from the AFM tip onto a surface (Figure 55). An electrochemical reaction can then immobilize the material on the surface. Material deposition is localized on the patterns traced by the AFM tip, thereby providing an intrinsically site-specific technique. In the

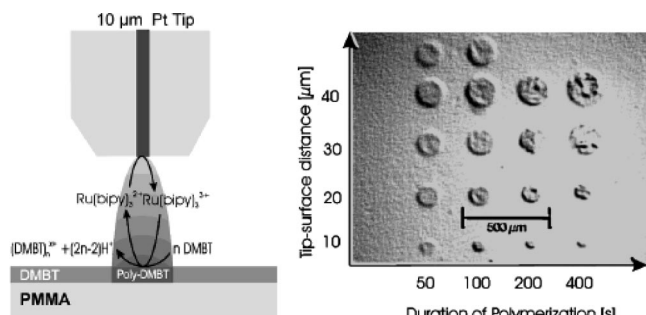


**Figure 53.** SECM experiment of the local polymerization of 4,4'-dimethoxybithiophene with a UME as oxidizing tip. Right image: Micropatterns of poly(4,4'-dimethoxybithiophene) on PMMA. Tip: 50  $\mu\text{m}$  Pt, RG (shielding ratio) = 50, potential = +1.2 V vs Ag/AgCl; electrolyte = 10 mM Ru(bipy)<sub>3</sub>Cl<sub>2</sub>, 10 mM Ru(NH<sub>3</sub>)<sub>6</sub>Cl<sub>3</sub>, and 100 mM NH<sub>4</sub>Cl. Reprinted with permission from ref 500. Copyright 2001 Wiley-VCH.



**Figure 54.** Micropattern of polythiophene obtained by local electrodeposition via SECM. Tip: 10  $\mu\text{m}$  Pt, RG (shielding ratio) = 10, electrolyte = 40 mM KNO<sub>3</sub>, 20 mM thiophene, 10 mM NaHCO<sub>3</sub>. Galvanostatic process = 20 nA; scan rate = 0.8  $\mu\text{m} \cdot \text{s}^{-1}$  at a distance of 8  $\mu\text{m}$  from the surface; pattern width = 20  $\mu\text{m}$ . Reprinted with permission from ref 502. Copyright 2001 American Chemical Society.

experiments by Liu et al., a typical experiment involved first the coating of a highly doped silicon AFM tip by immersion into a EDOT chloroform solution and subsequent drying.<sup>504</sup> Oxide-coated silicon wafers were used as substrates. Upon application of a negative bias between the AFM tip and the surface, EDOT is electropolymerized, leading to a tip-defined deposition of the polymer. Figure 55 shows two polymer lines written at different scan rates. Polyanilines, polypyrrroles, oligothiophene,<sup>505</sup> and polythiophene wires have been successfully written on semiconducting and insulating surfaces in the sub-100 nm regime with this method.

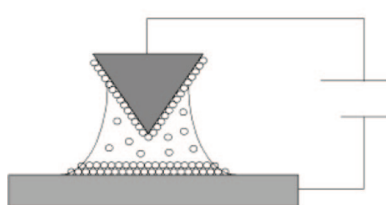


**Figure 55.** Schematic setup of the E-DPN setup. Two polythiophene wires written by E-DPN at 10 (left wire) and 1 nm/s (right wire). The voltage was -12 V. Polymer line width: 50 nm. Reprinted with permission from refs 503 and 504. Copyright 2001 and 2002 American Chemical Society.

## 7. Concluding Remarks

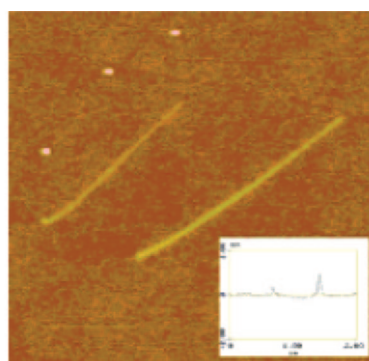
This review documents the substantial progress in the field of electrochemistry of CPs that has been gained during the few last years. Starting with the electrochemical formation mechanism of CPs, it has been clarified that oligomerization occurs in solution in front of the electrode and is preferably based on succeeding “dimerization” steps of ionic (radicalic) species. Deposition of the oligomers involves nucleation, growth, and solid state coupling processes. A chain propagation mechanism as postulated in the older literature seems to be very improbable. An important aspect concerns the  $\sigma$ -coupled intermediates which are formed after each oxidation of oligomeric species. Their stability increases as a function of chain length. There are also clear indications that  $\sigma$ -coupled chains are reversibly generated during charging/discharging of CPs. Besides, in the literature the existence of charged  $\pi$ -dimers is discussed.

The results of the oligomer approach prove that the redox charging of conjugated systems is due to potential-dependent successive redox steps, which may overlap, causing a faradaic plateau current. Experimental evidence of the existence of bipolarons as predicted by the band model is rare. In fact, there are increasing signs based on spectroscopic and electrical data that conducting polymers resemble molecular systems. Especially, recent conductivity measurements substantiate that conductivity is correlated with single redox states and reaches an optimum in overlapping mixed valence states.

The unconventional properties of CPs have triggered off considerable efforts to develop functionalized systems and to create new architectures (1D to 3D) on the molecular and mesoscopic level. Conceivable applications such as electrocatalysis, electronic devices, solar cells, or electrochromic windows are just a few challenges which have motivated researchers to refine strategies in preparing materials with tailor-made properties. In particular, nanoscience has proven to be a fascinating new area that touches the limits of macroscopic laws and includes quantum effects. Therefore, with regard to a correct interpretation of all these phenomena, it is necessary that the basic properties of CPs are well understood. It seems that experiment and theory are approaching this aim.

## 8. Acknowledgments

We would like to thank the BMBF, the DFG, the VW-Foundation, the GIF, and the BA-Wü-Research Programme



for generous financial support. It is a great pleasure to thank former and past co-workers of the Electrochemistry Group in Freiburg for their basic contributions to the electrochemistry of conducting polymers: Prof. K. Meerholz, Dr. M. Dietrich, Dr. A. Smie, Dr. P. Tschuncky, Dr. B. Geschke, Dr. M. Pagels, Dr. M. Zhou, Dr. A. Rasche, Dr. H. John, Dr. P. Espindola, and Dr. R. Alle. In addition, the inspiring successful cooperation with colleagues of the scientific community is gratefully acknowledged: Prof. K. Müllen (Mainz), Prof. P. Bäuerle (Ulm), Prof. T. Heinzel (Düsseldorf), Dr. M. Skompska (Warsaw), Prof. E. Vieil (Grenoble), Prof. M. Vorotyntsev (Dijon), Prof. F. Würthner (Würzburg), Prof. R. Holze (Chemnitz), Prof. S. Hüning (Würzburg), Prof. D. Mandler (Jerusalem). S.L. acknowledges funding within the Emmy-Noether Programme and the Freiburg Institute for Advanced Studies (FRIAS) of the DFG and the Landesstiftung BW. B.A.F. acknowledges a DAAD fellowship and a CONACYT-Mexico grant (No. 57856).

## 9. References

- (1) Lethaby, H. *J. Chem. Soc.* **1862**, *15*, 161.
- (2) Shirakawa, H.; Louis, E. J.; MacDiarmid, A. G.; Chiang, C. K.; Heeger, A. J. *J. Chem. Soc., Chem. Commun.* **1977**, 578.
- (3) Chiang, C. K.; Park, Y. W.; Heeger, A. J.; Shirakawa, H.; Louis, E. J.; MacDiarmid, A. G. *Phys. Rev. Lett.* **1977**, *39*, 1098.
- (4) Delamar, M.; Lacaze, P. C.; Dumousseau, J. S.; Dubois, J. E. *Electrochim. Acta* **1982**, *27*, 61.
- (5) Wnek, G. E.; Chien, J. C. W.; Karasz, F. E.; Lillya, C. P. *Polymer* **1979**, *20*, 1441.
- (6) Diaz, A. F.; Kanazawa, K. K.; Gardini, G. P. *J. Chem. Soc., Chem. Commun.* **1979**, 635.
- (7) Diaz, A. F. *Chem. Scr.* **1981**, *17*, 142.
- (8) Tourillon, G.; Garnier, F. *J. Electroanal. Chem.* **1982**, *135*, 173.
- (9) Diaz, A. F.; Logan, J. A. *J. Electroanal. Chem.* **1980**, *111*, 111.
- (10) Noufi, R.; Nozi, A. J.; White, J.; Warren, L. F. *J. Electrochem. Soc.* **1981**, *129*, 2261.
- (11) Heywang, G.; Jonas, F. *Adv. Mater.* **1992**, *4*, 116.
- (12) Dietrich, M.; Heinze, J.; Heywang, G.; Jonas, F. *J. Electroanal. Chem.* **1994**, *369*, 87.
- (13) Heeger, A. J. *Angew. Chem., Int. Ed.* **2001**, *40*, 2591.
- (14) MacDiarmid, A. G. *Angew. Chem., Int. Ed.* **2001**, *40*, 2581.
- (15) Shirakawa, H. *Angew. Chem., Int. Ed.* **2001**, *40*, 2575.
- (16) *Sci Finder*, March 2010.
- (17) Diaz, A. F.; Castillo, J. I.; Logan, J. A.; Lee, W. Y. *J. Electroanal. Chem.* **1981**, *129*, 115.
- (18) Genies, E. M.; Bidan, G.; Diaz, A. F. *J. Electroanal. Chem.* **1983**, *149*, 101.
- (19) Andrieux, C. P.; Audebert, P.; Hapiot, P.; Savéant, J. M. *J. Phys. Chem.* **1991**, *95*, 10158.
- (20) Andrieux, C. P.; Hapiot, P.; Audebert, P.; Guyard, L.; Nguyen, D. A. M.; Groenendaal, L.; Meijer, E. W. *Chem. Mater.* **1997**, *9*, 723.
- (21) Heinze, J.; Tschuncky, P. In *The Oligomer Approach*; Müllen, K., Wegner, G., Eds.; VCH-Wiley: Weinheim, 1998; p 479.
- (22) Ofer, D.; Crooks, R. M.; Wrighton, M. S. *J. Am. Chem. Soc.* **1990**, *112*, 7869.
- (23) Villeret, B.; Nechtschein, M. *Phys. Rev. Lett.* **1989**, *63*, 1285.
- (24) Freund, M. S.; Deore, B. *Self-Doped Conducting Polymers*; Wiley: Chichester, 2007.
- (25) Skotheim, T. A.; Reynolds, J. R., Eds. *Handbook of Conducting Polymers*, 3rd ed.; CRC Press: Boca Raton, FL, 2007.
- (26) Inzelt, G. *Conducting Polymers*; Springer: Heidelberg, 2008.
- (27) Baker, C. K.; Reynolds, J. J. *Electroanal. Chem.* **1988**, *251*, 307.
- (28) John, R.; Wallace, G. G. *J. Electroanal. Chem.* **1991**, *306*, 157.
- (29) Narula, P. M.; Noffle, R. E. *J. Electroanal. Chem.* **1999**, *464*, 123.
- (30) Sadki, S.; Schottland, P.; Brodie, N.; Sabouraud, G. *Chem. Soc. Rev.* **2000**, *29*, 283.
- (31) Heinze, J.; John, H.; Dietrich, M.; Tschuncky, P. *Synth. Met.* **2001**, *119*, 49.
- (32) Downard, A. J.; Pletcher, D. *J. Electroanal. Chem.* **1986**, *206*, 139.
- (33) Heinze, J. In *Encyclopedia of Electrochemistry*; Bard, A. J., Stratmann, M., Eds.; Wiley-VCH: Weinheim, Germany, 2004; Vol. 8, Chapter 16, p 607.
- (34) Andrieux, C. P.; Audebert, P.; Hapiot, P.; Savéant, J.-M. *J. Am. Chem. Soc.* **1990**, *112*, 2439.
- (35) Andrieux, C. P.; Audebert, P.; Hapiot, P.; Savéant, J.-M. *J. Phys. Chem.* **1991**, *95*, 10158.
- (36) Garcia, P.; Pernaut, J.-M.; Hapiot, P.; Wintgens, V.; Valat, P.; Garnier, F.; Delabouglise, D. *J. Phys. Chem.* **1993**, *97*, 513.
- (37) Audebert, P.; Hapiot, P. *Synth. Met.* **1995**, *575*, 95.
- (38) Guyard, L.; Hapiot, P.; Neta, P. *J. Phys. Chem. B* **1997**, *101*, 5698.
- (39) Hansen, G.; Henriksen, R. M.; Kumounah, F. S.; Lund, T.; Hamerich, O. *Electrochim. Acta* **2005**, *50*, 4936.
- (40) Hapiot, P.; Lorcy, D.; Tallec, A.; Carlier, R.; Robert, A. *J. Phys. Chem.* **1996**, *100*, 14823.
- (41) Heinze, J.; Willmann, C.; Bäuerle, P. *Angew. Chem., Int. Ed.* **2001**, *40*, 2861.
- (42) Meerholz, K.; Heinze, J. *Electrochim. Acta* **1996**, *41*, 1839.
- (43) Beck, F.; Oberst, M.; Jansen, R. *Electrochim. Acta* **1990**, *35*, 1841.
- (44) Zotti, G.; Schiavon, G.; Berlin, A.; Pagani, G. *Electrochim. Acta* **1989**, *34*, 881.
- (45) Zhou, M.; Heinze, J. *J. Phys. Chem. B* **1999**, *103*, 8451.
- (46) Heinze, J.; Hinkelmann, K.; Land, M. *DECHEMA Monogr.* **1989**, *112*, 75.
- (47) Zotti, G.; Schiavon, G.; Zecchin, S.; Sannicolo, F.; Brenna, E. *Chem. Mater.* **1995**, *7*, 1464.
- (48) Hill, M. G.; Mann, K. R.; Miller, L. L.; Penneau, J.-F. *J. Am. Chem. Soc.* **1992**, *114*, 2728.
- (49) Hill, M. G.; Penneau, J.-F.; Zinger, B.; Mann, K. R.; Miller, L. L. *Chem. Mater.* **1992**, *4*, 1106.
- (50) van Haare, J. A. E. H.; Groenendaal, L.; Havinga, E. E.; Janssen, R. A. J.; Meijer, E. W. *Angew. Chem., Int. Ed.* **1996**, *35*, 638.
- (51) Aperloo, J. J.; Janssen, R. A. J.; Malefant, P. R. L.; Groenendaal, L.; Fedet, J. N. *J. Am. Chem. Soc.* **2000**, *122*, 7042.
- (52) Hapiot, P.; Audebert, P.; Monnier, K.; Pernaut, J.-M.; Garcia, P. *Chem. Mater.* **1994**, *6*, 1549.
- (53) Smie, A.; Heinze, J. *Angew. Chem., Int. Ed.* **1997**, *36*, 363.
- (54) Tschuncky, P.; Heinze, J.; Smie, A.; Engelmann, G.; Koßmehl, G. *J. Electroanal. Chem.* **1997**, *433*, 223.
- (55) Heinze, J.; Willmann, C.; Bäuerle, P. *Angew. Chem., Int. Ed.* **2001**, *40*, 2861.
- (56) Merz, A.; Kronberger, J.; Dunsch, L.; Neudeck, A.; Petr, A.; Parkanyi, L. *Angew. Chem., Int. Ed.* **1999**, *38*, 1442.
- (57) Asavapiriyanon, S.; Chandler, G. K.; Gunawardena, G. A.; Pletcher, D. *J. Electroanal. Chem.* **1984**, *177*, 229.
- (58) Asavapiriyanon, S.; Chandler, G. K.; Gunawardena, G. A.; Pletcher, D. *J. Electroanal. Chem.* **1984**, *177*, 245.
- (59) Satoh, M.; Imanishi, K.; Yoshino, K. *J. Electroanal. Chem.* **1991**, *317*, 139.
- (60) Scharifker, B. R.; Garcia-Pastoriza, E.; Marino, W. *J. Electroanal. Chem.* **1991**, *300*, 85.
- (61) Debye, P. *Trans. Electrochem. Soc.* **1942**, *82*, 265.
- (62) Eigen, M.; Kruse, W.; Maas, G.; DeMayer, L. In *Progress in Reaction Kinetics*; Porter, C., Ed.; Pergamon Press: Oxford, 1964; pp 284–318.
- (63) El-Desoky, H.; Heinze, J.; Ghoneim, M. M. *Electrochim. Commun.* **2001**, *3*, 697.
- (64) Lacroix, J.-C.; Maurel, F.; Lacaze, P.-C. *J. Am. Chem. Soc.* **2001**, *123*, 1989.
- (65) Audebert, P.; Catel, J.-M.; Le Costumer, G.; Duchenet, V.; Hapiot, P. *J. Phys. Chem. B* **1995**, *99*, 11923.
- (66) Audebert, P.; Catel, J.-M.; Le Costumer, G.; Duchenet, V.; Hapiot, P. *J. Phys. Chem. B* **1998**, *102*, 8661.
- (67) Smie, A.; Synowczyk, A.; Heinze, J.; Alle, R.; Tschuncky, P.; Götz, G.; Bäuerle, P. *J. Electroanal. Chem.* **1998**, *452*, 87.
- (68) Lang, P.; Chao, F.; Costa, M.; Garnier, F. *Polymer* **1987**, *28*, 668.
- (69) Lukkar, J.; Alanko, M.; Pitkänen, V.; Kleemola, K.; Kankare, J. *J. Phys. Chem.* **1994**, *98*, 8525.
- (70) Ruiz, V.; Collina, A.; Heras, A.; Lopez-Palacios, J.; Seeber, R. *Helv. Chim. Acta* **2001**, *84*, 3628.
- (71) Hillman, A. R.; Mallen, E. F.; Hamnett, H. A. *J. Electroanal. Chem.* **1988**, *244*, 353.
- (72) Andrieux, C. P.; Hapiot, P.; Audebert, P.; Guard, L.; Nguyen Dinh An, M.; Groenendaal, L.; Meijer, E. W. *Chem. Mater.* **1997**, *9*, 723.
- (73) Audebert, P.; Catel, J.-M.; Le Costumer, G.; Duchenet, V.; Hapiot, P. *J. Phys. Chem. B* **1998**, *102*, 8661.
- (74) Tschuncky, P. Dissertation, Freiburg, 1995.
- (75) Tschuncky, P.; Heinze, J. *Synth. Met.* **1993**, *55*, 1603.
- (76) Randriamahazaka, H.; Sini, G.; Tran Van, F. *J. Phys. Chem. C* **2007**, *111*, 4553.
- (77) Heinze, J.; Rasche, A.; Pagels, M.; Geschke, B. *J. Phys. Chem. B* **2007**, *111*, 989.
- (78) Zotti, G.; Zecchin, S.; Vercelli, B.; Berlin, A.; Grimaldi, S.; Groenendaal, L.; Bertoncello, R.; Natali, M. *Chem. Mater.* **2005**, *17*, 3681.
- (79) Andrieux, C. P.; Dumas-Bouchiat, J. M.; Savéant, J. M. *J. Electroanal. Chem.* **1978**, *87*, 39.
- (80) Downard, A. J.; Pletcher, D. *J. Electroanal. Chem.* **1986**, *206*, 147.

- (81) Obretonov, W.; Schmidt, U.; Lorenz, W. J.; Staikov, G.; Budevski, E.; Carnal, D.; Müller, U.; Siegenthaler, H.; Schmidt, E. *J. Electrochem. Soc.* **1993**, *140*, 692.
- (82) Fleischmann, M.; Thirsk, H. R. In *Advances in Electrochemistry and Electrochemical Engineering*; Delahay, P., Ed.; Wiley-Interscience: New York, 1963; Vol. 3, p 123.
- (83) Raymond, D. E.; Harrison, D. J. *J. Electroanal. Chem.* **1993**, *361*, 65.
- (84) Villareal, I.; Morales, E.; Acosta, J. L. *Polymer* **2001**, *42*, 3779.
- (85) del Valle, M. A.; Cury, P.; Schrebler, R. *Electrochim. Acta* **2002**, *48*, 397.
- (86) Bade, K.; Tsakova, V.; Schultze, J. W. *Electrochim. Acta* **1992**, *37*, 2255.
- (87) Hwang, B.-J.; Santhanam, R.; Wu, C.-R.; Tai, Y.-W. *J. Solid State Electrochem.* **2003**, *7*, 678.
- (88) Hwang, B. J.; Santhanam, R.; Lin, Y.-L. *J. Electrochem. Soc.* **2000**, *147*, 2252.
- (89) Innocenti, M.; Loglio, F.; Pigani, L.; Seeber, R.; Terzi, F.; Udisti, R. *Electrochim. Acta* **2005**, *50*, 1497.
- (90) Bund, A.; Baba, A.; Berg, S.; Johannsmann, D.; Lübben, J.; Wang, Z.; Knoll, W. *J. Phys. Chem. B* **2003**, *107*, 6743.
- (91) Efimov, I.; Winkels, S.; Schultze, J. W. *J. Electroanal. Chem.* **2001**, *499*, 169.
- (92) Kvarnström, C.; Bilger, R.; Ivaska, A.; Heinze, J. *Electrochim. Acta* **1998**, *43*, 355.
- (93) Skompska, M. *Electrochim. Acta* **2000**, *45*, 3841.
- (94) Meerholz, K.; Heinze, J. *Angew. Chem., Int. Ed.* **1990**, *29*, 692.
- (95) Meerholz, K.; Heinze, J. *Synth. Met.* **1993**, *55–57*, 5040.
- (96) Meerholz, K.; Heinze, J. *Electrochim. Acta* **1996**, *41*, 1839.
- (97) Shacklette, L. W.; Eckhard, H.; Chance, R. R.; Miller, G. G.; Ivory, D. M.; Baughman, R. H. *J. Chem. Phys.* **1980**, *73*, 4098.
- (98) Bof Bufon, C. C.; Vollmer, J.; Heinzel, T.; Espindola, P.; John, H.; Heinze, J. *J. Phys. Chem. B* **2005**, *109*, 19191.
- (99) Burroughes, J. H.; Bradley, D. D. C.; Brown, A. R.; Marks, R. N.; Mackay, K.; Friend, R. H.; Burn, P. L.; Holmes, A. B. *Nature* **1990**, *347*, 539.
- (100) Kraft, A.; Grimsdale, A. C.; Holmes, A. B. *Angew. Chem., Int. Ed.* **1998**, *37*, 403.
- (101) Wessling, R. A. *J. Polym. Sci., Polym. Symp.* **1985**, *72*, 55.
- (102) Gilch, H. G.; Wheelwright, W. L. *J. Polym. Sci., Part A: Polym. Chem.* **1966**, *4*, 1337.
- (103) Louwet, F.; Vanderzande, D.; Gelan, J.; Mullens, J. *Macromolecules* **1995**, *28*, 1330.
- (104) Schwalm, T.; Rehahn, M. *Macromolecules* **2007**, *40*, 3921.
- (105) Utley, J. H. P.; Gruber, J. *J. Mater. Chem.* **2002**, *12*, 1613.
- (106) Girina, G. P.; Alpatova, N. M.; Feoktistov, L. G. *Russ. J. Electrochem.* **2006**, *42*, 102.
- (107) Alpatova, N. M.; Girina, G. P. *Russ. J. Electrochem.* **2006**, *42*, 670.
- (108) Pérez, L. O.; Utley, J. H. P.; Gruber, J. *Electrochim. Commun.* **2004**, *6*, 1141.
- (109) Cecile, C.; Mellah, M.; Labbé, E.; Nédélec, J. Y.; Périchon, J. *New J. Chem.* **2002**, *26*, 787.
- (110) Peres, L. O.; Varela, H.; Garcia, J. R.; Fernandes, M. R.; Torresi, R. M.; Nart, F. C.; Gruber, J. *Synth. Met.* **2001**, *118*, 65.
- (111) Kim, T.-H.; Park, S.-M. *Electrochim. Acta* **2005**, *50*, 1461.
- (112) Damlin, P.; Kvarnström, C.; Neugebauer, H.; Ivaska, A. *Synth. Met.* **2001**, *123*, 141.
- (113) Damlin, P.; Kvarnström, C.; Petr, A.; Neudeck, A.; Dunsch, L.; Ivaska, A. *Macromolecules* **2002**, *35*, 5789.
- (114) Damlin, P.; Kvarnström, C.; Petr, A.; El, P.; Dunsch, L.; Ivaska, A. *J. Solid State Electrochem.* **2002**, *6*, 291.
- (115) Damlin, P.; Kvarnström, C.; Kulovaara, H.; Ivaska, A. *Synth. Met.* **2003**, *135–136*, 309.
- (116) Hubbard, A. T.; Anson, F. C. In *Electroanalytical Chemistry*; Bard, A. J., Ed.; Marcel Dekker: New York, 1970; Vol. 4, p 129.
- (117) Hubbard, A. T. *J. Electroanal. Chem.* **1969**, *22*, 165.
- (118) Heinze, J. *Top. Curr. Chem.* **1990**, *152*, 1.
- (119) Roncali, J. *Chem. Rev.* **1992**, *92*, 711.
- (120) Meerholz, K.; Gregorius, H.; Müllen, K.; Heinze, J. *Adv. Mater.* **1994**, *6*, 671.
- (121) Chung, T. C.; Kaufman, J. H.; Heeger, A. J.; Wudl, F. *Phys. Rev.* **1984**, *30B*, 702.
- (122) Elsenbaumer, R. L.; Shacklette, L. W. In *Handbook of Conducting Polymers*; Skotheim, T. A., Ed.; Marcel Dekker: New York, 1986; p 213.
- (123) Kriscie, B.; Zagorska, M. *Synth. Met.* **1989**, *28*, 257.
- (124) Dietrich, M.; Heinze, J. *Synth. Met.* **1991**, *41–43*, 503.
- (125) Espindola, P.; Heinze, J. Manuscript in preparation.
- (126) Diaz, A. F.; Crowley, J.; Bargon, J.; Gardini, G. P.; Torrance, J. B. *J. Electroanal. Chem.* **1981**, *121*, 355.
- (127) Brédas, J. L.; Silbey, R.; Boudraux, D. S.; Chance, R. R. *J. Am. Chem. Soc.* **1983**, *105*, 6555.
- (128) Heinze, J. In *Encyclopedia of Electrochemistry*; Bard, A. J., Stratmann, M., Eds.; Wiley-VCH: Weinheim, Germany, 2004; Vol. 8, Chapter 4, p 93.
- (129) Heinze, J.; Tschuncky, P.; Smie, A. *J. Solid State Electrochem.* **1998**, *2*, 102.
- (130) Dunsch, L.; Rapta, P.; Schulte, N.; Schlüter, A. D. *Angew. Chem., Int. Ed.* **2002**, *41*, 2082.
- (131) Genies, E. M.; Syed, A. A. *Synth. Met.* **1984**, *10*, 21.
- (132) Heinze, J.; Störzbach, M.; Mortensen, J. *Ber. Bunsen-Ges. Phys. Chem.* **1987**, *91*, 960.
- (133) Feldberg, S. W.; Rubinstein, I. *J. Electroanal. Chem.* **1988**, *240*, 1.
- (134) Vorotnytsev, M. A.; Heinze, J. *Electrochim. Acta* **2001**, *46*, 3309.
- (135) Rasche, A.; Heinze, J. *Electrochim. Acta* **2008**, *53*, 3812.
- (136) Levillain, E.; Roncali, J. *J. Am. Chem. Soc.* **1999**, *121*, 8760.
- (137) Raimundo, J.-M.; Levillain, E.; Gallego-Planas, N.; Roncali, J. *Electrochim. Commun.* **2000**, *2*, 211.
- (138) Rapta, P.; Lukkari, J.; Tarabek, J.; Salomäki, M.; Jussila, M.; Yohannes, G.; Riekkkola, M.-L.; Kankare, J.; Dunsch, L. *Phys. Chem. Chem. Phys.* **2004**, *6*, 434.
- (139) Brédas, J. L.; Chance, R. R.; Silbey, R. *Phys. Rev. B* **1982**, *26*, 5843.
- (140) Brédas, J. L.; Street, G. B. *Acc. Chem. Res.* **1985**, *18*, 308.
- (141) Fesser, K.; Bishop, A. R.; Campbell, D. K. *Phys. Rev. B* **1983**, *27*, 4804.
- (142) Brédas, J. L.; Scott, J. C.; Yakuchi, K.; Street, G. B. *Phys. Rev. B* **1984**, *30*, 1023.
- (143) Deuchert, K.; Hünig, S. *Angew. Chem., Int. Ed.* **1978**, *17*, 875.
- (144) Cársky, P.; Zahradník, R. *Top. Curr. Chem.* **1973**, *43*, 1.
- (145) van Haare, J. A. E. H.; Havinga, E. D. E.; van Dongen, J. L. J.; Janssen, R. A. J.; Cornil, J.; Brédas, J. L. *Chem.—Eur. J.* **1998**, *4*, 1509.
- (146) Geskin, V. M.; Brédas, J. L. *ChemPhysChem* **2003**, *4*, 498.
- (147) Nechtschein, M.; Devreux, F.; Genoud, F.; Vieil, E.; Pernaut, J.-M.; Genies, E. *Synth. Met.* **1986**, *15*, 59.
- (148) Müllen, K., Wegner, G., Eds. *Electronic Materials: The Oligomer Approach*; Wiley-VCH: Weinheim, 1998.
- (149) Havinga, E. E.; Mutsaers, C. J.; Jenneskens, L. W. *Chem. Mater.* **1996**, *8*, 769.
- (150) Beljonne, D.; Brédas, J. L. In *Handbook of Conducting Polymers*, 3rd ed.; Skotheim, T. A., Reynolds, J. R., Eds.; CRC Press: Boca Raton, FL, 2007; pp 1–3.
- (151) Tolbert, L. M. *Acc. Chem. Res.* **1992**, *25*, 561.
- (152) Villaret, B.; Nechtschein, M. *Phys. Rev. Lett.* **1989**, *63*, 1285.
- (153) Inzelt, G. *Electrochim. Acta* **1989**, *34*, 83.
- (154) Kalaji, K.; Nyholm, L.; Peter, L. M. *J. Electroanal. Chem.* **1992**, *325*, 269.
- (155) Odin, C.; Nechtschein, M.; Hapiot, P. *Synth. Met.* **1992**, *47*, 329.
- (156) Zotti, G.; Schiavon, G. *Synth. Met.* **1989**, *31*, 347.
- (157) Aoki, K.; Kawase, M. *J. Electroanal. Chem.* **1994**, *377*, 125.
- (158) Otero, T. F.; Grande, H.; Rodriguez, J. *Electrochim. Acta* **1996**, *41*, 1863.
- (159) Otero, T. F.; Boyano, I. *J. Phys. Chem. B* **2003**, *107*, 6730.
- (160) Otero, T. F.; Abadías, R. *J. Electroanal. Chem.* **2007**, *610*, 96.
- (161) Heinze, J.; Rasche, A. *J. Solid State Electrochem.* **2006**, *10*, 148.
- (162) Wagner, K.; Pringle, J. M.; Hall, S. B.; Forsyth, M.; McFarlane, D. R.; Officer, D. L. *Synth. Met.* **2005**, *153*, 257.
- (163) Randriamahazaka, H.; Plesse, C.; Teyssi, D.; Chevrot, C. *Electrochim. Commun.* **2003**, *5*, 613.
- (164) Genies, E. M.; Pernaut, J.-M. *Synth. Met.* **1984**, *10*, 117.
- (165) Servagent, S.; Vieil, E. *J. Electroanal. Chem.* **1990**, *280*, 227.
- (166) Heinze, J.; Bilger, R. *Ber. Bunsen-Ges. Phys. Chem.* **1993**, *97*, 502.
- (167) Niu, L.; Kvarnström, C.; Ivaska, A. *J. Electroanal. Chem.* **2004**, *569*, 151.
- (168) Koehler, S.; Bund, A.; Efimov, I. *J. Electroanal. Chem.* **2006**, *589*, 82.
- (169) Chao, F.; Baudoin, J. L.; Costa, M.; Lang, P. *Makromol. Chem. Macromol. Symp.* **1987**, *8*, 173.
- (170) Zhou, Q.-X.; Kolaskie, C. J.; Miller, L. L. *J. Electroanal. Chem.* **1987**, *223*, 283.
- (171) Bruckensteiner, S.; Brzezinska, K.; Hillman, A. R. *Electrochim. Acta* **2000**, *45*, 3801.
- (172) Hillman, A. R.; Daisley, S. J.; Bruckensteiner, S. *Phys. Chem. Chem. Phys.* **2007**, *9*, 2379.
- (173) Zhou, M.; Pagels, M.; Geschke, B.; Heinze, J. *J. Phys. Chem. B* **2002**, *106*, 10065.
- (174) Lién, M.; Smyrl, W. H.; Morita, M. *J. Electroanal. Chem.* **1991**, *309*, 333.
- (175) Meerholz, K.; Heinze, J. *Mater. Sci. Forum* **1989**, *42*, 63.
- (176) Mastragostino, M.; Soddu, L. *Electrochim. Acta* **1990**, *35*, 463.
- (177) Borjas, R.; Buttry, D. A. *Chem. Mater.* **1991**, *3*, 72.
- (178) Arbizzani, C.; Mastragostino, M.; Meneghelli, L. *Electrochim. Acta* **1996**, *41*, 21.
- (179) Semenikhin, O. A.; Ovsyannikova, E. V.; Ehrenburg, M. R.; Alpatova, N. M.; Kazarinov, V. E. *J. Electroanal. Chem.* **2000**, *494*, 1.

- (180) Zotti, G.; Schiavon, G.; Zecchin, S. *Synth. Met.* **1995**, *72*, 275.
- (181) Casabore-Miceli, G.; Camaiori, N.; Geri, A.; Ridolfi, G.; Zanelli, A.; Gallazi, M. C.; Maggini, M.; Benincori, T. *J. Electroanal. Chem.* **2007**, *603*, 227.
- (182) Hillman, A. R.; Daisley, S. J.; Bruckenstein, S. *Electrochim. Acta* **2008**, *53*, 3763.
- (183) Zotti, G.; Salmaso, R.; Gallazi, M. C.; Marin, R. A. *Chem. Mater.* **1997**, *9*, 791.
- (184) Epstein, A. In *Handbook of Conducting Polymers*, 3rd ed.; Skotheim, T. A., Reynolds, J. R., Eds.; CRC Press: Boca Raton, FL, 2007; pp 15–3.
- (185) Naarmann, H.; Theophilou, N. *Synth. Met.* **1987**, *22*, 1.
- (186) Kaufman, F. B.; Schroeder, A. H.; Engler, E. M.; Kramer, S. R.; Chambers, J. Q. *J. Am. Chem. Soc.* **1980**, *102*, 483.
- (187) Chidsey, C. E. D.; Murray, R. J. *Phys. Chem.* **1986**, *90*, 1479.
- (188) Brédas, J. L.; Thémans, B.; Fripiat, J. G.; André, J. M.; Chance, R. R. *Phys. Rev. B* **1984**, *29*, 6761.
- (189) Zotti, G.; Schiavon, G. *Chem. Mater.* **1991**, *3*, 62.
- (190) Roncali, J.; Garreau, R.; Yassar, A.; Marque, P.; Garnier, F.; Lemaire, M. *J. Phys. Chem.* **1987**, *91*, 6706.
- (191) Chance, R. R.; Brédas, J. L.; Silbey, R. *Phys. Rev. B* **1984**, *29*, 4491.
- (192) Chance, R. R.; Boudreux, D. S.; Brédas, J. L.; Silbey, R. In *Handbook of Conducting Polymers*; Skotheim, T. A., Ed.; Marcel Dekker: New York, 1986; p 825.
- (193) Kaiser, A. B. *Rep. Prog. Phys.* **2001**, *64*, 1.
- (194) John, H.; Bauer, R.; Espindola, P.; Sonar, P.; Heinze, J.; Müllen, K. *Angew. Chem., Int. Ed.* **2005**, *44*, 2447.
- (195) Smie, A.; Synowczyk, A.; Heinze, J.; Alle, R.; Tschunky, P.; Götz, G.; Bäuerle, P. *J. Electroanal. Chem.* **1998**, *452*, 87.
- (196) Torrance, J. B. *Acc. Chem. Res.* **1979**, *12*, 79.
- (197) Yurchenko, O.; Heinze, J.; Ludwigs, S. *ChemPhysChem* **2010**, *11*, 1637.
- (198) Kaneto, K.; Ura, S.; Yoshino, K.; Inuishi, Y. *Jpn. J. Appl. Phys., Part 2* **1984**, *23*, 189.
- (199) Crooks, R. M.; Chyan, O. M. R.; Wrighton, M. S. *Chem. Mater.* **1989**, *1*, 4.
- (200) Skompska, M.; Mieczkowski, J.; Holze, R.; Heinze, J. *J. Electroanal. Chem.* **2005**, *577*, 9.
- (201) Ahonen, H. J.; Lukkari, J.; Kankare, J. *Macromolecules* **2000**, *33*, 6787.
- (202) Chiang, J. C.; MacDiarmid, A. G. *Synth. Met.* **1986**, *13*, 193.
- (203) MacDiarmid, A. G.; Chiang, J. C.; Richter, A. F.; Epstein, A. J. *Synth. Met.* **1987**, *18*, 285.
- (204) Bard, A. J.; Faulkner, L. *Electrochemical Methods—Fundamentals and Applications*, 2nd ed.; J. Wiley: New York, 2001.
- (205) Li, Y. *Electrochim. Acta* **1997**, *42*, 203.
- (206) Heinze, J.; Dietrich, M.; Mortensen, J. *Makromol. Chem., Macromol. Symp.* **1987**, *8*, 73.
- (207) Heinze, J. In *Encyclopedia of Electrochemistry*; Bard, A. J., Stratmann, M., Eds.; Wiley-VCH: Weinheim, 2004; Vol. 8, Chapter 16.
- (208) Otero, T. F.; DeLretta, E. *Synth. Met.* **1988**, *26*, 79.
- (209) Kiani, M. S.; Mitchell, G. R. *Synth. Met.* **1992**, *48*, 203.
- (210) Ruiz, V.; Colina, A.; Heras, A.; López-Palacios, J. *Electrochim. Acta* **2004**, *50*, 59.
- (211) Sánchez, J. V.; Díaz, R.; Herrasti, P.; Ocon, P. *Polym. J.* **2001**, *33*, 514.
- (212) Zhou, M.; Heinze, J. *Electrochim. Acta* **1999**, *44*, 1733.
- (213) Zhou, M.; Heinze, J. *J. Phys. Chem. B* **1999**, *103*, 8443.
- (214) Ogasawara, M.; Funahashi, K.; Demura, T.; Hagiwara, T.; Iwata, K. *Synth. Met.* **1986**, *14*, 61.
- (215) Yoon, C. O.; Sung, H. K.; Kim, J. H.; Barsoukov, E.; Kim, J. H.; Lee, H. *Synth. Met.* **1999**, *99*, 201.
- (216) Lee, K.; Menon, R.; Yoon, C. O.; Heeger, A. J. *Phys. Rev. B* **1995**, *52*, 4779.
- (217) Bof Bufon, C. C.; Heinzel, T.; Espindola, P.; Heinze, J. *J. Phys. Chem.* **2010**, *114*, 714.
- (218) Ko, J. M.; Rhee, H. W.; Park, S.-M.; Kim, C. Y. *J. Electrochem. Soc.* **1990**, *137*, 905.
- (219) Bagno, A.; Scorrano, G. *J. Am. Chem. Soc.* **1988**, *110*, 4577.
- (220) Zhou, M.; Heinze, J. *J. Phys. Chem. B* **1999**, *103*, 8451.
- (221) Suárez, M. F.; Compton, R. G. *J. Electroanal. Chem.* **1999**, *462*, 211.
- (222) Fuvre, C.; Abello, L.; Delubougline, D. *Adv. Mater.* **1997**, *9*, 722.
- (223) Wang, Y.; Zhang, C.; Huang, J.; Zhang, W.; Zhou, X. *J. Electroanal. Chem.* **1998**, *441*, 51.
- (224) Temsamani, K. R.; Mark, H. B., Jr.; Kutner, W.; Stalcup, A. M. *J. Solid State Electrochem.* **2002**, *6*, 391.
- (225) Aubert, P.-H.; Groenendaal, L.; Louwet, F.; Lutsen, L.; Vanderzande, D.; Zotti, G. *Synth. Met.* **2002**, *126*, 193.
- (226) Zotti, G.; Zecchin, S.; Schiavon, G.; Louwet, F.; Groenendaal, L.; Crispin, X.; Osikowicz, W.; Salaneck, W.; Fahlman, M. *Macromolecules* **2003**, *36*, 3337.
- (227) Schwuger, M.-L.; Stickdorn, K.; Schomaecker, R. *Chem. Rev.* **1995**, *95*, 849.
- (228) Tsakova, V.; Winkels, S.; Schultze, J. W. *Electrochim. Acta* **2000**, *46*, 759.
- (229) Lagrost, C.; Jouini, M.; Tanguy, J.; Aeiyach, S.; Lacroix, J. C.; Chané-Ching, K. I.; Lacaze, P. C. *Electrochim. Acta* **2001**, *46*, 3985.
- (230) Fall, M.; Dieng, M. M.; Aaron, J.-J.; Aeiyach, S.; Lacaze, P. C. *Synth. Met.* **2001**, *118*, 149.
- (231) Barr, G. E.; Sayre, C. N.; Connor, D. M.; Collard, D. M. *Langmuir* **1996**, *12*, 1395.
- (232) Mani, A.; Phani, K. L. N. *J. Electroanal. Chem.* **2001**, *513*, 126.
- (233) Kanungo, M.; Kumar, A.; Contractor, A. Q. *J. Electroanal. Chem.* **2002**, *528*, 46.
- (234) Sakmeche, N.; Aeiyach, S.; Aaron, J.-J.; Jouini, M.; Lacroix, J. C.; Lacaze, P.-C. *Langmuir* **1999**, *15*, 2566.
- (235) Stromberg, C.; Tsakova, V.; Schultze, J. W. *J. Electroanal. Chem.* **2003**, *547*, 125.
- (236) Schweiss, R.; Lübben, J. F.; Johannsmann, D.; Knoll, W. *Electrochim. Acta* **2005**, *50*, 2849.
- (237) Moustafid, T. E.; Gregory, R. V.; Brenneman, K. R.; Lessner, P. M. *Synth. Met.* **2003**, *135*–136, 435.
- (238) Groenendaal, L.; Jonas, F.; Freitag, D.; Pielartzik, H.; Reynolds, J. R. *Adv. Mater.* **2000**, *12*, 481.
- (239) Sakmeche, N.; Aeiyach, S.; Aaron, J.-J.; Jouini, M.; Lacroix, J. C.; Lacaze, P.-C. *Langmuir* **1999**, *15*, 2566.
- (240) Asami, R.; Atobe, M.; Fuchigami, T. *J. Am. Chem. Soc.* **2005**, *127*, 13160.
- (241) Chen, W.; Xue, G. *Prog. Polym. Sci.* **2005**, *30*, 783.
- (242) Jin, S.; Xue, G. *Macromolecules* **1997**, *30*, 5753.
- (243) Xu, J.; Shi, G.; Xu, Z.; Chen, F.; Hong, X. *J. Electroanal. Chem.* **2001**, *514*, 16.
- (244) Eley, D. D. In *Chemistry of Cationic Polymerization*; Plech, P. H., Ed.; Macmillan: New York, 1983; p 393.
- (245) Topchiev, A. V.; Zavgorodnii, S. V.; Paushkin, Y. M. *Boron Fluoride and its Compounds as Catalysts in Organic Chemistry*; Pergamon Press: New York, 1959.
- (246) Shi, G.; Jin, S.; Xue, G.; Li, C. *Science* **1995**, *267*, 994.
- (247) Krische, B.; Zargorska, M. *Synth. Met.* **1989**, *28*, 263.
- (248) Shi, G.; Li, C.; Liang, Y. *Adv. Mater.* **1999**, *11*, 1145.
- (249) Shi, G.; Li, C.; Yu, B.; Ye, W. *Polymer* **1997**, *38*, 1247.
- (250) Zhou, L.; Xue, G. *Synth. Met.* **1997**, *87*, 193.
- (251) Alkan, S.; Cutler, C. A.; Reynolds, J. R. *Adv. Funct. Mater.* **2003**, *13*, 331.
- (252) Wan, X.; Yan, F.; Jin, S.; Liu, X.; Xue, G. *Chem. Mater.* **1999**, *11*, 2400.
- (253) Liu, C.; Zhang, J.; Shi, G.; Zhao, Y. *J. Phys. Chem. B* **2004**, *108*, 2195.
- (254) Alakhlas, F.; Holze, R. *Synth. Met.* **2007**, *157*, 109.
- (255) Xu, J. K.; Nie, G. M.; Zhang, S. S.; Han, X. J.; Pu, S. Z.; Shen, L.; Xiao, Q. *Eur. Polym. J.* **2005**, *41*, 1654.
- (256) Fan, B.; Qu, L.; Shi, G. *J. Electroanal. Chem.* **2005**, *575*, 287.
- (257) Xu, J.; Hou, J.; Pu, S.; Nie, G.; Zhang, S. *J. Appl. Polym. Sci.* **2006**, *101*, 539.
- (258) Galinski, M.; Lewandowski, A.; Stepniak, I. *Electrochim. Acta* **2006**, *52*, 5567.
- (259) Endres, F.; Abedin, S. Z. *E. Phys. Chem. Chem. Phys.* **2006**, *8*, 2101.
- (260) Ohno, H., Ed. *Electrochemical Aspects of Ionic Liquids*; Wiley-Interscience: 2005.
- (261) MacFarlane, D.; Forsyth, M.; Howlett, P. C.; Pringle, J. M.; Sun, J.; Armat, G.; Neil, W.; Izgorodina, E. I. *Acc. Chem. Res.* **2007**, *40*, 1165.
- (262) Hapiot, P.; Lagrost, C. *Chem. Rev.* **2008**, *108*, 2238.
- (263) Mazurkiewicz, J. H.; Innis, P. C.; Wallace, G. G.; MacFarlane, D. R.; Forsyth, M. *Synth. Met.* **2003**, *135*–136, 31.
- (264) Pringle, J. M.; Efthimiadis, J.; Howlett, P. C.; Efthimiadis, J.; MacFarlane, D. R.; Chaplin, A.; Hall, S. B.; Officer, D. L.; Wallace, G. G.; Forsyth, M. *Polymer* **2004**, *45*, 1447.
- (265) Boxall, D. L.; Osteryoung, R. A. *J. Electrochem. Soc.* **2004**, *151*, E41.
- (266) Damlin, P.; Kvärnström, C.; Ivaska, A. *J. Electroanal. Chem.* **2004**, *570*, 113.
- (267) Randriamahazaka, H.; Plesse, C.; Teyssi, D.; Chevrot, C. *Electrochem. Commun.* **2004**, *6*, 299.
- (268) Pringle, J. M.; Forsyth, M.; MacFarlane, D. R.; Wagner, K.; Hall, S. B.; Officer, D. L. *Polymer* **2005**, *46*, 2047.
- (269) Geetha, S.; Trivedi, D. C. *Synth. Met.* **2005**, *155*, 232.
- (270) Zein El Abedin, S.; Borrisenko, N.; Endres, F. *Electrochem. Commun.* **2004**, *6*, 422.
- (271) Schneider, O.; Bund, A.; Ispas, A.; Borrisenko, N.; Zein El Abedin, S.; Endres, F. *J. Phys. Chem. B* **2005**, *109*, 7159.
- (272) Sekiguchi, K.; Atobe, M.; Fuchigami, T. *J. Electroanal. Chem.* **2003**, *557*, 1.
- (273) Lu, W.; Fadeev, A. G.; Qi, B.; Mattes, B. R. *Synth. Met.* **2003**, *135*–136, 139.

- (274) Lu, W.; Fadeev, A. G.; Qi, B.; Smela, E.; Mattes, B. R.; Ding, J.; Spinks, G. M.; Mazurkiewicz, J.; Zhou, D.; Wallace, G. G.; MacFarlane, D. R.; Forsyth, S. A.; Forsyth, M. *Science* **2002**, 297, 983.
- (275) Ding, J.; Zhou, D.; Spunks, G.; Wallace, G.; Forsyth, S.; Forsyth, M.; Mac Farlane, D. *Chem. Mater.* **2003**, 15, 2392.
- (276) Sekiguchi, K.; Atobe, M.; Fuchigami, T. *Electrochim. Commun.* **2002**, 4, 881.
- (277) Pringle, J. M.; MacFarlane, D. R.; Forsyth, M. *Synth. Met.* **2005**, 155, 684.
- (278) Han, D.; Qiu, X.; Shen, Y.; Guo, H.; Zhang, Y.; Niu, L. J. *Electroanal. Chem.* **2006**, 596, 33.
- (279) Dong, B.; Zhang, S.; Zheng, L.; Xu, J. *J. Electroanal. Chem.* **2008**, 619–620, 193.
- (280) Lu, W.; Fadeev, A. G.; Qi, B.; Smela, E.; Mattes, B. R.; Ding, J.; Spinks, G. M.; Mazurkiewicz, J.; Zhou, D.; Wallace, G. G.; MacFarlane, D. R.; Forsyth, S. A.; Forsyth, M. *Science* **2002**, 297, 983.
- (281) Pang, Y.; Xu, H.; Li, X.; Ding, H.; Cheng, Y.; Shi, G.; Jin, L. *Electrochim. Commun.* **2006**, 8, 1757.
- (282) Lu, W.; Fadeev, A. G.; Qi, B.; Mattes, B. R. *Synth. Met.* **2003**, 135–136, 139.
- (283) Mu, S. *Electrochim. Acta* **2007**, 52, 7827.
- (284) Lange, U.; Roznyatovskaya, N. V.; Mirsky, V. M. *Anal. Chim. Acta* **2008**, 614, 1.
- (285) McQuade, D. T.; Pullen, A. E.; Swager, T. M. *Chem. Rev.* **2000**, 100, 2537.
- (286) Monk, P. M. S.; Mortimer, R. J.; Rosseinsky, D. R. *Electrochromism: Fundamentals and Applications*; VCH: Weinheim, 1995.
- (287) Ko, H. C.; Kang, M.; Moon, B.; Lee, H. *Adv. Mater.* **2004**, 16, 1712.
- (288) Deronzier, A.; Moutet, J.-C. *Coord. Chem. Rev.* **1996**, 147, 339.
- (289) Cravino, A.; Zerza, G.; Neugebauer, H.; Maggini, M.; Bucella, S.; Menna, E.; Svensson, M.; Andersson, M. R.; Brabec, C. J.; Sariciftci, N. S. *J. Phys. Chem. B* **2002**, 106, 70.
- (290) Halls, J. J. M.; Walsh, C. A.; Greenham, N. C.; Marseglia, E. A.; Friend, R. H.; Moratti, S. C.; Holmes, A. B. *Nature* **1995**, 376, 498.
- (291) Schmidt-Mende, L.; Fechtenköetter, A.; Müllen, K.; Moons, E.; Friend, R. H.; MacKenzie, J. D. *Science* **2001**, 293, 1119.
- (292) Huynh, W. U.; Dittmer, J. J.; Alivisatos, A. P. *Science* **2002**, 295, 2425.
- (293) Brabec, C. J. *Sol. Energy Mater. Sol. Cells* **2004**, 83, 273.
- (294) Padinger, F.; Rittberger, R. S.; Sariciftci, N. S. *Adv. Funct. Mater.* **2003**, 13, 85.
- (295) Heeger, A. J. *Rev. Mod. Phys.* **2001**, 73, 681.
- (296) Cravino, A.; Sariciftci, N. S. *J. Mater. Chem.* **2002**, 12, 1931.
- (297) Roncali, J. *Chem. Soc. Rev.* **2005**, 34, 483.
- (298) Beninori, T.; Brenna, E.; Sannicolo, F.; Trimarco, L.; Zotti, G.; Sozzani, P. *Angew. Chem., Int. Ed.* **1996**, 35, 648.
- (299) Ferraris, J. P.; Yassar, A.; Loveday, D. C.; Hmyene, M. *Opt. Mater.* **1998**, 9, 34.
- (300) Yamazaki, T.; Murata, Y.; Komatsu, K.; Furukawa, K.; Morita, M.; Maruyama, N.; Yamao, T.; Fujita, S. *Org. Lett.* **2004**, 6, 4865.
- (301) Segura, J. L.; Gómez, R.; Reinold, E.; Bäuerle, P. *Org. Lett.* **2005**, 7, 2345.
- (302) Segura, J. L.; Gómez, R.; Blanco, R.; Reinold, E.; Bäuerle, P. *Chem. Mater.* **2006**, 18, 2834.
- (303) Audebert, P.; Bidan, G.; Lapkowski, M. *J. Electroanal. Chem.* **1987**, 219, 165.
- (304) Catellani, M.; Luzzati, S.; Lupsac, N.-O.; Mendichi, R.; Consonni, R.; Famulari, A.; Meille, S.; Giacalone, F.; Segura, J. L.; Martin, N. *J. Mater. Chem.* **2004**, 14, 67.
- (305) Catellani, M.; Luzzati, S.; Lupsac, N.-O.; Mendichi, R.; Consonni, R.; Giacalone, F.; Segura, J. L.; Martín, N. *Thin Solid Films* **2004**, 451, 2.
- (306) Blanco, R.; Seoane, C.; Segura, J. L. *Tetrahedron Lett.* **2008**, 49, 2056.
- (307) Zerza, G.; Cravino, A.; Neugebauer, H.; Sariciftci, N. S.; Gómez, R.; Segura, J. L.; Martín, N.; Svensson, M.; Andersson, M. R. *J. Phys. Chem. A* **2001**, 105, 4172.
- (308) Micaroni, L.; Nart, F. C.; Hümmelgen, I. A. *J. Solid State Electrochem.* **2002**, 7, 55.
- (309) Pommerene, J.; Vestweber, H.; Guss, W.; Mahrt, R. F.; Bässler, H.; Porsch, M.; Daub, J. *Adv. Mater.* **1995**, 7, 551.
- (310) Tanaka, S.; Yamashita, Y. *Chem. Mater.* **1996**, 8, 570.
- (311) Akoudad, S.; Roncali, J. *Chem. Commun.* **1998**, 2081.
- (312) Blanco, R.; Gómez, R.; Seoane, C.; Segura, J. L.; Mena-Osteritz, E.; Bäuerle, P. *Org. Lett.* **2007**, 9, 2171.
- (313) Chen, S.; Liu, Y.; Qiu, W.; Sun, X.; Ma, Y.; Zhu, D. *Chem. Mater.* **2005**, 17, 2208.
- (314) You, C. C.; Saha-Möller, C. R.; Würthner, F. *Chem. Commun.* **2004**, 2030.
- (315) Fischer, M. K. R.; Kaiser, T. E.; Würthner, F.; Bäuerle, P. *J. Mater. Chem.* **2009**, 198, 1129.
- (316) Dominey, R. N.; Lewis, T. J.; Wrighton, M. S. *J. Phys. Chem.* **1983**, 87, 5345.
- (317) Monk, P. M. S. *The Viologens: Physicochemical Properties, Synthesis and Applications of the Salts of 4,4'-Bipyridine*; John Wiley and Sons: Chichester, 1998.
- (318) Mortimer, R. J. *Electrochim. Acta* **1999**, 44, 2971.
- (319) Da Silva, S.; Cosnier, S.; Almeida, M. G.; Moura, J. J. G. *Electrochim. Commun.* **2004**, 6, 404.
- (320) Da Silva, S.; Shan, D.; Cosnier, S. *Sens. Actuators, B* **2004**, 103, 397.
- (321) Bidan, G.; Deronzier, A.; Moutet, J.-C. *J. Chem. Soc., Chem. Commun.* **1984**, 1185.
- (322) Komura, T.; Yamaguchi, T.; Furuta, K.; Siroco, K. *J. Electroanal. Chem.* **2002**, 534, 123.
- (323) Komura, T.; Yamaguchi, T.; Sirono, K.; Kura, K. *Electroanalysis* **2002**, 14, 823.
- (324) Park, S.; Ko, H. C.; Paik, W.; Lee, H. *Synth. Met.* **2003**, 139, 439.
- (325) Ko, H. C.; Park, S.; Paik, W.; Lee, H. *Synth. Met.* **2002**, 132, 15.
- (326) Ko, H. C.; Kim, S.; Lee, H.; Moon, B. *Adv. Funct. Mater.* **2005**, 15, 905.
- (327) Besbes, M.; Trippé, G.; Levillain, E.; Mazari, M.; Le Derf, F.; Perepichka, I. F.; Derdour, A.; Gorgues, A.; Sallé, M.; Roncali, J. *Adv. Mater.* **2001**, 13, 1249.
- (328) Thobie-Gautier, C.; Gorgues, A.; Jubault, M.; Roncali, J. *Macromolecules* **1993**, 26, 4094.
- (329) Huchet, L.; Akoudad, S.; Roncali, J. *Adv. Mater.* **1998**, 10, 541.
- (330) Lyskawa, J.; Le Derf, F.; Levillain, E.; Mzari, M.; Salle, M.; Dubois, L.; Viel, P.; Bureau, C.; Palacin, S. *J. Am. Chem. Soc.* **2004**, 126, 12194.
- (331) Eloï, J.-C.; Chabanne, L.; Whittell, G. R.; Manners, I. *Mater. Today* **2008**, 11, 28.
- (332) Holliday, B. J.; Stanford, T. B.; Swager, T. M. *Chem. Mater.* **2006**, 18, 5649.
- (333) Kingsborough, R. P.; Swager, T. M. *Chem. Mater.* **2000**, 12, 872.
- (334) Kingsborough, R. P.; Swager, T. M. *Prog. Inorg. Chem.* **1999**, 48, 123.
- (335) Shioya, T.; Swager, T. M. *Chem. Commun.* **2002**, 1364.
- (336) Reddinger, J. L.; Reynolds, J. R. *Chem. Mater.* **1998**, 10, 3.
- (337) Deronzier, A.; Moutet, J. C. *Curr. Top. Electrochim. Chem.* **1994**, 3, 159.
- (338) Lamy, C.; Leger, J.-M.; Garnier, F. In *Handbook of Organic Conducting Molecules and Polymers*; Nalwa, H. S., Ed.; Wiley: New York, 1997; Vol. 3, p 471.
- (339) Pickup, P. J. *Mater. Chem.* **1999**, 9, 1641.
- (340) Holliday, B. J.; Swager, T. M. *Chem. Commun.* **2005**, 23.
- (341) Zotti, G.; Schiavon, G.; Zecchin, S.; Berlin, A.; Pagani, G.; Canavesi, A. *Synth. Met.* **1996**, 76, 255.
- (342) Malinski, T. *Porphyrin Handb.* **2000**, 6, 231.
- (343) Otsubo, T.; Aso, Y.; Takimiya, K. *J. Mater. Chem.* **2002**, 12, 2565.
- (344) Paul-Roth, C.; Rault-Berthelot, J.; Simonneaux, G.; Letessier, J.; Bergamini, J.-F. *J. Electroanal. Chem.* **2007**, 606, 103.
- (345) Yuasa, M.; Oyaizu, K.; Yamaguchi, A.; Ishikawa, M.; Eguchi, K.; Kobayashi, T.; Toyoda, Y.; Tsutsui, S. *Polym. Adv. Technol.* **2005**, 16, 616.
- (346) Ballarin, B.; Seiber, R.; Tassi, L.; Tonelli, D. *Synth. Met.* **2000**, 114, 279.
- (347) Schäferling, M.; Bäuerle, P. *J. Mater. Chem.* **2004**, 14, 1132.
- (348) Too, C. O.; Wallace, G. G.; Burrell, A. K.; Collis, G. E.; Officer, D. L.; Boge, E. W.; Brodie, S. G.; Evans, E. J. *Synth. Met.* **2001**, 123, 53.
- (349) Chen, J.; Burrel, A. K.; Campbell, W. M.; Officier, D. L.; Too, C. O.; Wallace, G. G. *Electrochim. Acta* **2004**, 49, 329.
- (350) Chen, J.; Officer, D. L.; Pringle, J. M.; MacFarlane, D. R.; Too, C. O.; Wallace, G. G. *Electrochem. Solid State Lett.* **2005**, 8, A528.
- (351) Moretto, G. L.; Markwitz, A.; Hall, S. B.; Burrell, A. K.; Officer, D. L.; Campbell, W. M.; Collis, G. E. *Mod. Phys. Lett. B* **2001**, 15, 1411.
- (352) Allietta, N.; Pansu, R.; Bied-Charreton, C.; Albin, V.; Bedioui, F.; Devynck, J. *Synth. Met.* **1996**, 81, 205.
- (353) Clark, J. C.; Fabre, B.; Fronczeck, F. R.; Vicente, M.; Graca, H. *J. Porphyrins Phthalocyanines* **2005**, 9, 803.
- (354) Diab, N.; Schuhmann, W. *Electrochim. Acta* **2001**, 47, 265.
- (355) Johanson, U.; Marandi, M.; Sammelselg, V.; Tamm, J. *J. Electroanal. Chem.* **2005**, 575, 267.
- (356) Cosnier, S.; Gondran, C.; Wessel, R.; Montforts, F.-P.; Wedel, M. *J. Electroanal. Chem.* **2000**, 488, 83.
- (357) Lin, C. Y.; Hung, Y. C.; Liu, C. M.; Lo, C. F.; Lin, Y. C.; Lin, C. L. *Dalton Trans.* **2005**, 2, 396.
- (358) Schäferling, M.; Bäuerle, P. *Synth. Met.* **2001**, 119, 289.
- (359) Poriel, C.; Ferrand, Y.; Le Maux, P.; Paul-Roth, C.; Simonneaux, G.; Rault-Berthelot, J. *J. Electroanal. Chem.* **2005**, 583, 92.
- (360) Poriel, C.; Ferrand, Y.; Le Maux, P.; Rault-Berthelot, J.; Simonneaux, G. *Chem. Commun.* **2003**, 1104.

- (361) Poriel, C.; Ferrand, Y.; Le Maux, P.; Paul-Roth, C.; Rault-Berthelot, J.; Simmoneaux, G. *Chem. Commun.* **2003**, 2308.
- (362) Ruhlmann, L.; Schulz, A.; Giradeau, A.; Messerschmidt, C.; Fuhrhop, J. H. *J. Am. Chem. Soc.* **1999**, *121*, 6664.
- (363) Li, G.; Wang, T.; Schulz, A.; Bhosale, S.; Lauer, M.; Espindola, P.; Heinze, J.; Fuhrhop, J.-H. *Chem. Commun.* **2004**, 552.
- (364) Vorotyntsev, M. A.; Vasilyeva, S. V. *Adv. Colloid Interface Sci.* **2008**, *139*, 97.
- (365) Vorotyntsev, M. A.; Casalta, M.; Pousson, E.; Roullier, L.; Boni, G.; Moise, C. *Electrochim. Acta* **2001**, *46*, 4017.
- (366) Skompska, M.; Vorotyntsev, M. A.; Goux, J.; Moise, C.; Heinz, O.; Cohen, Y. S.; Levi, M. D.; Goferd, Y.; Salitra, G.; Aurbach, D. *Electrochim. Acta* **2005**, *50*, 1635.
- (367) Skompska, M.; Vorotyntsev, M. A.; Refczynska, M.; Goux, J.; Lesniewska, E.; Boni, G.; Moise, C. *Electrochim. Acta* **2006**, *51*, 2108.
- (368) Brisset, H.; Navarro, A.-E.; Moustrou, C.; Perepichka, I. F.; Roncali, J. *Electrochim. Commun.* **2004**, *6*, 249.
- (369) Patil, A. O.; Ikenoue, Y.; Wudl, F.; Heeger, A. J. *J. Am. Chem. Soc.* **1987**, *109*, 1858.
- (370) Patil, A. O.; Ikenoue, Y.; Basescu, N.; Colaneri, N.; Chen, J.; Wudl, F.; Heeger, A. J. *Synth. Met.* **1987**, *20*, 151.
- (371) Bäuerle, P.; Gaudl, K.-U.; Würthner, F.; Sariciftci, N. S.; Neugebauer, H.; Mehring, M.; Zhong, C.; Doblhofer, *Adv. Mater.* **1990**, *2*, 490.
- (372) Yue, J.; Wang, Z. H.; Cromack, K. R.; Epstein, A. J.; MacDiarmid, A. G. *J. Am. Chem. Soc.* **1991**, *113*, 2665.
- (373) Tran-Van, F.; Carrier, M.; Chevrot, C. *Synth. Met.* **2004**, *142*, 251.
- (374) Han, C.-C.; Lu, C.-H.; Hong, S.-P.; Yang, K.-F. *Macromolecules* **2003**, *36*, 7908.
- (375) Mažeikiene, R.; Malinauskas, A. *Mater. Chem. Phys.* **2004**, *83*, 184.
- (376) Zhang, L. *J. Solid State Electrochem.* **2007**, *11*, 365.
- (377) Cano Márquez, A. G.; Torres Rodríguez, L. M.; Montes Rojas, A. *Electrochim. Acta* **2007**, *52*, 5294.
- (378) Deore, B. A.; Yu, I.; Freund, M. S. *J. Am. Chem. Soc.* **2004**, *126*, 52.
- (379) Ma, Y.; Ali, S. R.; Dodoo, A. S.; He, H. *J. Phys. Chem. B* **2006**, *110*, 16359.
- (380) Deore, B.; Freund, M. S. *Analyst* **2003**, *128*, 803.
- (381) Ng, S. C.; Chan, H. S. O.; Huang, H. H.; Ho, P. K. H. *J. Chem. Soc., Chem. Commun.* **1995**, 1327.
- (382) Viinikanoja, A.; Lukkari, J.; Ääritalo, T.; Laiho, T.; Kankare, J. *Langmuir* **2003**, *19*, 2768.
- (383) Zhang, N.; Wu, R.; Li, Q.; Pakbaz, K.; Yoon, C. O.; Wudl, F. *Chem. Mater.* **1993**, *5*, 1598.
- (384) Berlin, A.; Schiavon, G.; Zecchin, S.; Zotti, G. *Synth. Met.* **2001**, *119*, 153.
- (385) Zotti, G.; Zecchin, S.; Schiavon, G.; Berlin, A.; Pagani, G.; Canavesi, A. *Chem. Mater.* **1997**, *9*, 2940.
- (386) Ito, S.; Murata, K.; Teshima, S.; Aizawa, R.; Asako, Y.; Takahashi, K.; Hoffman, B. M. *Synth. Met.* **1998**, *96*, 161.
- (387) Wei, X. L.; Wang, Y. Z.; Long, S. M.; Bobeczk, C.; Epstein, A. J. *J. Am. Chem. Soc.* **1996**, *118*, 2545.
- (388) Lukachova, L. V.; Shkerin, E. A.; Puganova, E. A.; Karyakina, E. E.; Kiseleva, S. G.; Orlov, A. V.; Karpacheva, G. P.; Karyakin, A. A. *J. Electroanal. Chem.* **2003**, *544*, 59.
- (389) Karyakina, E. E.; Neftyakova, L. V.; Karyakin, A. A. *Anal. Lett.* **1994**, *27*, 2871.
- (390) Ngamna, O.; Morrin, A.; Moulton, S. E.; Killard, A. J.; Smyth, M. R.; Wallace, G. G. *Synth. Met.* **2005**, *153*, 185.
- (391) Karyakin, A. A.; Strakhova, A. K.; Yatsimirsky, A. K. *J. Electroanal. Chem.* **1994**, *371*, 259.
- (392) Ikenoue, Y.; Tomozawa, H.; Saida, Y.; Kira, M.; Yashima, H. *Synth. Met.* **1991**, *40*, 333.
- (393) Sonmez, G.; Schwendeman, I.; Schottland, P.; Zong, K. W.; Reynolds, J. R. *Macromolecules* **2003**, *36*, 639.
- (394) Yang, C.-H.; Chih, Y.-K.; Wu, W.-C.; Chen, C.-H. *Electrochim. Solid State Lett.* **2006**, *9*, C5.
- (395) Yang, C.-H.; Huang, L.-R.; Chih, Y.-K.; Lin, W.-C.; Liu, F.-J.; Wang, T.-L. *Polymer* **2007**, *48*, 3237.
- (396) Barbero, C.; Miras, M. C.; Schnyder, B.; Haas, O.; Kotz, R. *J. Mater. Chem.* **1994**, *4*, 1775.
- (397) Rahmanifar, M. S.; Mousavi, M. F.; Shamsipur, M. *J. Power Sources* **2002**, *110*, 229.
- (398) Willicut, R. J.; McCarley, R. L. *J. Am. Chem. Soc.* **1994**, *116*, 10823.
- (399) Willicut, R. J.; McCarley, R. L. *Adv. Mater.* **1995**, *7*, 759.
- (400) Smela, E.; Kariis, H.; Yang, Z.; Mecklenburg, M.; Liedberg, B. *Langmuir* **1998**, *120*, 13452.
- (401) Karris, H.; Smela, E.; Udval, K.; Wirde, M.; Gelius, U.; Liedberg, B. *J. Phys. Chem. B* **1998**, *102*, 6529.
- (402) Liedberg, B.; Yang, Z.; Enquist, I.; Wirde, M.; Gelius, U.; Götz, G.; Bäuerle, P.; Rummel, R.-M.; Ziegler, C.; Göpel, W. *J. Phys. Chem. B* **1997**, *101*, 5951.
- (403) Mitchalish, R.; El-Kasmi, A.; Lang, P.; Yassar, A.; Garnier, F. *J. Electroanal. Chem.* **1998**, *457*, 129.
- (404) Berlin, A.; Zotti, G.; Schiavon, G.; Zecchin, S. *J. Am. Chem. Soc.* **1998**, *120*, 13453.
- (405) Harm, U.; Bürgler, R.; Fürbeth, W.; Mangold, K.-M.; Jüttner, K. *Macromol. Symp.* **2002**, *187*, 65.
- (406) Ocafraint, M.; Tran, T. K.; Blanchard, P.; Roncali, J. *Adv. Funct. Mater.* **2008**, *18*, 2163.
- (407) Noble, C. O., IV; McCarley, R. L. *J. Am. Chem. Soc.* **2000**, *122*, 6518.
- (408) Newkome, G. R.; Moorefield, C. N.; Vögtle, F. *Dendritic Molecules. Concepts, Syntheses, Perspectives*; VCH: Weinheim, 1996.
- (409) Wong, K.-T.; Lin, Y.-H.; Wu, H.-H.; Fungo, F. *Org. Lett.* **2007**, *9*, 4531.
- (410) Sebastian, R.-M.; Caminade, A.-M.; Majoral, J.-P.; Levillain, E.; Huchet, L.; Roncali, J. *Chem. Commun.* **2000**, 507.
- (411) Alvarez, J.; Sun, L.; Crooks, R. M. *Chem. Mater.* **2002**, *14*, 3995.
- (412) Crooks, R. M.; Zhao, M.; Sun, L.; Chechik, V.; Yeung, L. K. *Acc. Chem. Res.* **2001**, *34*, 181.
- (413) Roncali, J.; Thobie-Gautier, C.; Brisset, H.; Favard, J. F.; Guy, A. J. *Electroanal. Chem.* **1995**, *381*, 257.
- (414) Roquet, S.; deBettignies, R.; Leriche, P.; Cravino, A.; Roncali, J. *J. Mater. Chem.* **2006**, *16*, 3040.
- (415) Piron, F.; Leriche, P.; Mabon, G.; Grosu, I.; Roncali, J. *Electrochim. Commun.* **2008**, *10*, 1427.
- (416) Love, J. C.; Estroff, L. A.; Kriebel, J. K.; Nuzzo, R. G.; Whitesides, G. M. *Chem. Rev.* **2005**, *105*, 1103.
- (417) Finklea, H. O.; Avery, S.; Lynch, M.; Furtsch, T. *Langmuir* **1987**, *3*, 409.
- (418) Boldt, F.; Baltes, N.; Borgwarth, K.; Heinze, J. *Surf. Sci.* **2005**, *1*–*3*, 51.
- (419) Sayre, C. N.; Collard, D. M. *Langmuir* **1997**, *13*, 714.
- (420) Wang, J.; Zeng, B.; Fang, C.; He, F.; Zhou, X. *Electroanalysis* **1999**, *11*, 1345.
- (421) Mazur, M.; Krzysinski, P. *J. Phys. Chem. B* **2002**, *106*, 10349.
- (422) Baba, A.; Knoll, W. *Adv. Mater.* **2003**, *15*, 1015.
- (423) Vercelli, B.; Zotti, G.; Berlin, A.; Grimoldi, S. *Chem. Mater.* **2006**, *18*, 3754.
- (424) Gao, Z.; Siow, K. S.; Chan, H. S. O. *Synth. Met.* **1995**, *75*, 5.
- (425) Zhai, L.; Laird, D. W.; McCullough, R. D. *Langmuir* **2003**, *19*, 6492.
- (426) Simon, R. A.; Rico, A. J.; Wrighton, M. S. *J. Am. Chem. Soc.* **1982**, *104*, 2031.
- (427) Wurm, D. B.; Kim, Y.-T. *Langmuir* **2000**, *16*, 4533.
- (428) Dahlgren, G.; Smith, A.; Wurm, D. B. *Synth. Met.* **2000**, *113*, 289.
- (429) Kang, J. F.; Perry, J. D.; Tian, P.; Kilbey, S. M. *Langmuir* **2002**, *18*, 10196.
- (430) Fulghum, T.; Karim, S. M. A.; Baba, A.; Taranekar, P.; Nakai, T.; Mauda, T.; Advincula, R. C. *Macromolecules* **2006**, *39*, 1467.
- (431) Berlin, A.; Zotti, G. *Macromol. Rapid Commun.* **2000**, *21*, 301.
- (432) Hata, K.; Fujihara, H. *Chem. Commun.* **2002**, 2714.
- (433) Ito, M.; Tsukatani, T.; Fujihara, H. *J. Mater. Chem.* **2005**, *15*, 960.
- (434) Zotti, G.; Vercelli, B.; Berlin, A. *Chem. Mater.* **2008**, *20*, 397.
- (435) Fave, C.; Noel, V.; Ghilane, J.; Trippé-Allard, G.; Randriamahazaka, H.; Lacroix, J. C. *J. Phys. Chem. C* **2008**, *112*, 18638.
- (436) Gabriel, S.; Cécus; Fleury-Frenette, M. K.; Cossement, D.; Hecq, M.; Ruth, N.; Jérôme, R.; Jérôme, C. *Chem. Mater.* **2007**, *19*, 2364.
- (437) Jérôme, C.; Jérôme, R. *Angew. Chem., Int. Ed.* **1998**, *37*, 2488.
- (438) Jérôme, C.; Labaye, D. E.; Jérôme, R. *Synth. Met.* **2004**, *142*, 207.
- (439) Hatano, T.; Bae, A.-H.; Takeuchi, M.; Fujita, N.; Kaneko, K.; Ihara, H.; Takafuji, M.; Shinkai, S. *Angew. Chem., Int. Ed.* **2004**, *43*, 465.
- (440) Ge, D.; Wang, J.; Wang, S.; Ma, J.; He, B. *J. Mater. Sci. Lett.* **2003**, *22*, 839.
- (441) Hatano, T.; Takeuchi, M.; Ikeda, A.; Shinkai, S. *Org. Lett.* **2003**, *5*, 1395.
- (442) Hatano, T.; Takeuchi, M.; Ikeda, A.; Shinkai, S. *Chem. Lett.* **2003**, *32*, 314.
- (443) Shi, W.; Ge, D.; Wang, J.; Jiang, Z.; Ren, L.; Zhang, Q. *Macromol. Rapid Commun.* **2006**, *27*, 926.
- (444) Shi, W.; Liang, P.; Ge, D.; Wang, J.; Zhang, Q. *Chem. Commun.* **2007**, 2414.
- (445) Hulvat, J. F.; Stupp, I. *Angew. Chem., Int. Ed.* **2003**, *42*, 778.
- (446) Huang, L.; Wang, Z.; Wang, H.; Cheng, X.; Mitra, A.; Yan, Y. *Mater. Chem.* **2002**, *12*, 388.
- (447) Goto, H.; Akagi, K. *Macromol. Rapid Commun.* **2004**, *25*, 1482.
- (448) Goto, H. *J. Electrochim. Soc.* **2007**, *154*, E63.
- (449) Goto, H.; Nomura, N.; Akagi, K. *J. Polym. Sci.* **2005**, *43*, 4298.
- (450) Goto, H.; Akagi, K. *Chem. Mater.* **2006**, *18*, 255.
- (451) Nonaka, T.; Fuchigami, T. In *Organic Electrochemistry*, 4th ed.; Lund, H., Hammerich, O., Eds.; Marcel Dekker Inc.: 2001; pp 1084–1085.
- (452) Qu, L.; Shi, G.; Chen, F.; Zhang, J. *Macromolecules* **2003**, *36*, 1063.
- (453) Qu, L.; Shi, G. *Chem. Commun.* **2003**, 206.

- (454) Qu, L.; Shi, G.; Yuan, J.; Han, G.; Chen, F. *J. Electroanal. Chem.* **2004**, *561*, 149.
- (455) Yuan, J. Y.; Zhang, D. Q.; Qu, L. T.; Shi, G. Q.; Hong, X. Y. *Polym. Int.* **2004**, *53*, 2125.
- (456) Qu, L.; Shi, G. *J. Polym. Sci., Part A* **2004**, *42*, 3170.
- (457) Han, D.; Yang, G.; Song, J.; Niu, L.; Ivaska, A. *J. Electroanal. Chem.* **2007**, *602*, 24.
- (458) Wang, Z.; Jiao, L.; You, T.; Niu, L.; Dong, S.; Ivaska, A. *Electrochem. Commun.* **2005**, *7*, 875.
- (459) Song, J.; Han, D.; Guo, L.; Niu, L. *Nanotechnology* **2006**, *17*, 824.
- (460) Bajpai, V.; He, P.; Dai, M. *Adv. Funct. Mater.* **2004**, *14*, 145.
- (461) Hui, F.; Li, B.; Hu, J.; Fang, Y. *Electrochem. Commun.* **2009**, *11*, 639.
- (462) Martin, C. R. *Science* **1994**, *266*, 1966.
- (463) Martin, C. R. *Acc. Chem. Res.* **1995**, *28*, 61.
- (464) Braun, P. V.; Wiltzius, P. *Curr. Opin. Colloid Interface Sci.* **2002**, *7*, 116.
- (465) Tian, S.; Wang, J.; Jonas, U.; Knoll, W. *Chem. Mater.* **2005**, *17*, 5726.
- (466) Han, S.; Briseno, A. L.; Shi, X.; Mah, D. A.; Fzhou, M. R. *J. Phys. Chem. B* **2002**, *106*, 6465.
- (467) Sumida, T.; Wada, Y.; Kitamura, T.; Yanagida, S. *Chem. Commun.* **2000**, 1613.
- (468) Cassagneau, T.; Caruso, F. *Adv. Mater.* **2002**, *14*, 1837.
- (469) Bartlett, P. N.; Birkin, P. R.; Ghanem, M. A.; Toh, C.-S. *J. Mater. Chem.* **2001**, *11*, 849.
- (470) Ghanem, M. A.; Bartlett, P. N.; de Groot, P.; Zhukov, A. *Electrochem. Commun.* **2004**, *6*, 447.
- (471) Luo, X.; Killard, A. J.; Morrin, A.; Smyth, M. R. *Chem. Commun.* **2007**, 3207.
- (472) Cho, S. I.; Lee, S. B. *Acc. Chem. Res.* **2008**, *41*, 699.
- (473) Joo, J.; Kim, B. H.; Park, D. H.; Kim, H. S.; Seo, D. S.; Shim, J. H.; Lee, S. J.; Ryu, K. S.; Kim, K.; Jin, J.-I.; Lee, T. J.; Lee, C. J. *Synth. Met.* **2005**, *153*, 313.
- (474) Xiao, R.; Cho, S. I.; Liu, R.; Lee, S. B. *J. Am. Chem. Soc.* **2007**, *129*, 4483.
- (475) Demoustier-Champagne, S.; Ferrain, E.; Jérôme, C.; Jérôme, R.; Legras, R. *Eur. Polym. J.* **1998**, *34*, 1767.
- (476) Delvaux, M.; Duchet, J.; Stavaux, P. Y.; Legras, R.; Demoustier-Champagne, S. *Synth. Met.* **2000**, *113*, 275.
- (477) Duvail, J. L.; Retho, P.; Garreau, S.; Louarn, G.; Godon, C.; Demoustier-Champagne, S. *Synth. Met.* **2002**, *131*, 123.
- (478) Cho, S. I.; Choi, D. H.; Kim, S.-H.; Lee, S. B. *Chem. Mater.* **2005**, *17*, 4564.
- (479) Demoustier-Champagne, S.; Stavaux, P.-Y. *Chem. Mater.* **1999**, *11*, 829.
- (480) Cao, Y.; Mallouk, T. E. *Chem. Mater.* **2008**, *20*, 5260.
- (481) Lee, J. I.; Cho, S. H.; Park, S.-M.; Kim, J. K.; Kim, J. K.; Yu, J.-W.; Kim, Y. C.; Russell, T. P. *Nano Lett.* **2008**, *8*, 2315.
- (482) Bates, F. S.; Fredrickson, G. H. *Phys. Today* **1999**, *52*, 32.
- (483) Bates, F. S.; Fredrickson, G. H. *Annu. Rev. Phys. Chem.* **1990**, *41*, 525.
- (484) Thurn-Albrecht, T.; Schotter, J.; Kästle, G. A.; Emley, N.; Shibauchi, T.; Krusin-Elbaum, L.; Guarini, K.; Black, C. T.; Tuominen, M. T.; Russell, T. P. *Science* **2000**, *290*, 2126.
- (485) Crossland, E. J. W.; Ludwigs, S.; Hillmyer, M. A.; Steiner, U. *Soft Matter* **2007**, *3*, 94.
- (486) Crossland, E. J. W.; Nedelcu, M.; Ducati, C.; Ludwigs, S.; Hillmyer, M. A.; Steiner, U.; Snaith, H. J. *Nano Lett.* **2009**, *9*, 2813.
- (487) Parthasarathy, R. V.; Martin, C. R. *Chem. Mater.* **1994**, *6*, 1627.
- (488) Van Dyke, L. S.; Martin, C. R. *Langmuir* **1990**, *6*, 1118.
- (489) Park, D. H.; Kim, M.; Kim, M. S.; Kim, D.-C.; Song, H.; Kim, J.; Joo, J. *Electrochem. Solid State Lett.* **2008**, *11*, K69.
- (490) Cho, S. I.; Kwon, W. J.; Choi, S. J.; Kim, P.; Park, S. A.; Kim, J.; Son, S. J.; Xiao, R.; Kim, S. H.; Lee, S. B. *Adv. Mater.* **2005**, *17*, 171.
- (491) Cho, S. I.; Choi, D. H.; Kim, S.-H.; Lee, S. B. *Chem. Mater.* **2005**, *17*, 4564.
- (492) Hurst, S. J.; Payne, E. K.; Qin, L. D.; Mirkin, C. A. *Angew. Chem., Int. Ed.* **2006**, *45*, 2672.
- (493) Park, S.; Chung, S. W.; Mirkin, C. A. *J. Am. Chem. Soc.* **2004**, *126*, 11772.
- (494) Liu, R.; Lee, S. B. *J. Am. Chem. Soc.* **2008**, *130*, 2942.
- (495) Wuu, Y.-M.; Fan, F.-R.-F.; Bard, A. J. *J. Electrochem. Soc.* **1989**, *136*, 885.
- (496) Kranz, C.; Ludwig, M.; Gaub, H. E.; Schuhmann, W. *Adv. Mater.* **1995**, *7*, 38.
- (497) Zhou, J.; Wipf, D. O. *J. Electrochem. Soc.* **1997**, *144*, 1202.
- (498) Turyan, I.; Mandler, D. *J. Am. Chem. Soc.* **1998**, *120*, 10733.
- (499) Borgwarth, K.; Rohde, N.; Ricken, C.; Hallensleben, M. L.; Mandler, D.; Heinze, J. *Adv. Mater.* **1999**, *11*, 1221.
- (500) Marck, C.; Borgwarth, K.; Heinze, J. *Adv. Mater.* **2001**, *13*, 47.
- (501) Borgwarth, K.; Heinze, J. *J. Electrochem. Soc.* **1999**, *146*, 3285.
- (502) Marck, C.; Borgwarth, K.; Heinze, J. *Chem. Mater.* **2001**, *13*, 747.
- (503) Li, Y.; Maynor, B. W.; Liu, J. *J. Am. Chem. Soc.* **2001**, *123*, 2105.
- (504) Maynor, B. W.; Filocamo, S. F.; Grinstaff, M. W.; Liu, J. *J. Am. Chem. Soc.* **2002**, *124*, 522.
- (505) Jang, S.-Y.; Marquez, M.; Sotzing, G. A. *J. Am. Chem. Soc.* **2004**, *126*, 9476.

CR900226K